UNIVERSITY OF VAASA
FACULTY OF TECHNOLOGY

COMMUNICATIONS AND SYSTEMS ENGINEERING

Sai Raghu Kezheke Variam

HIERARCHICAL CONTROL OF AC MICROGRIDS

Master's thesis for the degree of Master of Science in Technology submitted for assessment, Vaasa, 16 May 2018

Supervisor Professor Mohammed Elmusrati

Instructor Asst. Professor Ali Altowati

ACKNOWLEDGMENT

I would like to thank the people who shared their knowledge with me for helping me to complete my thesis. Firstly, I would like to thank Dr. Ali Altowati and Professor Mohammad Elmusrati, who hava encouraged me to take this topic and helping me throughout the process of writing. I was not prepared to take this topic, but Dr. Altowati's motivation helped me to take this as a challenge and succeed in it. Secondly, I would also like to thank Tobias Glocker, who has helped me to gain knowledge and skills through my course work.

My deep gratitude goes towards the staff of University of Vaasa and Tritonia for their support and cooperation throughout my study period.

Last, but not the least I would like to thank all my friends and family, who have supported me through the difficult phase of my thesis.

TABLE OF CONTENTS **Page**

ABBREVIATIONS 8

ABSTRACT 10

1. INTRODUCTION 11
   1.1 Introduction to microgrids 11
   1.2 Thesis motivation 12
   1.3 Research methods 12
   1.4 Thesis outline and contribution 13

2. LITERATURE REVIEW 15
   2.1 Structure of a microgrid 15
   2.2 Types of microgrids 17
      2.2.1 AC Microgrid 17
      2.2.2 DC Microgrid 18
   2.3 Difference between AC and DC microgrids 18

3. POWER CONVERTERS IN MICROGRIDS 20
   3.1 Microgrid classification based on operations 20
      3.1.1 Grid forming power converters 21
      3.1.2 Grid feeding power converters 23
         3.1.2.1 Current control methods 24
         3.1.2.2 Current control based on the resonant controller in a stationary reference frame 25
      3.1.3 Grid supporting type power converters 27
         3.1.3.1 Grid supporting converter operating as voltage source 28
         3.1.3.2 Grid supporting converter operating as current source 30

4. HIERARCHICAL CONTROL OF MICROGRIDS 33
4.1 General introduction 33
4.2 Concept analysis 36
4.2.1 Voltage and current control loops 36
4.2.2 Primary control 38
4.2.2.1 Active load sharing 40
4.2.2.2 Droop control 45
4.2.3 Secondary control 61
4.2.3.1 Centralized secondary control of a microgrid 62
4.2.3.2 Distributed secondary control of a microgrid 65
4.2.4 Tertiary control 73

5. SIMULATIONS AND RESULTS 76

6. CONCLUSION 99

7. REFERENCES 101

8. APPENDICES 105

LIST OF TABLES AND FIGURES

Table 1 Classification of grid-connected components according to their electrical behavior 32
Table 2 Parameter values used in for simulation 98

Figure 1 Structure of microgrids 17
Figure 2 Grid forming converters equivalent circuit 21
Figure 3 Grid forming power converters 22
Figure 4 The equivalent control structure of grid feeding 23
Figure 5 Grid feeding control 24
Figure 6 Grid feeding stationary reference frame 26
Figure 7 The equivalent control structure of grid supporting power converters acting as voltage source 28
Figure 8 Voltage source grid supporting 29
Figure 9 The equivalent control structure of grid supporting power converters acting as current source 30
Figure 10 Current source grid supporting 31
Figure 11 Hierarchical control mechanism 34
Figure 12 Reference voltage generation for voltage control loops 37
Figure 13 Zero level voltage control loop for multiple energy resources 38
Figure 14 Primary control structure 39
Figure 15 Centralized controller for a parallel UPS system 41
Figure 16 Block diagram of master and slave module 42
Figure 17 The equivalent circuit for parallel UPS system controlled through MS strategy 43
Figure 18 Average power sharing in ALS 44
Figure 19 3C method block diagram 45
Figure 20 Conventional droop technique 46
Figure 21 Simplified diagram of converter connected to the MG 46

Figure 22 Small signal model of conventional active power model 48
Figure 23 The small-scale model of the adjustable active power control 49
Figure 24 The small-scale signal model for reactive power control 50
Figure 25 Droop/boost characteristic of low-voltage microgrid 52
Figure 26 Block diagram for virtual power frame transformation 53
Figure 27 Virtual output impedance 54
Figure 28 Two DER system 55
Figure 29 Signal injection method updated block diagram 59
Figure 30 Control block diagram for harmonic cancellation technique 60
Figure 31 h^{th} harmonic equivalent circuit of a DER 61
Figure 32 Secondary control structure in a MG 62
Figure 33 The centralized way of secondary control in a MG 63
Figure 34 Networked control system in MG 65
Figure 35 Distributed secondary control 68
Figure 36 Secondary control response vs primary control response 69
Figure 37 Small signal model for distributive frequency control for a DG unit 70
Figure 38 Small signal model of distributed control of a DG unit in a low R/X islanded microgrids 72
Figure 39 Block diagram of tertiary control 74
Figure 40 Single inverter control model 77
Figure 41 PV array circuit 78
Figure 42 Internal control structure 80
Figure 43 Active Power from inverter 81
Figure 44 Reactive Power from the inverter 81
Figure 45 Three phase voltage from the output of inverter 82
Figure 46 Current across output of inverter 82
Figure 47 Frequency of Vabc output of inverter 82
Figure 48 Single inverter MG in grid-connected mode 83
Figure 49 Active and reactive power during transition from islanding to grid-connected mode 84

Figure 50 Frequency transition between islanding and grid-connected mode 84
Figure 51 Voltage at inverter output 85
Figure 52 Two inverters connected in parallel 86
Figure 53 Active power of parallel inverters 87
Figure 54 Reactive power of parallel inverters 87
Figure 55 Frequency restoration from P-F 88
Figure 56 Active load sharing and frequency between two inverters with switching time at t =0.3, 0.6 and 0.9 seconds 88
Figure 57 Voltage transition between two inverters 89
Figure 58 Current transition between two inverters 89
Figure 59 Inner control of de-centralized parallel inverter 90
Figure 60 Frequency restoration of centralized MG 90
Figure 61 Voltage restoration of centralized MG 90
Figure 62 Model snapshot of centralized control inside droop strategy 91
Figure 63 Active power in load during centralized MG control 91
Figure 64 Reactive power in load during centralized MG control 91
Figure 65 Frequency of centralized MG control with distributive load 92
Figure 66 Active power of centralized MG control with distributive load 92
Figure 67 Reactive power of centralized MG control with distributive load 92
Figure 68 Inverter output voltage of centralized MG control with distributive load 93
Figure 69 Inverter output current of centralized MG control with distributive load 93
Figure 70 Grid connected in parallel inverter operation 94
Figure 71 Frequency restoration in grid-connected mode 95
Figure 72 Current at output of inverter during grid-connected mode 95
Figure 73 Voltage at the output of inverter during grid-connected mode 96
Figure 74 Active power during transition 96
Figure 75 Voltage at PCC in grid-connected mode 97
Figure 76 Current output of inverter during and after switching to grid 97

ABBREVIATIONS

AC	Alternating current
DER	Distributive energy resources
CHP	Combined heat and power
CSI	Current source inverter
DC	Direct current
DG	Distributive generation
DS	Distributed source
DSOGI	Dual second order generalized integrator
EES	Electrical energy storage
HC	Harmonic compensator
IC	Integrated circuit
IGBT	Insulated-gate bipolar transistor
ISA	International society of automation
LVDS	Low voltage distribution systems
LVRT	Low voltage ride through
MATLAB	Matrix laboratory
MG	Microgrid
MPPT	Maximum power point tracker
PCC	Point of common coupling
PI	Proportional integral
PID	Proportional integral directive
PLL	Phase lock loop
PR	Proportional resonant
PV	Photovoltaic
RES	Renewable energy resources
RMS	Root mean square
SOGI	Second order generalized integrator

THD	Total harmonic distortion
UPS	Uninterrupted power supply
VSC	Voltage source converters
VSI	Voltage source inverter
WT	Wind turbine

UNIVERSITY OF VAASA
Faculty of Technology
Author: Sai Raghu Kezheke Variam
Topic of the Thesis: Hierarchical control of AC microgrids
Supervisor: Professor Mohammed Elmusrati
Instructor: Asst. Professor Ali Altowati
Degree: Master of Science in Technology
Degree Programme: Degree Programme in Communications and Systems Engineering
Major: Communications and Systems Engineering
Year of Entering the University: 2014
Year of Completing the Thesis: 2018 **Pages:** 116

ABSTRACT:

Microgrids are a group of localized electrical resources mainly using renewable resources as a main source of power, which can operate independently or in collaboration with utility grid. When connection of a microgrid is concerned, switching from an islanding to grid-connected mode is always a difficult task for a microgrid mainly due to transients and mismatching in synchronization. Hierarchical control structure of a microgrid eradicates this issue by separating the control structure in multiple levels. This thesis explains different levels of hierarchical control strategies, which constitute primary control, secondary and tertiary control.

The primary control is based on droop control including output virtual impedance, secondary control performs restoration of voltage and frequency performed by primary and tertiary control maintain the power flow between the micro grid and external utility.

In first step, this thesis covers the technical overview of traditional control methods of power converters and then the latter part consists of detailed description of all three levels of hierarchical control with synchronization and power flow analysis. Various types of primary controls, like with and without communication, and improvements to droop control are discussed and compared. In the end, concepts explained in previous chapters, are done in practice and simulated results are discussed.

KEYWORDS: Microgrids, Hierarchical control, Droop, Primary control, Secondary control, Tertiary control

1. INTRODUCTION

1.1 Introduction to microgrids

Electricity generation is seeing a rapid change with escalating environmental concerns and responding to consumer demands. Smart grids evolved as a recent development to these changes that introduced an intelligent and self-sufficient electrical network. Among these developments, the introduction of Renewable Energy Sources (RES) is mainly looked up because of its availability and sustainability. In the past, the Distributive Energy Resources (DERs) like DG (Distributed generators) and DS (Distributed source) were self-operational with very low controlling mechanisms from the transmission grids, which resulted in non-flexibility of operation of these resources and hence we could not exploit the usage of these resources to the maximum. However, the technical constraints predominantly focusing on voltage and power fluctuations of these, DER has raised concerns about their usage as intelligent grids. To overcome these problems microgrids are used nowadays, which plays a crucial role in generation and distribution of electrical networks. Microgrids are a part of electric power distribution networks that combine considerable number of DERs like PV (Photovoltaic), wind etc. and storage devices like flywheel, which may connect or disconnect itself from the main grid under emergency situation either intended or unintended. It operates under two modes namely grid-connected and islanding mode. The standalone operation of microgrid, when it disconnects itself from the main grid, is called islanding mode of microgrid. Due to this increasing demand for higher power quality, DERs are getting more attention in recent years (Mastromauro 2014:1). One of the main benefits of microgrids are generalized by having its CHP (Combined heat and power) technology, which is because of its environmentally friendly and economical benefits. When there is waste fuel after the generation of power in small generators by means of CHP, the wasted power can be reused by local consumers, hence making use of the resources efficiently. Modern day DG systems that are one of the main sources of MG (microgrid) have higher controllability and operability than traditional generators, which makes them a key player for electrical networks in the future.

1.2 Thesis Motivation

Both AC (Alternating current) and DC (Direct current) MGs can be used for variety of applications and islanded MGs are more suitable for marine and avionics industries, which are mostly offshore based. These MGs are interfaced by special power electronic power converters called VSI (Voltage Source Inverters), which can be connected in parallel to other MGs. When a single inverter is used in MG then initial level of control is enough to generate power. There are quite many challenges when MGs are connected to grid. The grid frequency and phase should match the inverter frequency and phase so as to maintain the operation smoothly. Similarly, when multiple VSI's are connected to the source then there is need for proper synchronization between those connected inverters to achieve good power quality. Synchronization is always an issue, when inverters are trying to connect in parallel or when inverters are trying to connect to the grid because both frequency and phase need to be same when trying to connect to the load.

1.3 Research Methods

In case of parallel inverters, droop control method is always the first choice. These control loops consist of active power-frequency and voltage-reactive power characteristics, which have been used to connect inverters to uninterrupted power supply (UPS). These droop control techniques come with both advantages and disadvantages, which will be looked into in detail in chapter 4. Droop controls are not suitable for parallel-connected inverter systems with non-linear loads, because control units should take care of both current harmonics and active and reactive power. To overcome this, control loops are adjusted with output impedance using virtual reactance or resistance along with droop control, hence harmonic current component will be shared evenly. Another disadvantage of droop control is its load-dependent frequency deviation, which involves phase deviation of output voltage frequency of the UPS system and the input voltage provided by the utility mains. This method can be only used for islanding mode of operation, hence the synchronization is not achieved in MG while transitioning between islanding and grid-connected modes. Some improvements have

been made by using an integrator in droop control to avoid frequency deviation (Guerrero et al. 2011: 158-172). There are many ways to achieve synchronization, one of the ways is to manually switch from mains to islanded whenever phase and frequencies of both are same. For this the inverter always needs to be near bypass switch. However, this way is dangerous and can cause further transients, as the frequencies while closing the switch might be uneven. Hence, this method is very impractical as the reliability to achieve synchronization is very less. So communication type droop method seems unavoidable as it's non-critical as compared to previous methods. In droop method the virtual impedance technique is used, which is also called adaptive voltage restoration, that has been designed to improve transient response of systems with low voltage applications. Maintaining the power quality is always the main issue for islanded microgrids, especially when there are more number of sensible loads available whose performance depends on these dips and harmonics of voltages. In case there are more energy resources that are connected in parallel, then the power sharing is also a key factor, i.e. if two or more inverters are connected in parallel, then they need to be synchronized properly to deliver equal power to the load. The implementation of a smart control technique, namely hierarchical control, will eliminate the problem of synchronization and power quality as well. In hierarchical control, primary control have droop or other lower control loops, secondary control will deal with synchronization issues when multiple inverters are connected in parallel in both islanding and grid-connected modes, and tertiary control can be used to control bidirectional power flow when micro grids are connected to utility or mains. Hierarchical controls in past were very limited to AC systems, but nowadays these are used in DC systems like wind-farms, battery, photovoltaic systems (PV) etc. Hence with the use of hierarchical controls, the power-electronic converters, which operate both in grid-connected and islanding mode, can achieve battery synchronization.

1.4 Thesis outline and contribution

In this thesis, chapter 2 comprises basic introduction about microgrid and its structure, then in chapter 3 various types of power converters used in microgrids for both islanding mode and grid-connected mode, their comparison depending upon the type of operation and lastly

the control techniques for these power converters are discussed. In chapter 4 primary, secondary and tertiary control of hierarchical model for single and multiple DER systems are explained. Different types of primary control methods are compared with traditional droop and in secondary control centralized and de-centralized systems are compared. The final objective of this thesis is to achieve synchronization when multiple inverters are connected together both in islanding and grid-connected mode.

2. LITERATURE REVIEW

A microgrid is the collection of distributed energy resources (DER) connected together as stand-alone or tied-up with the utility grid to meet load demands. The DERs constitute of various resources both renewable (solar, wind, geo, etc.) and non-renewable (fossil fuels), which generate the power from their resources to meet the demand. It can also be defined as part of main grid consisting of energy movers, power electronic converters, DER and local loads. A microgrid should be able to operate independently and also be able to work in connection with utility grid in case of power shortage. During the connection from microgrid to utility, the energy transfer should be seamless, not intermittent. Nowadays MGs are representing a new prototype by working in low voltage distribution systems (LVDS) based on generation by PV array, prime movers, small and medium wind turbines, etc. For working with these power generation sources, power electronic interfaces (ac-dc or dc-ac or dc-dc) are needed to transmit the generated power to either local load or utility. These power electronic converters have full control over the transient response and also, they do not have inherent inertia unlike the generator machines, which make the system stable, and hence steady-state synchronization is achieved (Mastromauro 2014: 1-2). To achieve better synchronization virtual inertias are implemented inside the control loops generally known as droop control, which works very similar to that of synchronous machines. This control helps to achieve constant active and reactive power at the output by controlling the system frequency and voltage. Hence the MG helps to maintain the stability and consistency of grid system by maintaining both active and reactive powers and by keeping the RMS (root mean square) voltage constant.

2.1 Structure of a microgrid

Microgrid's DER itself acts as a source grid hence it can be connected to utility grid by means of Point of common coupling (PCC). PCC in either parallel MG or grid-connected MG, can

be regulated by controlling the active power flow in/out between grids or DERs. The components inside MG are as follows:

1. Distributed Generators (DG): Microgrids can accommodate different types of resources under their belt so that they can utilize the available resources like air water, wind, biomass, etc. DG can operate as a voltage source or a current source inverter (CSI) build upon the modes in which it operates. When a DER is operating as a current source inverter, then the main objective is to supply the power generated to the load and also regulate the voltage and frequency of both MG and utility. Hence, it's not commonly used in MG, especially when it is serving a purpose for only stand-alone operation, but for grid-connected mode, it works aforementioned. VSI is used mostly for Energy Storage System (ESS) whereas CSI is implemented for Photovoltaic (PV) or Wind Turbine (WT), which requires maximum power tracking algorithms to generate reference powers to the controller. (Mastromauro 2014: 1).

2. Energy Storage: Energy storage is a new technology and has a diverse role in MG, where the power generated by these DGs is stored. These improve the stability, power quality and reliability of the power generators (Kundur 1993). ESS enables the MG to operate without the emission of CO2, which helps the DG to synchronize the inverters with or without the presence of the grid. Before ESS all renewable sources need to have a voltage source in order to function, where the voltage source is typically a main grid without which the system could not operate. In case of utility failure, the energy resources could have only been operated using diesel engines, which was not economical. It helps to maintain the irregular PV power flow and stabilizing the voltage at the grid.

3. Load: Load of MG can vary from industrial to residential. These loads can be critical or non-critical, linear or non-linear, balanced or unbalanced depending on the specific operation. These include priority service to critical loads, power quality and reliability improvement of loads as mentioned above. In cases of load imbalances, protection devices are introduced so that harmonics and disturbances can be avoided.

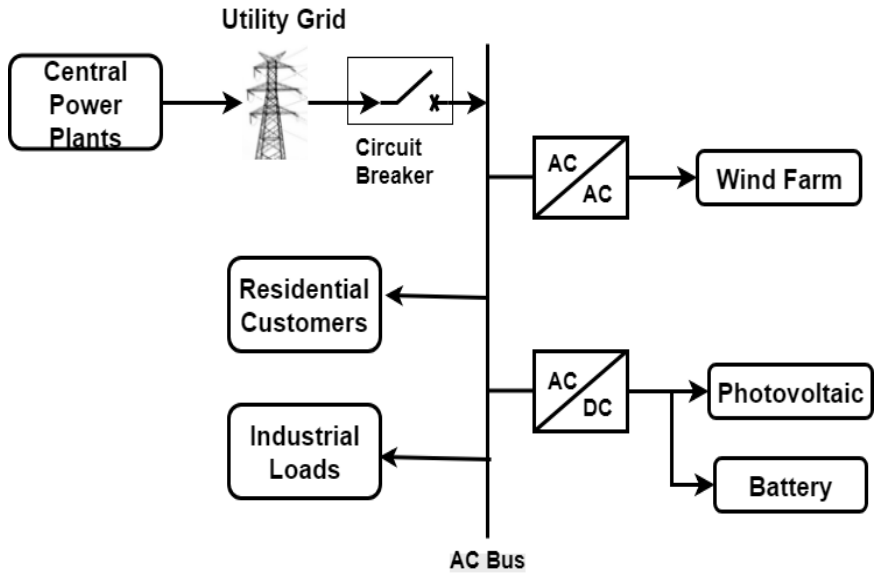

Figure 1. Structure of a microgrid

2.2 Types of microgrids

As shown in Figure 1 the microgrids can be classified into two types: AC microgrids and DC microgrids. Majority of the distributed systems in the globe use ac grids, that is mainly because of the advantages of AC MGs over DC ones. The protection system for microgrids mainly constitutes of protective relays, protective devices, measuring equipment's, grounding, etc. MG operates mainly in two modes: grid-connected and islanding or stand-alone mode both consisting of AC and DC sources, hence hybrid MGs nowadays use both AC and DC source to control the power flow between the grids. For advanced control of microgrids, a hierarchical control method is being adopted in this thesis namely primary, secondary and tertiary control. The two types of microgrids are explained below:

2.2.1 AC microgrid

As the renewable energy sources are naturally dispersed, hence it's an enormous challenge for power systems to maintain a countless, yet still growing and discontinuously distributed power generation in a traditional way. In order to make a whole distributive systems work, a

systematic arrangement is necessary. When we integrate different generation sources, a microgrid is formed. Traditionally in all microgrids, the generation source is mostly AC source. A three-phase AC bus is deployed near the point of common coupling (PCC), which is normally set as the only power interface between utility and the microgrid. A microgrid can be connected in grid-connected mode and islanding mode depending on the operation needs. Hence a very fast switching need to be placed between PCC and utility grid, which will act as a cut-off between utility and the microgrid. As discussed, a microgrid consist of both distributive generation resource and an energy storage system (ESS). Renewable resources try to extract maximum power from the natural environment and then integrates to the main grid. Since most of the renewable resources aforementioned are DC type, so there need to be multiple stages for conversion of these DC sources to AC which adds the complexity to AC microgrids in (Manandhar et al. 2016: 1).

2.2.2 DC microgrid

DC microgrid was proposed after the emergence of AC microgrids. As the name suggests, DC MGs are generally designed to distribute DC power source, energy storage device like batteries and DC loads. The main purpose of DC microgrids is to increase PV distribution lines, reduce the energy dissipation and costs for conversion of AC-DC power using IGBT's (Insulated-gate bipolar transistor) or MOSFET's (Metal oxide semiconductor field effect transistor) and last but not the least to provide continuous power to the loads without any interruption.

2.3 Difference between AC and DC microgrids

Since a MG consists of both AC, DC and mixed AC/DC distribution line as showed in Figure 1. Comparison of both AC and DC microgrids is done by Chen and L. Xu (2017).

A. Conversion Efficiency: DC MG has taken over its counterpart AC microgrids for its efficiency especially when power storage is considered. For example for PV-to battery charging case, the power flow from an AC MG has to go through a DC-AC conversion which includes complex operation, but power flow in DC microgrids skips the conversion stage and there hence improves performance and efficiency.

B. One-off cost on converters: A normal DC-AC converter is used to convert power source from DC microgrid to AC microgrid, whereas in an AC microgrid power converters are needed to be placed in every distribution source. Since the power rating of normal DC/AC converter is less than total power rating but greater than any of the individual unit ratings in AC microgrids, hence the cost of manufacturing and installation is reduced.

C. Transmission/ distribution efficiency: In DC power transmission there is no issue of reactive power, thereby the transmission loss caused by the reactive power can be mitigated.

D. Power supply reliability: The important improvement of microgrid distribution system over traditional distribution is the reliability of power. In AC microgrids it's hard to determine when to switch between grid-connected to islanding mode as there is a contradiction between LVRT (Low Voltage Ride Through) grid code requirements and seamless switch. As DC microgrids are not directly coupled with AC grids then the storage system on DC side can recover the voltage fluctuation immediately when abnormalities are detected. Hence DC microgrids provide seamless power supply.

E. Controllability: DC power system provides a good stability to the system, hence DC voltage regulation is the only main issue to maintain the stability of the DC power system. Regulations in AC power systems need to be performed for both voltage (amplitude) and frequency respectively, there hence making the system more difficult to achieve stability.

F. Load availability: As power is especially made for AC systems because electrical equipment manufacturers design mainly for AC power systems, but DC loads also have huge potential. Digital loads are more compatible with DC loads than its AC counterparts. A DC bus helps to reduce the costs on the rectifying side.

3. POWER CONVERTERS IN MICROGRIDS

3.1 Microgrid classification based on operations

The power inverters, which are connected in parallel to the utility, are made to transfer power between the grid and DGs. this power is more or less equal to the required rated power and the power converter contributes to the information of grid voltage and frequency. Traditionally the distributed power generation system (DPGS) or DGs in grid-connected mode of operation are current-controlled and it delivers specified real power to the distributed network, unlike in islanded mode, where DPGS is connected in voltage-controlled and it is responsible for both active power and voltage control, in this case, DPGS converters are grid forming type (Mastromauro 2014: 3). Depending on the type of operation of MG, Rocabert et al. (2012: 4735) have classified the power converters as:

- Grid forming
- Grid feeding
- Grid supporting

Grid forming power converters act as an ideal voltage source, which can supply constant voltage and frequency to the control loop as shown in Figure 2, where the amplitude E^* and the frequency w^* act as a reference to the inner control loop. Grid feeding type on the other hand is mainly designed to deliver the power to the utility grid. These converters act as a current source with high output impedance in parallel with the controlled current source. Grid feeding type is mainly used in grid-connected operation and can never be separated from the main grid. Here as shown in Figure 4, active and reactive powers ($P^*$and Q^*) are fed to the control loop and are delivered to the load. They act like a current source converter and work only if there is power source or generator to produce grid voltage. For regulating these P^* and Q^*, the current source should be synchronized with AC voltage source at grid. Grid supporting type power converters are represented either as current or voltage source depending on the type of operation. These converters regulate their output voltage and current to make grid voltage and frequency near to rated value.

3.1.1 Grid forming power converters

Grid forming power converters are predominantly used in islanding mode of operations as these are voltage controlled and act as an AC voltage source by themselves. These power converters are controlled using a closed loop mechanism to work as an ideal AC voltage source with specified voltage and frequency levels (Mastromauro 2014: 2-3). Grid forming has a low output impedance by setting the voltage amplitude and frequency of local grid using control loop mechanism. The equivalent circuit of grid forming converters (Figure 2) constitutes a voltage source and low series impedance. Because it acts itself as a grid, these converters can provide reference values for grid supporting type and grid feeding type converters when connected to the grid. In some cases when grid supporting is also used in islanding mode, then one of these converters should behave as grid forming. Uninterrupted power supplies are the best examples of grid forming converters, which generate AC voltage when there is shortage of or failure in the grid voltage.

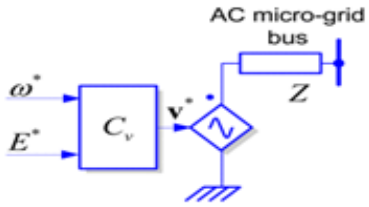

Figure 2. Grid forming converters equivalent circuit (Rocabert et al. 2012: 4735)

As discussed before, they perform autonomous operation i.e. acting as an ideal AC voltage source with a fixed frequency and maintaining the DGs and the loads. Figure 3 shows the basic circuit diagram for the grid forming power converter in three phases, which consists of two cascaded control systems (voltage and current control) in a dq reference frame, here the outer loop is responsible for controlling the voltage and inner loop is responsible for controlling the current. In this circuit, the voltage amplitude is measured at point of common coupling (PCC) and current is measured near inductor line impedance, which is then transformed in dq frame by using Park transformation, and then these values are compared with actual reference values and then fed to $dq - abc$ transformation for generating three

phase voltage signal. The three-phase voltage is then passed to the modulator, whose task is to generate pulses based on Vabc values and then fed to voltage source inverter. The modulator can be a simple pulse width modulation (PWM) or space vector pulse width modulation (SV-PWM) depending on the needs. Here in this control scheme both active power and reactive power can be segregated to regulate the voltage by taking fixed frequency as a reference. This power control is done by d and q frames, like current i_d will control active component and so i_q controls the reactive component. The current through the inductor L_f will charge the capacitor C_f so as to maintain the output voltage close to the reference value. In voltage control loop the reference value of a direct voltage component V_d^* is compared with voltage component from PCC (V_d) and the similar way is performed for quadrature componentV_q. The resultant will pass through a controller to obtain direct and quadrature current reference values i_d^* and i_q^*.

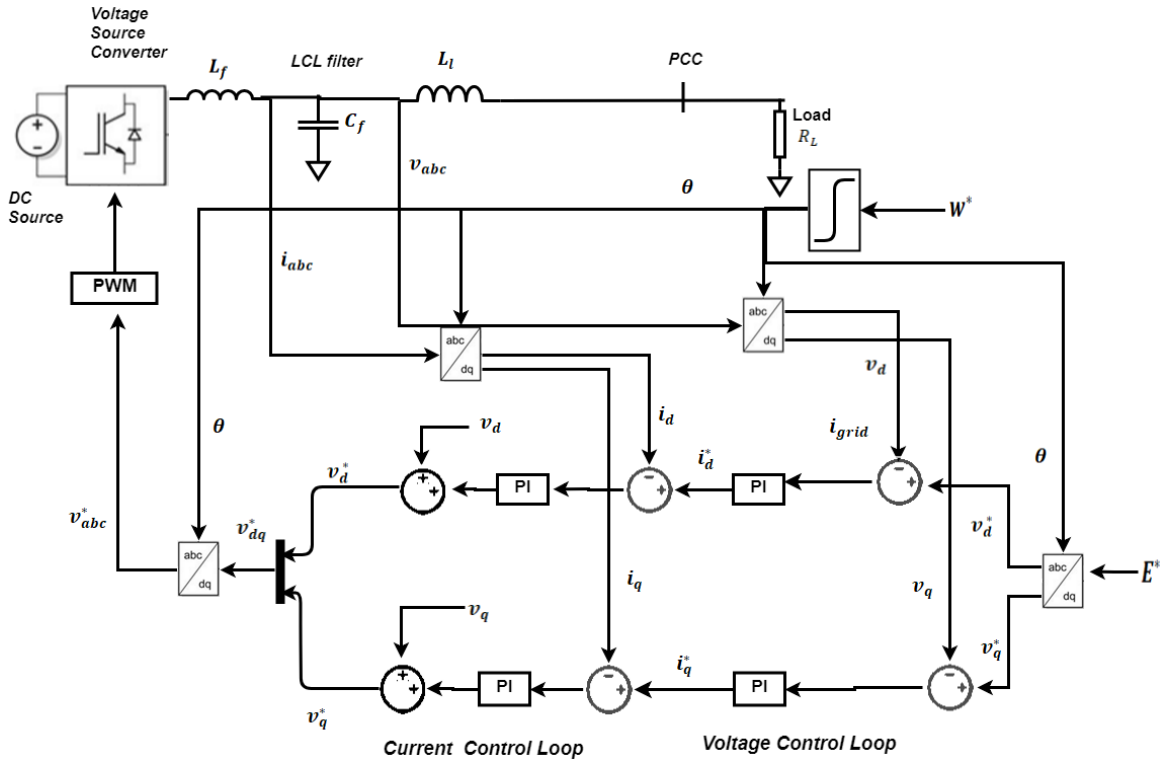

Figure 3. Grid forming power converters

3.1.2. Grid feeding power converters

These converters are current controlled and have high output impedance and are used to deliver both active power and reactive power to the grid. These components do not contribute to power balancing (Mastromauro 2014: 3). These power converters are suitable to install in parallel with other grid-feeding converters in grid-connected mode. The most common places, where grid feeding type converter are used are PV, hybrid systems (diesel, fuel cells) etc. The equivalent circuit of these power converters is shown here:

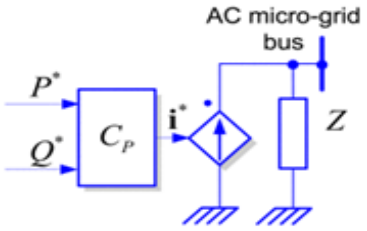

Figure 4. The equivalent control structure of grid feeding (Rocabert et al. 2012: 4735)

Since these converters are current controlled, hence an ideal current source with a high output impedance (Z) is shown. P^* and Q^* are active and reactive powers to be delivered to the load. Here the key point is the current source should be synchronized with AC voltage at PCC in order to deliver both P^* and Q^* to the grid, therefore the phase lock loop (PLL) is necessary. In the circuit shown in Figure 4 P^* and Q^* are active and reactive powers to be delivered respectively. Since here the motivation is not to control the output voltage, only current control loop is needed. These converters cannot be operated in islanded mode if there is no grid forming or grid supporting type of converters connected. The regulation of both P^* and Q^* are always done by controllers like Maximum Power Point Tracker (MPPT) or power plant controllers. The control of grid feeding power converter depends on current control loops, which regulate the current fed in to the grid (Blaabjerg et al. 2006: 1400). A reference current, which is injected in current control loop is normally feed-forward signal calculated as a reference to active and reactive powers (Rodriguez et al. 2009: 1798-1799).

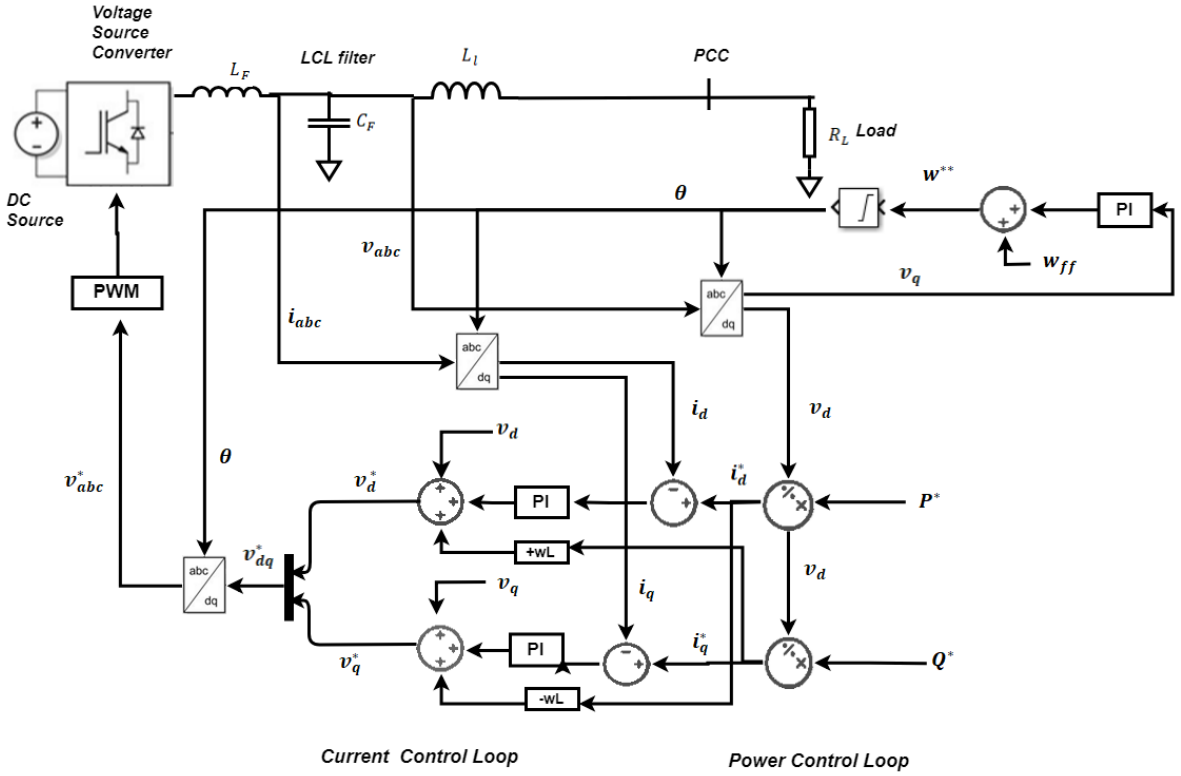

Figure 5. Grid feeding control

The most commonly used control method for three phase AC systems is using PI or PID (Proportional-Integrate-Derivative) controllers with frame-transformed components. A proportional integral (PI) controller can be implemented in both dq reference frame and also resonant controller based on $\alpha\beta$ stationary reference frame (Blaabjerg et al. 2006: 1400-1401). The other ways like non-linear control structure includes hysteresis, sliding, and predictive controllers are also providing a fast and sturdy response. The two control methods, which can be implemented in grid feeding converters are:

3.1.2.1 Current control methods

These control methods based on dq synchronous reference frame are broadly used in control of AC currents in three-phase systems. In general, we use Clark transform to calculate two phase orthogonal currents i_α and i_β from three phase currents (i_a, i_b, i_c). Then i_α and i_β in

the fixed coordinate stator are transformed into two stationary components i_{sd} and i_{sq} in d and q frame with Park transform. In this reference frame, two independent control loops will regulate both d (direct) and q (quadrature) components. The sinusoidal currents under control using Park transformation can be represented as DC values in an orthogonal dq frame while rotating synchronously at a fundamental frequency of the grid. As we can see in the Figure 5, the reference currents i_d^* and i_q^* are provided by Power Control Loop which regulates both active and reactive power delivered to the grid. The instantaneous active and reactive power components are calculated by (Rocabert et al. 2012:4739)

$$p = v_d i_d + v_q i_q \quad (1)$$

An overall overview of current control methods of grid-connected MGs is discussed in Blaabjerg et al. (2006: 1398-1409). In Figure 6 the structure of dq-based synchronous current control, including grid feed-forward and decoupling network is used to improve the performance and efficiency (Timbus et al. 2009: 655–656). Proportional integral controllers used in the given figure are unable to synchronize the oscillations that appear in dq-frame during unbalanced load conditions. To overcome this drawback, two dq synchronous controllers are implemented to produce positive and negative sequence components of the injected current (Liserre et al. 2006: 836–837). The detail analysis of different current controllers like PI, dead-beat controllers, hysteresis controllers, and proportional resonant controllers are done in Timbus et al. (2009: 656).

3.1.2.2 Current control based on the resonant controller in a stationary reference frame

Normally current regulators from AC regulators are hysteresis controllers. The main objective of this controller is to have a zero phase and magnitude error. This kind of controllers work with AC variables expressed in $\alpha\beta$ stationary reference frame. Here the disadvantage of PI is resolved by using PR (proportional resonant) controller, whose resonant frequency is tuned to grid frequency.

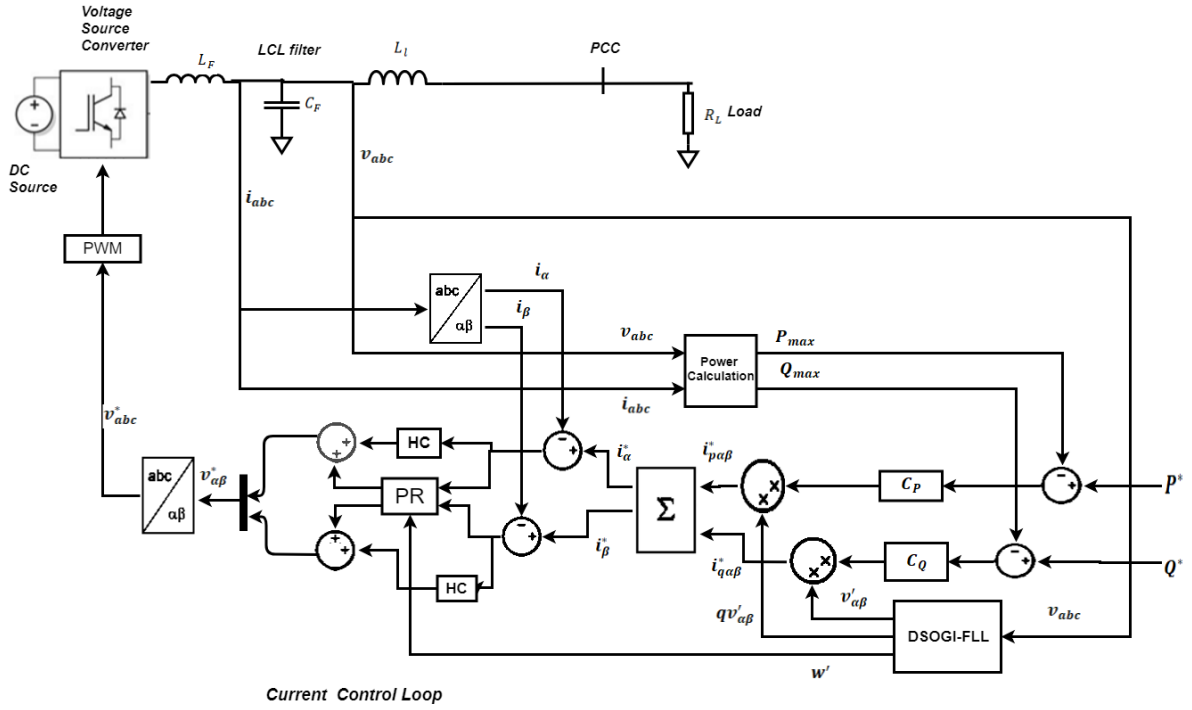

Figure 6. Grid feeding stationary reference frame

Transfer function of this system is as shown below Rocabert et al. 2012:4739):

$$G_{PR}^{\alpha\beta} = k_P + \frac{k_R s}{S^2+w_0^2} + \sum_{h=2}^{n} \frac{k_{ih} s}{(s^2+hw_0{}^2)} \quad (2)$$

In the above equation k_P is a proportional gain of PI controller, k_R is a resonant gain of PR (Proportional Resonant) controller at grid frequency and $k_{ih}s$ is a resonant gain at h-harmonic and w_0 is fundamental frequency of the system. Just like in dq synchronous controllers, the reference currents i_α^* and i_β^* are controlled using power controller by regulating both active and reactive power exchange with the grid. The instantaneous active power and reactive power components in $\alpha\beta$ stationary reference frame are calculated (Rocabert et al. 2012:4739).

$$p = v_\alpha i_\alpha + v_\beta i_\beta \quad \text{and} \quad q = v_\beta i_\alpha + v\_\alpha \, i\_\beta \quad (3)$$

In general, PI in synchronous reference frame results in resonant (PR) controllers when transformed to a stationary reference frame. There are considerable benefits of using PR controllers in stationary reference frame over PI controllers in synchronous reference frame when an unbalanced load is considered. In this case, PR controller is able to control both

positive and negative sequence components with a single PR block. When PR controllers are used then decoupling of networks or independent sequential control are not needed to be implemented. Because of these benefits, PR controllers are best suitable for regulation of current injection in grid-feeding converters even during grid failures. In stationary reference frame control type of grid feeding converter, a dual second-order generalized integrator (DSOGI) is used instead of traditional PLL. Moreover, harmonic compensators (HC) are connected in parallel, which can be implemented by tuning multiple PR controllers at desired harmonic frequency hw' (Rocabert et al. 2012: 4738).

3.1.3 Grid supporting type power converters

Grid supporting power converters are only responsible to extract maximum active power from the energy source and to provide support services to obtain high power quality in the grid. Grid supporting power converters are designed to control voltage of AC grid and frequency of either islanding or grid-connected operation (Bouzid et al. 2015: 10). In these converters, the circulating current between two parallel grid-forming inverters is ruled out by introducing droop coefficients in the inverter frequency and voltage control. Grid supporting converters are used for controlling power sharing in microgrid. Different current sharing strategies for parallel-connected inverters are proposed in microgrid like master-slave, centralized controllers, average load sharing. These controllers will work flawlessly only if the inverters are connected close to each other and are connected using a communication channel. Hence, these controllers are not apt for the microgrid when inverters are far apart from each other, which will make the system more expensive. To overcome this non-communication based strategies are implemented like droop control method, which removes the problems arisen due to the limitation of distance between the inverters and there hence improving the overall performance of MGs (Guerrero et al. 2006: 1461–1470). Droop control algorithm is implemented to control the power sharing in microgrids without using communication schemes. Here active and reactive powers are regulated so as to keep grid voltage E and frequency f in limits. These converters can be operated in two modes.

3.1.3.1 Grid supporting converter operating as voltage source

The main objective of these power converters is to regulate grid voltage and grid frequency near to their respected values there hence controlling active and reactive power delivered to the grid. Grid supporting voltage source converters are designed and controlled such a fashion that the energy sources copies the behavior of synchronous generators. If there are any discrepancies between measured and nominal power then the frequency of an inverter drifts from the nominal value. These types of behavior are generated by using droop mechanism.

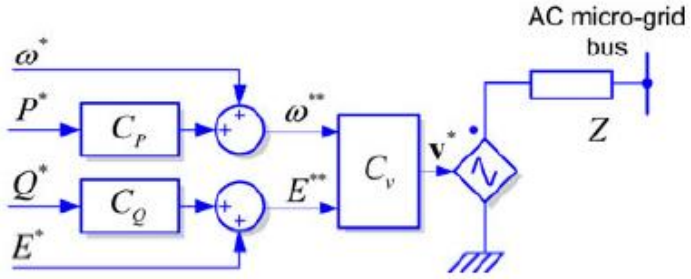

Figure 7. The equivalent control structure of Grid supporting power converters acting as voltage source (Rocabert et al. 2012: 4735)

These kinds of converters have a link impedance can operate both in grid-connected as well as islanding mode, just like synchronous generators which operate in traditional grid systems. Figure 7 shows voltage source where the dependent voltage source gets value from voltage controller and through link impedance it's passed on to the grid or to the local load. Here C_p , C_q and C_v are controllers which produce finally controlled three phase voltages to the DER and Z act as a series link impedance. The power converter is modeling the controlled behavior of an AC source whose operation is homogeneous to that of synchronous generators (Driesen & Visscher 2008: 2). In this control scheme, the active power and reactive power delivered by the power converter is a function of AC grid voltage, the AC voltage of the simulated AC source as discussed in (Kundur 1993) . Throughout the operation of these types of converters, the effect of link impedance is calculated by inner control loop. In Figure 8 we can see that power generated in the droop control is a function of grid voltage and grid current (V_{abc} and I_{abc}) respectively.

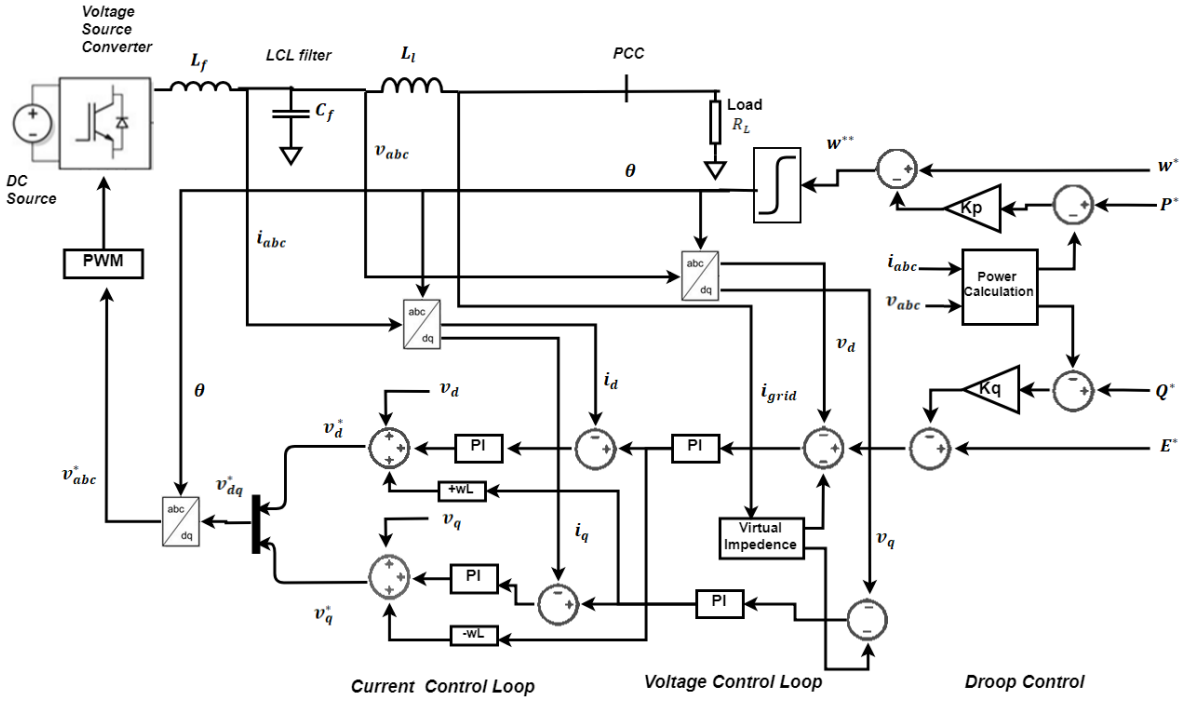

Figure 8. Voltage source grid supporting

The link impedance Z shown in these power converters are usually a physical device connected between VSI and the grid, or a virtual component emulated within current control loop. (Rocabert et al. 2012: 4740). These converters can regulate both amplitude and frequency of grid voltage in grid-connected or islanding mode of operations. The virtual impedance shown in the figure can be either resistive or inductive or combination of all three. Here the phase angle is calculated by passing power difference (actual power - reference power) to a proportional controller and then passed over to integrator to produce θ.

$$\theta = \int w(t)dt \tag{4}$$

The above formula is the relationship between angular frequency and phase angle. This phase angle is then given to abc to dq converter, which in turn produces V_d, V_q, I_d, I_q in synchronous frame. The controlled voltage is the passed to PWM generator, which produces the pulses to trigger the IGBT depend on space vector algorithm.

3.1.3.2 Grid supporting converter operating as current source

These converters are represented as an ideal AC current source connected in parallel to shunt admittance. Just like supporting voltage source converters, these also control the output current to keep the value of grid frequency and grid voltage near to the actual limits. This converter can only be used in grid-connected operation, unlike voltage source type converters, which can be used in both islanding, and grid-connected mode. Figure 9 shows the equivalent circuit of current-controlled grid supporting converters, where we see the dependent current source is activated by power controller which receives controlled power input from frequency and voltage controller.

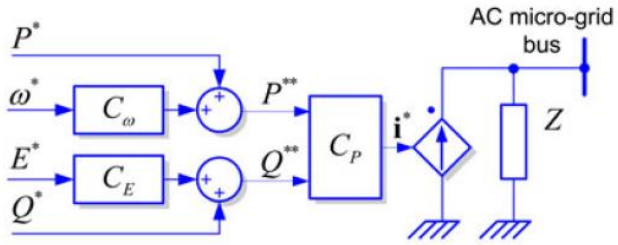

Figure 9. The equivalent control structure of grid supporting power converters acting as current source (Rocabert et al. 2012: 4735)

These controllers have two objectives, firstly to supply load connected to the microgrid and secondly to regulate both amplitude and frequency of both AC grid and microgrid, which is done by the implementation of droop control. This usage of droop control comes from the idea of synchronous generators, which have self-regulation abilities in grid-connection mode by reducing delivered active power (Rocabert et al. 2012: 4736 – 4738). In Figure 10 the system will remain stable if droop gains are not too high. Grid supporting using current source is far less used than its grid supporting using voltage source, the reason for this might be because droop control was initially introduced in UPS based systems which uses grid forming type control mechanism. Hence, when parallel inverter operation is considered then the possible transformation to grid supporting converter as voltage source was optimum solution (Bouzid et al. 2015: 9-10).

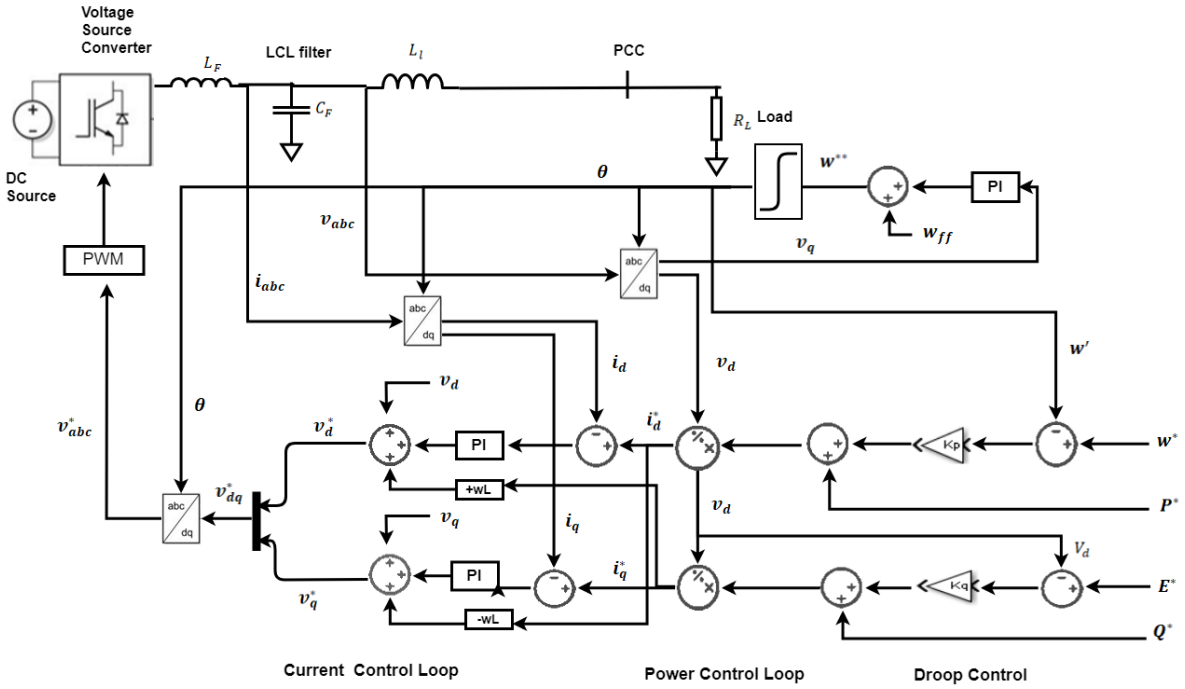

Figure 10. Current source grid supporting

The operation of current source grid supporting converters are same as voltage source type converter, except for the introduction of power control loop instead of voltage control loop in voltage source grid supporting converters as explained in Rocabert et al. (2012: 4737). The below table shows summarized analysis of power converters.

Table 1. Classification of grid-connected components according to their electrical behavior (Bouzid et al. 2015: 10)

Contribution to the grid	**Classification of Grid-Connected**		
	Grid-Forming	**Grid-feeding**	**Grid-Supporting**
Source type	Ideal voltage source	Ideal current source	Non-ideal voltage or current source
Control type	Constant frequency/voltage control	PQ control	Droop control
Combination	Series	Parallel	Parallel or series
Output impedance	$Z_d = 0$	$Z_d = \infty$	Finite, non-zero
Output frequency	Fixed Frequency	Grid synchronized	Frequency droop
Application	Islanded	Grid-connected	Grid-connected or islanded

4. HIERARCHICAL CONTROL OF MICROGRIDS

4.1 General introduction

Microgrids have different power generators with different technologies working in same time, so we need a control mechanism to minimize the operating cost and maximize the efficiency, sustainability and controllability. Standards in MG controls are related to the new grid codes that are expected to appear in the future. ANSI/ISA or ISA-95 are most commonly used international standards for developing an automated interface between enterprise and control systems. The main objective of ISA-95 is to provide consistent terminology that has a basic foundation for manufacturers and suppliers, hence proving a consistent information and operation models for simplifying application functionality. The ISA standard can be described as a multi-level hierarchical control as proposed in Ambrosio et al. (2007: 1–5) and Hamilton et al. (2006: 927–931). The following ISA-95 hierarchical level control for microgrid was discussed in Guerrero et al. (2011: 160).

Level 0. **Device:** The device level explains set of field devices that senses and provides actuation of physical processes within environmental and production systems.

Level 1. **Unit:** The unit level incorporates management level control systems to monitor the state and behaviors of unit automation or manufacturing cell.

Level 2. **Area:** The area or production line incorporates management and control policies required to administer states and behavior of specific area or production line.

Level 3. **Building:** The building or production setup incorporates the management and control policies required to administer the states and behaviors of a building and its environment and production systems.

Level 4. **Plant:** The plant level incorporates the superior level management policies of a branch or operational division of an enterprise, usually including the elements of enterprise financial section that are directly associated with that business entity.

Level 5. **Enterprise**: In enterprise level, the superior management policies and development responsible for the entire enterprise, including all of its plants and respective production lines.

The aforementioned levels show hierarchical command structure starting from 5 to level 0. Hence, it is important to note that command level from a higher level to lower levels will have a lower impact on system stability and robustness, so the bandwidth must increase with decrease in control level. Similar to ISA-95, MG control is classified into three levels as discussed in and shown in Figure 11. Power ratings, distribution of loads and generating systems, electricity prices, generation cost from a random primary resource are the main issues while designing the operations of microgrid. Hence a hierarchical control mechanism is needed in order to distribute these features in separate sets and each takes care of its own task to increase the efficiency of the MG.

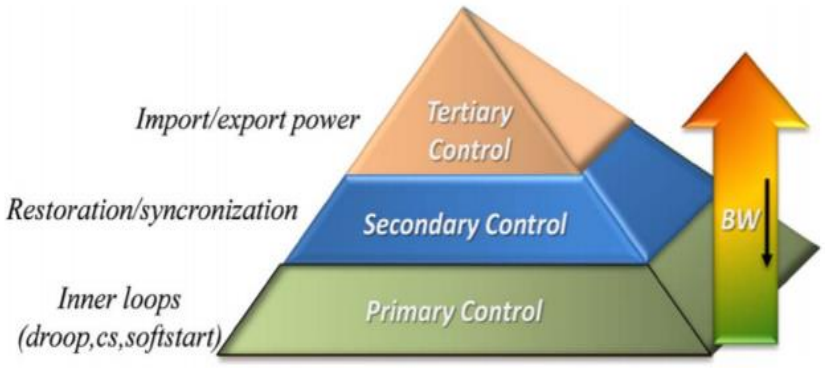

Figure 11. Hierarchical control mechanism (Guerrero et al. 2011: 160)

The levels of hierarchical control can be classified as follows:

***Level 0*. Inner control loop:** This is the first stage in hierarchical control systems, which sorts out the regulation problems of other control levels. Voltage and current control implementation, feedback and feed forward synchronization, linear and non-linear control loops are performed to regulate voltage and current to make the system stable.

***Level 1*: Primary control:** This level comprises the second stage of hierarchical control structure, where mode of communication is designed, for example if we need wired or wireless bus link for control. For wired link droop control and for wireless various other control structures like 3C. In this stage the main focus is given to make system more stable and damped. The additional structure includes virtual impedance control loop as discussed before to simulate output impedance.

***Level 2*: Secondary control:** This stage ensues if the electrical values are within the required range, in addition it provides a synchronization mechanism for logically connect or disconnect the MG from utility grid. Secondary control acts as a centralized automatic generation controller, where MG voltage and frequency values are checked and restored to their nominal values. This control consist of slow control loops, a low bandwidth communication at certain points in order to measure a certain parameter in MG and send it back to each DGs. In Shafiee et al. (2014: 1020-1025) a detailed explanation of secondary control approach is explained for islanding mode of operation.

***Level 3*: Tertiary control:** This is the upper most layer in hierarchical control, which is responsible for enhancing the MG operation and also interacting with distribution network for providing active and reactive power reference for individual DG units. Tertiary state controls the power flow between microgrid and utility. This holds the responsibility of importing or exporting of energy for the microgrid (Rocabert et al. 2012: 4743).

As discussed in Guerrero et al. (2011: 158-172), AC microgrid can operate both in grid-connected and islanding mode, so the bypass switch will be responsible for reconnecting MG back to the grid. Here a bypass switch is designed to meet grid interconnection standards example IEEE 1547 and UL 1541 in US. "Now the IEEE PI1547.4 *"Draft Guide for Design, Operation, and Integration of Distributed Resource Island Systems with Electric Power systems"* is in draft form" Guerrero et al. (2011: 160) & Kroposki et al. (2009: 3). This draft covers microgrids and intentional islands that contain distributed energy with utility power systems. The draft provides a different approach for design, the operation of connection and reconnection to the grid. The transition of grid connection to islanding mode will be due to intentional or unintentional events like grid failures or grid disturbances. Hence for islanding mode, the microgrid must provide active power and reactive power and the operating voltage should be within the limits. A proper synchronization technique is be needed to match voltage, frequency and phase angle of the microgrid.

4.2 Concept analysis

In the past stand-alone and islanding microgrids are considered as separate scenarios. Present technologies made it easy to integrate both islanding and grid-connected mode into one chain. This integration is a demanding task as it includes a combination of different power electronics technologies, telecommunication and other energy storage technologies. Islanding microgrids are more sophisticated than grid-connected microgrids, as there need to be synchronization between transitions. Hence more precise level control system is needed to be implemented to overcome the issue of non-smooth transitions. Apart from these risks, other factors, which raise concerns for combining grid-connected and islanding MGs, were faulty monitoring, protective maintenance etc. Here we will discuss detailed analysis of each level inside proposed hierarchical control. Guerrero et al. (2011: 161) explain about UCTE (Union for Co-ordination of Transmission of Electricity) Continental Europe, which has defined this hierarchical control for large power systems. These MGs are high powered synchronous machines with high inertia and reactive network, but the power electronics based power systems have no-inertia and nature of networks are mostly resistive. Hence there is a good amount of differences between these two power systems, so special considerations are taken into account while designing these systems.

4.2.1 Voltage and current control loops

These are part of inner control loops, which also include power control loops. These are considered as level 0 of hierarchical control system. These controls play a crucial role in designing as we discussed in previous chapter. Their implementation decides if it's going to be implemented for grid-connection or both grid-connection and islanding mode of operation. Voltage and current control loops are present in all power converter designs (grid-feeding, grid-forming and grid-supporting) as discussed in previous chapter. These are the final stages of control in MG.

There are two types of modes inside level 0 control. They are PQ control mode or current control VSI (CCVSI) or current source inverter (CSI) and voltage control VSI (VCVSI) or

voltage source inverter (VSI). These models were explained in grid supporting type converters in chapter 3. CSI consists of inner current loop along with PLL (phase lock loop) for synchronization with the grid on the other hand voltage source inverter (VSI) consists of both current and voltage loop doing the same. VSI's are more commonly used in MGs because they can be used in both grid-connected and islanding mode and thus they don't need any external reference signal to stay synchronized. Similarly, VSI has other functionalities like ride-through capability and power-quality enhancement of distributed power systems. In VSI, the current signal is fed to the system using feed-forward path through virtual impedance method as discussed before. Talking about power quality, this factor plays a crucial role, when connected in islanding mode because of its non-linear and single-phase loads and MGs having low inertia (Bidram et al. 2012: 1964-1965).

When VSI operates only in grid-connected mode then it acts as a current source and voltage source when operating in islanding mode. Hence to operate in both the modes VSI is supposed to control the imported or exported power to the grid to stabilize the MG. Both VSI and CSI can operate together in a microgrid, for example, VSI's can connect to energy storage devices like battery, fly wheel etc., and CSI can connect to photo-voltaic (PV) and wind turbines (WT) which need more power tracking algorithms (MPPT). A simplified VSI model is shown in Figure 12 where reference voltage for the inverter is generated from grid voltage or source voltage (v_0 and i_0)

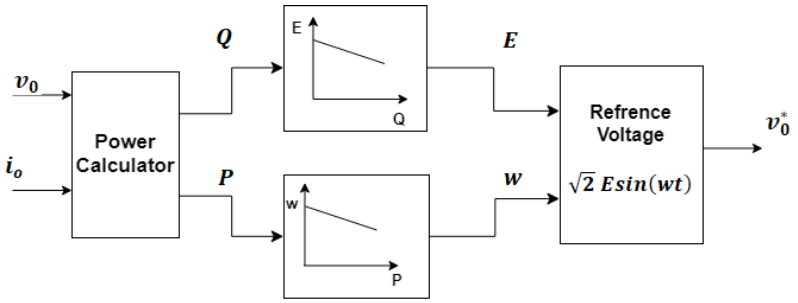

Figure 12. Reference voltage generation for voltage control loops (Bidram et al. 2012: 1964)

As we mentioned above, these VSI's can operate in parallel with each other. Hence to improve the power quality of multiple energy resources connected in parallel islanding MG in Figure 12 can be used.

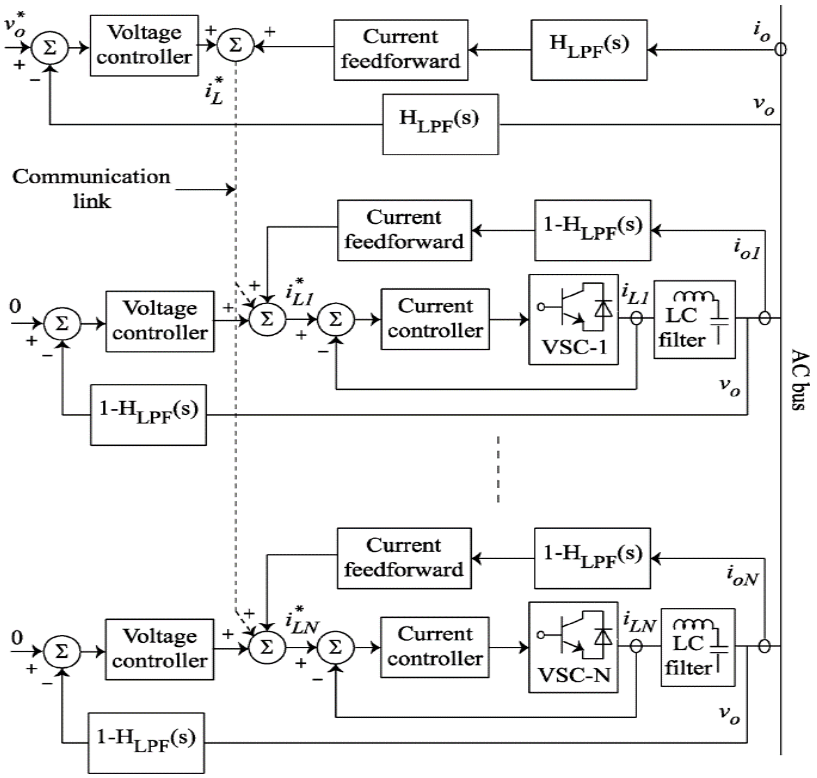

Figure 13. Zero level voltage control loop for multiple energy resources (Bidram et al. 2012: 1964)

In Figure 13 $H_{LPF}(s)$ is a low pass filter transfer function. Here we can see that the reference point for voltage control loop is produced by primary control. The current controller in the VSI produces better power quality and controls the harmonic contents of the supplied current to common AC bus. Bidram et al. (2012: 1964).

4.2.2 Primary control

Primary control is level 1 in hierarchical control system, which is responsible for frequency and voltage reference amplitude and then passes on to voltage and current control loops. In chapter 2, while discussing grid-supporting type converters we saw that those power converters are used more commonly in MG operation because of its flexibility of connecting on and off grid smoothly. In those designs, the main essence was droop control, which helps to maintain stability in a MG and also to achieve synchronization. Apart from droop control,

primary control in DER system can also be implemented using active load sharing technique as specified in Guerrero et al. (2008: 2847-2851).

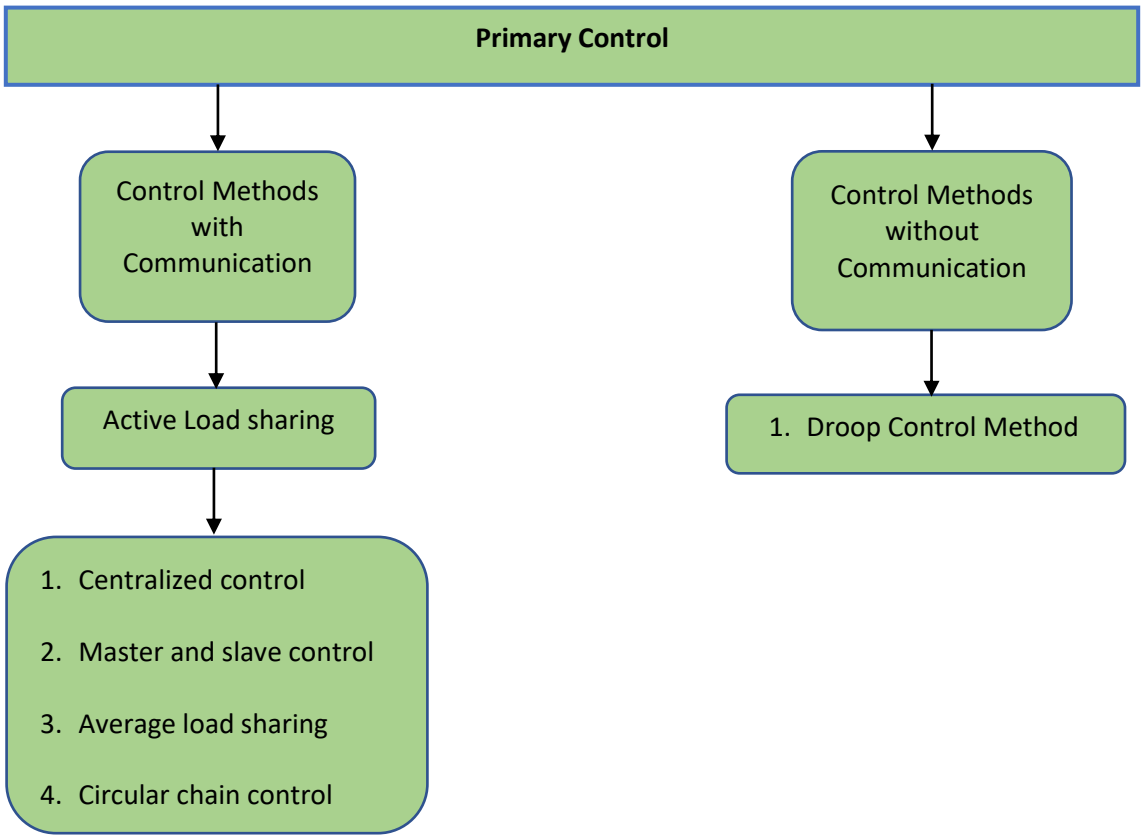

Figure 14. Primary Control structure.

As we can see from above figure, the primary control can be divided into two categories, control methods with communication and control methods without communication. Control method with communication has communication links between central controller and other units. Similarly, control without communication does not interlink with central controller, for example droop control. This type of control is more reliable and more cost effective and can be implemented in projects with longer distances (Vandoorn et al. 2013: 613-628).

4.2.2.1 Active load sharing

In active load sharing, active power and reactive power are controlled using inter-communication links. These methods receive less focus mainly because of its low redundancy and limited flexibility of UPS (Uninterrupted Power Supply) system, but still this method improves total harmonic distortion (THD) in the system. Active load sharing technique can be classified into four sections namely: centralized control, master and slave, average load sharing (ALS) and circular chain control (3C) (Guerrero et al. 2008: 2847).

A. Centralized control

This control method is also called a concentrated control, where active and reactive control is handled using a centralized controller. The centralized controller can be seen from figure 16. Here the total load current i_L can be divided with a total number of DER systems (N) to obtain current reference for each module. (Martins et al. 1995: 584-585 & Iwade et al. 2003: 482).

$$i_j^* = \frac{i_j}{N} \quad for \ j = 1 \dots \dots \dots \dots . N \tag{5}$$

The current reference is then subtracted from the current from the individual modules to produce error signal $\Delta i = i_j^* - i_j$. Then this error signal can be used to produce in-phase and quadrature components (Δi_p and Δi_q) so as to adjust phase and amplitude of output voltage reference of each UPS unit. Here the controlled parameter is current, which is common to all the parallel DERs unlike its centralized control system. In this method, it is mandatory to calculate load current i_L so that it can not be used for large-scale distribution system and along with this a central control board is necessary to control all the parallel DERs. (Guerrero et al. 2008: 2847). Figure 15 shows the centralized control for a parallel UPS system where reference current i^* is provided to all individual DER systems.

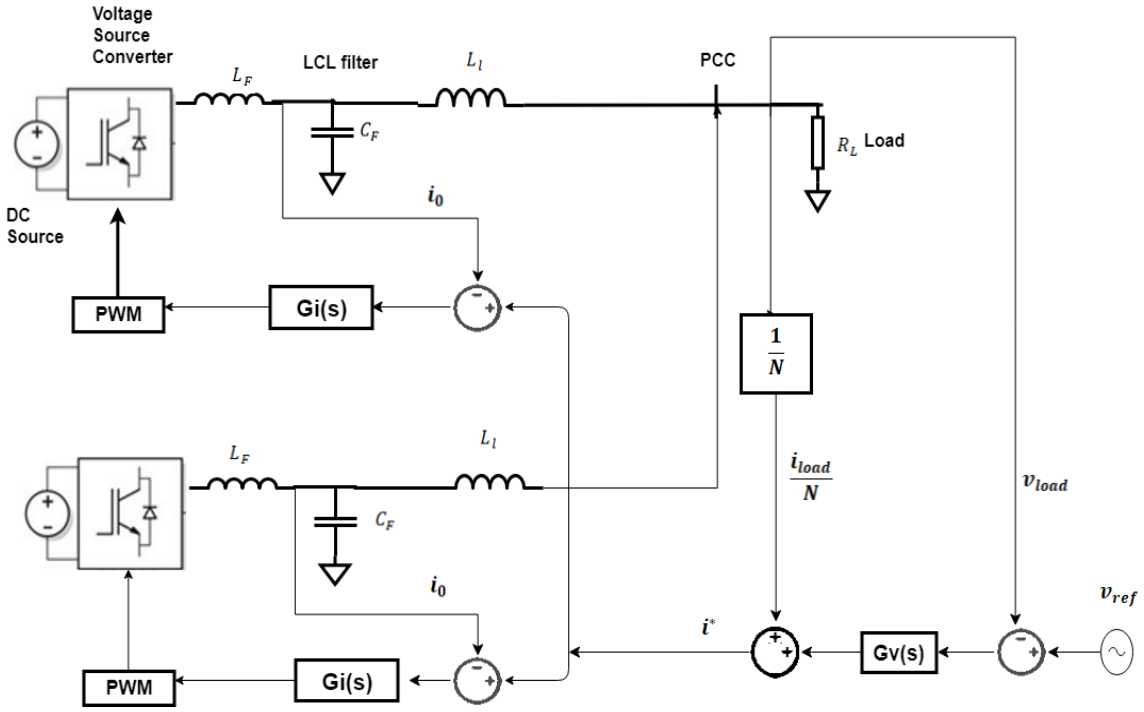

Figure 15. Centralized controller for a parallel UPS system

B. Master and slave control

In this control, the master will control the slave devices by regulating master current i_M. Master current for a MG can be written as (Guerrero et al. 2008: 2847):

$$i_S^* = i_M \qquad for \qquad S = 2 \ldots . N \tag{6}$$

Similarly, the block diagram for master and slave control can be seen in Figure 16. In this system, if master fails for some reason then another module will take the masters role and continue to perform the operation. The master can be centralized or de-centralized depending on the fixed module to generate maximum root mean square current. Depending on the type of operation, the master and slave method can be written in different variants:

- Dedicated: Here the master acts as a lone controller or to say it acts as a fixed module.
- Rotary: When master gets disconnected or fails to continue then next one is chosen.
- High crest current: Here the master can be fixed by the module, which can provide maximum root mean square (RMS) or crest current. Unitriode ICs can be implemented,

which senses the module with maximum current and then it becomes automatically the master module. (Guerrero et al. 2008: 2847-2848).

In grid-connection mode with this strategy and the central controller, the utility will act as the master, hence there is no need for any special control for grid-connection and islanding mode (Palizban & Kauhaniemi 2015: 803). In Figure 16 we can see that master control acting as a voltage source inverter whereas slave acting as current source inverter. Therefore, if master fails due to some reason then another module will take the responsibility of master and system continues.

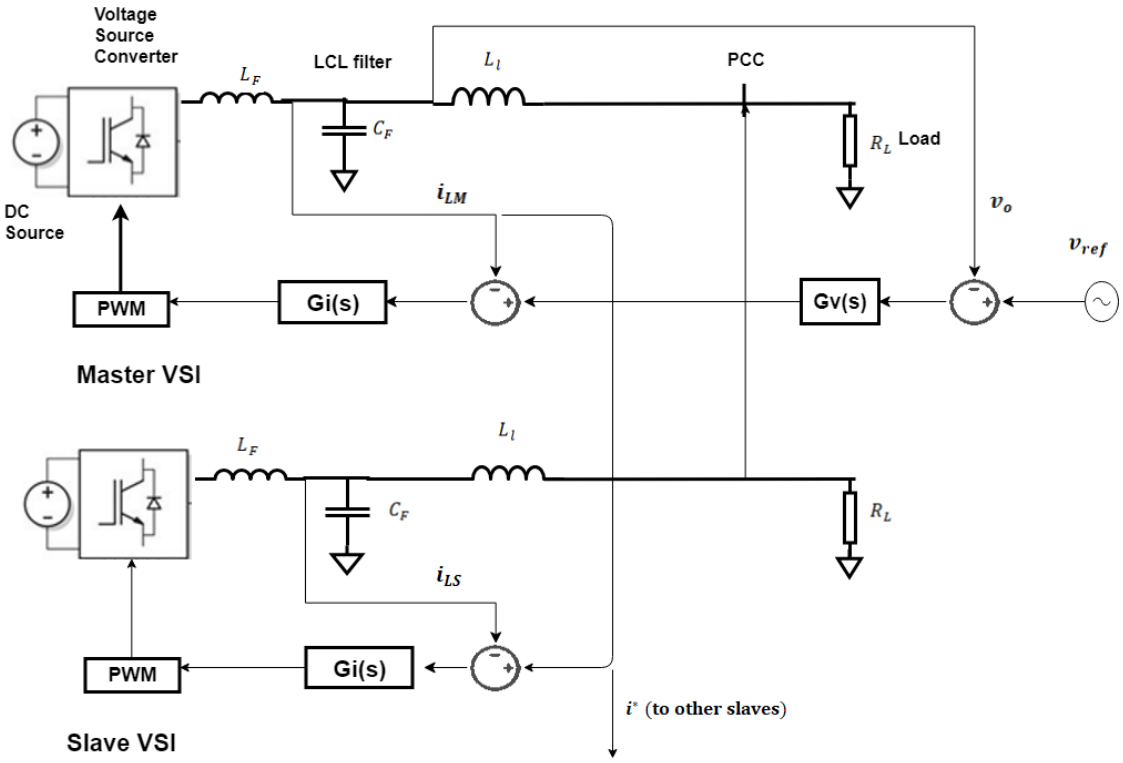

Figure 16. Block diagram of master and slave module

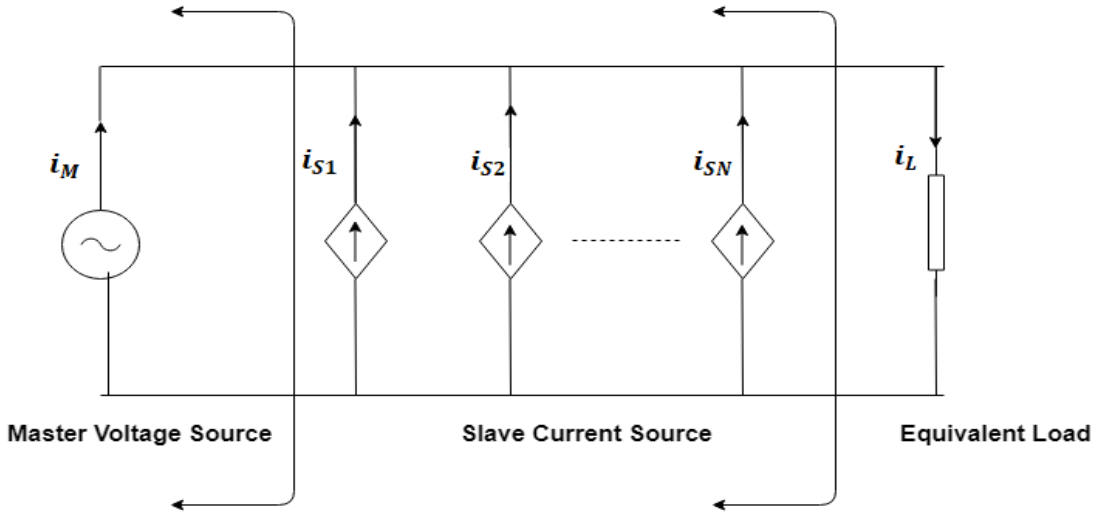

Figure 17. The equivalent circuit for parallel UPS system controlled through MS strategy (Guerrero et al. 2008: 2848)

C. Average load sharing

In this method, all modules can draw the average current from the other modules. The idea behind this method is similar to that of parallel dc/dc converter, where current sharing resistors are connected in parallel to a common information bus. The bus will give current information from all other connected modules and this is later used to average current from each module. This average current from each and every module will act as a reference to each unit. In this control, as there is no master or slave ideology present, hence the reliability of this method is much better. Current distribution control is acting as a variant for this method (Hsieh et al. 2005: 955). The reference current for each module is written as (Guerrero et al. 2008: 2848):

$$i_k^* = \frac{1}{N}\sum_{j=1}^{N} i_j \qquad for \quad k = 1,2,\ldots.N \tag{7}$$

Then these references current will pass to inner control loops like MS method discussed above. When outer current loop uses the current reference then voltage loop will have a narrow bandwidth, hence the need of compensator becomes evident. Another method is to use active power or reactive power instead of the current, as the dynamic response of current is very slow, which in turn provokes poor current sharing during transients. Hence, active power and reactive power can be used to adjust phase and amplitude of individual DER

modules instead of current. Average power sharing method is shown in Figure 18, here the average active and reactive power for each DER can be written as (Guerrero et al. 2008:2849)

$$P_k^* = \frac{1}{N}\sum_{j=1}^{N} P_j \qquad k = 1, \dots \dots \dots N \tag{8}$$

$$Q_k^* = \frac{1}{N}\sum_{j=1}^{N} Q_j \qquad k = 1 \dots \dots N \tag{9}$$

Since this method does not need any master or slave unit, so only low-bandwidth communication channel is required for active and reactive load sharing. Even with aforementioned advantages of this method, unbalances between power stages and power lines can produce large circulating harmonics between each module (Guerrero et al. 2008: 2848-2849).

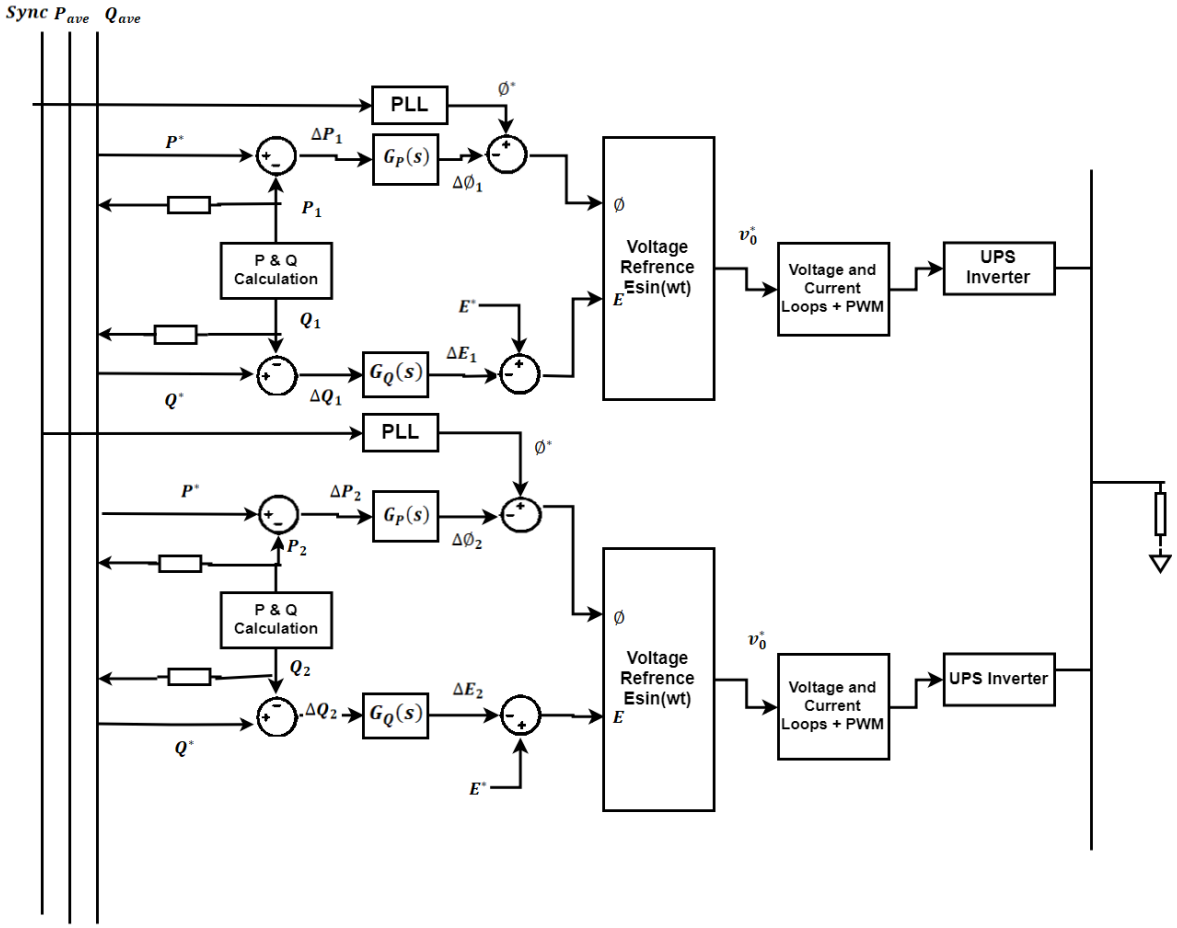

Figure 18. Average power sharing in ALS (Guerrero et al. 2008: 2850)

D. Circular chain control

In this control scheme, the current reference from each module as mentioned in previous modules is used to form a control ring (Wu et.al 2000: 273-277). Figure 19 shows block diagram of 3C model, here the current reference can be written as (Guerrero et al. 2008:2849)

$$\begin{cases} i_1^* = i_N \\ i_k^* = i_{k-1} \end{cases} \quad for\ k = 2, \dots\dots\dots N \qquad (10)$$

Current limitation control acts as a variant for current chain control method, here the load voltage is controlled by master unit while the slave units are only sharing the load current. So the current from the previous unit is taken as the reference for next DER unit, but for the master unit the reference current will be same. The connection of all control units can form a circular chain, hence any unit can act as master. Therefore, in this method any of the units can act as master or slave. (Guerrero et al. 2008: 2850-2851).

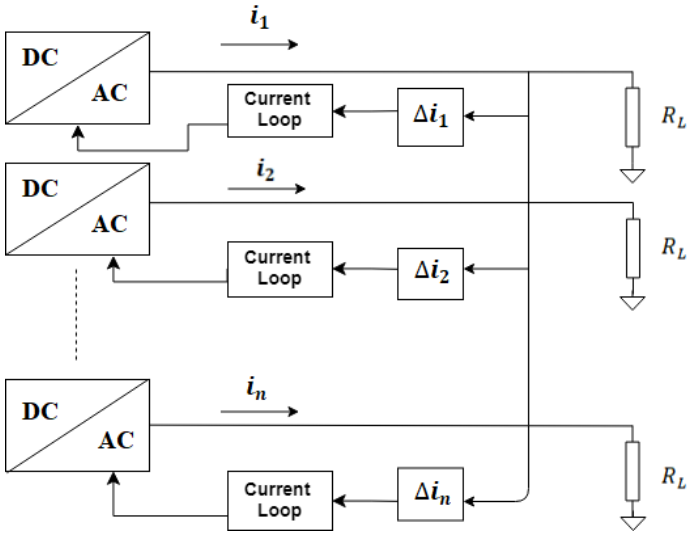

Figure 19. 3C method block diagram (Guerrero et al. 2008: 2851)

4.2.2.2 Droop control

The droop control is one of the communicationless approaches, where there is no interlinks between the different DER units and hence can be called as autonomous or independent control. Primary control copies the behavior of synchronous generators, which reduce the frequency when active power increases (Visscher & Haan 2008: 2-3). This principle, which

is implemented in primary control, is called droop control. Droop control is independent, autonomous and wireless communication based control technique. The conventional droop control method is shown in Figure 20

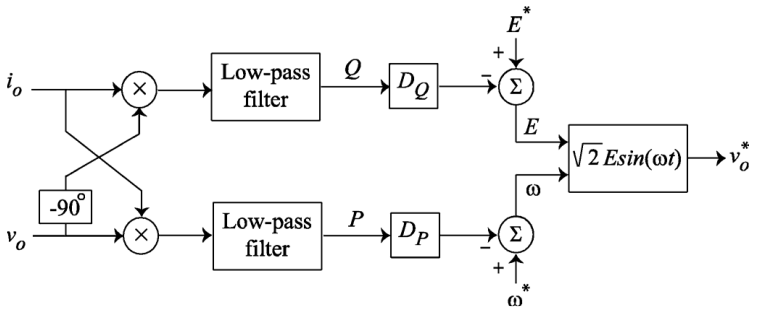

Figure 20. Conventional droop technique (Bidram et al. 2012: 1965)

Droop control is typically an active power control or frequency droop characteristic and reactive power control or voltage droop characteristic. The traditional droop method, as shown Figure 20 is implemented in grid supporting converters acting as voltage source as discussed in chapter 2.

In Bidram et al. (2012: 1965-1966), the droop control is explained from the equivalent circuit of a VSC connected to an AC bus as shown in Figure 21.

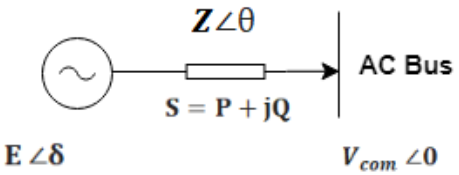

Figure 21. Simplified diagram of converter connected to the MG (Bidram et al. 2012: 1965)

If switching ripples and high frequencies are neglected then the VSC can be considered as AC source with voltage amplitude E and phase $\emptyset$. Let's assume AC bus have a phasor voltage $V_{com}\angle 0$ and output impedance and line impedance are taken as an effective line impedance $\angle\,\theta$. Hence, the apparent power can be calculated as (Bidram et al. 2012: 1965)

$$S = V_{com}I^* = \frac{V_{com}E\angle\,\theta-\emptyset}{Z} - \frac{V_{com}^2\angle\,\theta}{Z} \qquad (11)$$

From apparent power, real and reactive power can be calculated as follows (Bidram et al. 2012: 1965):

$$P = \frac{V_{com}E}{Z}\cos(\theta - \emptyset) - \frac{V_{com}^2}{Z}\cos(\theta) \quad (12)$$

$$Q = \frac{V_{com}E}{Z}\sin(\theta - \emptyset) - \frac{V_{com}^2}{Z}\sin(\theta) \quad (13)$$

Effective line impedance $Z \angle \theta$ is assumed to be purely inductive so phase angle $\theta = 90^{\circ}$, so the equation 12 and 13 can reduced to following (Bidram et al. 2012: 1965):

$$P = \frac{V_{com}E}{Z}\sin(\emptyset) \quad (14)$$

$$Q = \frac{V_{com}E}{Z}\cos(\emptyset) - \frac{V_{com}^2}{Z} \quad (15)$$

Now if the phase difference between the output of converter AC voltage and AC bus is very small then, $\cos(\emptyset) \approx 1$ and $\sin(\emptyset) = \emptyset$. Hence we can tune voltage and frequency droop characteristic to fine tune reference voltage to level 0 control loop as discussed in (Zhong & Weiss 2009: 2-5).

As droop method copies the idea of synchronous generator of decreasing angular frequency with raise in active power, so the relation between w and P is shown below (Bidram et al. 2012: 1965)

$$\omega = \omega^* - D_P P \quad (16)$$

Similarly, relation between voltage amplitude E and reactive power Q in droop method is (Bidram et al. 2012: 1965):

$$E = E^* - D_Q Q \quad (17)$$

Here E^* and ω^* are output RMS voltage and frequency of a DER during no load respectively. D_P and D_Q are droop coefficients, which can also be modeled as a proportional gain controller, whose value is fixed and can be obtained by:

$$D_P = \frac{\Delta\omega}{P_{max}} \quad (18)$$

$$D_Q = \frac{\Delta E}{2Q_{max}} \quad (19)$$

Hence these droop coefficients provide a static deviation, which then plays a very important role to keep the system synchronized and within voltage stability limits. $\Delta\omega$ and ΔE are frequency and voltage deviations and P_{max} and Q_{max} are maximum active and reactive power respectively. When MG is operated in grid-connected operation, then E and ω are

enforced by the grid. Hence, DER's active and reactive power references can be adjusted through E^* and ω^* as shown below (Lopes et al. 2006: 918).

$$P^{Ref} = \frac{\omega^* - \omega}{D_P} \tag{20}$$

$$Q^{Ref} = \frac{E^* - E}{D_Q} \tag{21}$$

The dynamic response of the conventional primary control on simplified systems in Figure 22 can be seen by linearizing equations (14), (15), (16) and (17). As we normally linearize an equation to reduce the complexity, likewise frequency and power droop equations on (14) and (15) can also be linearized as follows (Bidram et al. 2012: 1965):

$$\Delta P = G\Delta \tag{22}$$

$$\Delta\omega = \Delta\omega^* - D_P\Delta P \tag{23}$$

Here G and $\Delta\delta$ can be elaborated as (Bidram et al. 2012: 1966):

$$G = \frac{V_{com0}E_0}{Z}cos\delta_0 \quad and \quad \Delta\delta = \int \Delta\omega dt \tag{24}$$

From the above equation, we can make a small signal model for active power control, which is shown in Figure 22.

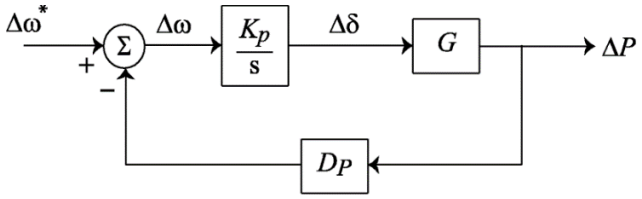

Figure 22. Small signal model of conventional active power model
(Bidram et al. 2012: 1966).

Therefore, the transfer function of the small-signal active power model can be written as (Bidram et al. 2012: 1966):

$$\Delta P(s) = \frac{G}{s + D_P G}\Delta\omega^*(s) \tag{25}$$

As we see in droop control equation D_P effects the angular frequency of DER, hence there should be some trade-off between time constant of the control system and frequency regulation's (Sao et al. 2005: 1009-1011). Even though conventional droop technique is non-

communicational type control, which makes it more reliable, still there are some pit-falls in this control as, explained in (Bidram et al. 2012: 1965-1966).

- As there is one control variable available in each characteristic then it's impossible to control multiple objectives, so trade-offs are expected like the one explained above.
- The conventional droop control is designed with high inductive impedance between VSC and AC bus, so in low voltage MGs or purely resistive MGs, the droop control will not perform well.
- Unlike frequency, voltage is not a global quantity in microgrid, so reactive droop power control effects badly.
- In case of nonlinear loads, these conventional droop methods are unable to recognize load current harmonics from circulating current.

The potential drawbacks as mentioned above have following solutions and are explained in Bidram et al. (2012: 1966-1972):

A. Adjustable load sharing methods

In this technique, the time constant of proposed active and reactive power controllers can be adjusted without causing any impact on DER voltage and frequency (Sao et al. 2005: 1013). Active power controller uses traditional droop controller as explained above, but the phase angle can me showed as (Bidram et al. 2012: 1966):

$$\delta = K_P \int \omega \, dt \tag{26}$$

Here K_P is integral gain. The small-scale model of the adjustable load sharing method is shown below:

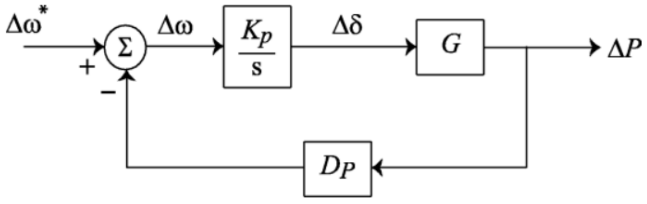

Figure 23. The small-scale model of the adjustable active power control (Sao et al. 2005: 1013).

The transfer function of the small scale model can be written as (Bidram et al. 2012: 1966):

$$\Delta P(s) = \frac{K_P G}{s + K_P D_P G} \Delta\omega^*(s) \quad (27)$$

The eigen values of negative feedback linearized system is (Bidram et al. 2012: 1966):

$$\gamma = -K_P D_P G \quad (28)$$

Here gain G is discussed above in equation (24), K_P is a proportional constant and D_P is droop coefficient, hence closed loop time constant can be controlled by varying proportional gain (K_P). Since D_P will not change with changes in K_P so the frequency droop for active power control will not have any notable changes due to time constant adjustments. Similarly, V_{com0}, E_0 and δ_0 from equation (18) can be represented using small scale signal control model for reactive power control in droop equation can be seen as:

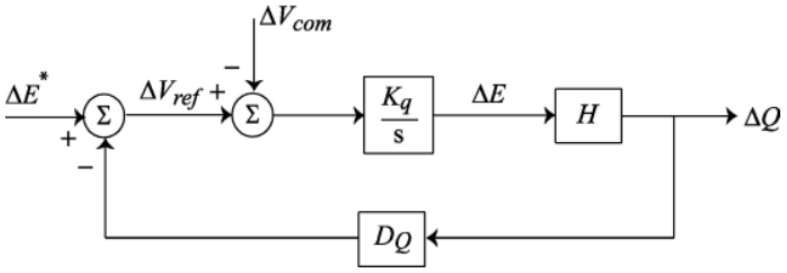

Figure 24. The small-scale signal model for reactive power control (Sao et al. 2005: 1014).

Here ΔQ can be modeled as (Bidram et al. 2012: 1966):

$$\Delta Q(s) = \frac{H}{1 + D_Q H} \Delta E^*(s) \quad (29)$$

Where,

$$H = \frac{V_{com0} cos\delta_0}{Z} \quad (30)$$

ΔQ is a linear function of reference signal $\Delta E^*$and H is a function of δ_0, Z (line impedance) and operating voltage (V_{com0}), which shows how traditional reactive power can be controlled using operating parameters of microgrid. In adjustable load sharing control method, the integral control can be used to regulate common bus voltage as shown in Figure 25 where,

$$E = K_q \int (V_{ref} - V_{com}) dt \quad (31)$$

and K_q is integral gain and reference voltage (V_{ref}) is (Bidram et al. 2012: 1966):

$$V_{ref} = E^* - D_Q Q \tag{32}$$

During steady state both V_{ref} and V_{com0} are equal making the reference signal ΔE^* to pass through the integrator. Similarly, the steady state reactive power can be calculated as (Bidram et al. 2012: 1967):

$$Q = \frac{E^* - V_{com}}{D_Q} \tag{33}$$

Hence, as we see from the above equations, the microgrid parameters will no longer affect the reactive power control and voltage compensation across the bus is assured. The closed loop transfer function of small signal model for reactive power control can be written as (Bidram et al. 2012: 1966):

$$\Delta Q(s) = \frac{K_q H}{s + K_q D_Q H} \Delta E^*(s) - \frac{K_q H}{s + K_q D_Q H} \Delta V_{com(s)} \tag{34}$$

Here we can see that dynamic response of reactive power control as proposed by Bidram et al. (2012: 1966) can be adjusted directly by adjusting K_q without changing D_Q, hence the voltage variation in reactive droop control (17) will no longer be affected.

B. VPD/FQB droop method

Voltage-active power droop (VPD) and frequency-reactive boost droop (FQB) control method can be implemented in low voltage MGs where the line impedance is most probably resistive. Therefore, resistive effective line impedance can be assumed, which in turn makes phase angle 0 i.e. $\theta = 0^{\circ}$ and $\sin\delta \approx \delta$. Considering the above assumptions, the active and reactive power from equations 14 and 15 can be written as (Bidram et al. 2012: 1966):

$$\begin{cases} P \approx \frac{V_{com}E - V_{com}^2}{Z} \\ Q \approx \frac{-V_{com}E\,\delta}{Z} \end{cases} \tag{35}$$

From VPD/FQB characteristics, the voltage and frequency relations as mentioned below can also be considered where E^* and ω^* are output voltage and angular frequency and D_Q and D_P are droop and boost coefficients of DER system under no-load conditions.

$$\begin{cases} E = E^* - D_P E \\ \omega = \omega^* + D_Q \omega \end{cases} \tag{36}$$

Droop and boost characteristics of VPD/FQB can be seen in Figure 25. Hence, this way of controlling powers gives improved performance for low-voltage resistive MGs. However, the performance largely depends on system parameters. In any case, it unequivocally relies upon system parameters limiting its application. In addition to that, this technique will fail in case of any load fluctuations for example introduction of non-linear loads and hence cannot guarantee correct voltage regulation.

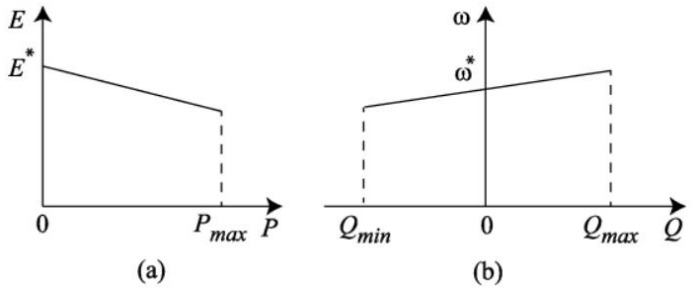

Figure 25. Droop /Boost characteristic of low-voltage microgrid. (a) voltage-active droop characteristic (b) frequency-reactive power boost characteristics (Bidram et al. 2012: 1967).

Just like in adjustable load sharing method, in VPD/FQB method the time constant can be modified without causing fluctuations in voltage and frequency (Sao et al. 2005: 1099-1011). In the VPD control mode, the common bus voltage V_{comm}, is controlled to follow a reference voltage V_{ref} (Bidram et al. 2012: 1967).

$$E = \left(K_{P1} + \frac{K_{I1}}{s}\right)\left(V_{ref} - V_{com}\right) \tag{37}$$

Where,

$$V_{ref} = E^* - D_P P \tag{38}$$

K_{P1} and K_{I1} are proportional and integral constant of active power controller respectively. Similarly, in FQB control mode, δ is determined by another PI controller as shown below (Bidram et al. 2012: 1967):

$$\delta = \left(K_{P2} + \frac{K_{I2}}{s}\right)\omega \tag{39}$$

Here, K_{P2} and K_{I2} are proportional and integral gains of reactive power. Hence as explained above, in Bidram et al. (2012: 1967) the time constants in VPD/FQB of a closed loop controller are adjusted directly by proportional and integral gains respectively.

C. Virtual frame transformation method

In this virtual frame transformation method the orthogonal linear transformation matrixT_{PQ}, is used to transfer active/reactive power reference, where powers are independent of effective impedance (Vasquez et al. 2009: 4089-4090). T_{PQ} can be shown as (Bidram et al. 2012: 1967):

$$\begin{bmatrix} P' \\ Q' \end{bmatrix} = T_{PQ} \begin{bmatrix} P \\ Q \end{bmatrix} = \begin{bmatrix} sin\theta & -cos\theta \\ cos\theta & sin\theta \end{bmatrix} \begin{bmatrix} P \\ Q \end{bmatrix} \quad (40)$$

After frame transformation the P' and Q' are used in droop equations as shown in equation (17). Similarly, virtual frequency/voltage frame transformation is shown here (Bidram et al. 2012: 1967):

$$\begin{bmatrix} \omega' \\ E' \end{bmatrix} = T_{\omega E} \begin{bmatrix} \omega \\ E \end{bmatrix} = \begin{bmatrix} sin\theta & cos\theta \\ -cos\theta & sin\theta \end{bmatrix} \begin{bmatrix} \omega \\ E \end{bmatrix} \quad (41)$$

Voltage amplitude E and angular frequency (ω) are calculated using droop equations as discussed before. These frames' transformed values of E' and ω' are used as reference values for controlling VSC as discussed in Li et al. 2009: 2491-2494. The block diagram for virtual frame transformation method is shown below:

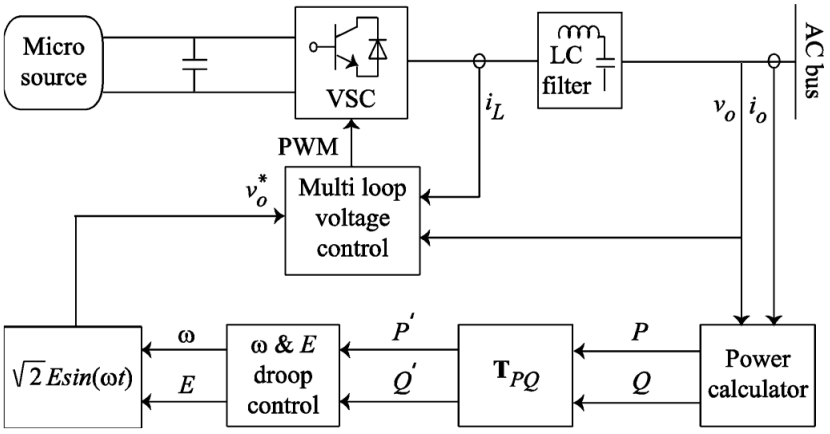

Figure 26. Block diagram for virtual power frame transformation (Bidram et al. 2012: 1968).

In this diagram, we can see that virtual frame transformation decouples active power and reactive power control. But this type of control method has an issue, since there are no precautions done for taking care for non-linear loads hence this method doesn't guarantee a

regulated voltage and thus comprises some trade-offs between control loop time constant and amplitude and frequency regulations.

D. Virtual output impedance

Traditional P/f and Q/E control is sufficient for better performance of microgrids even when load conditions are unbalanced. However, when it comes to efficiency, then we need more sophisticated kind of control. Virtual impedance control can be modified to adjust the output impedance of VSCs (Guerrero et al. 2011: 161-162).

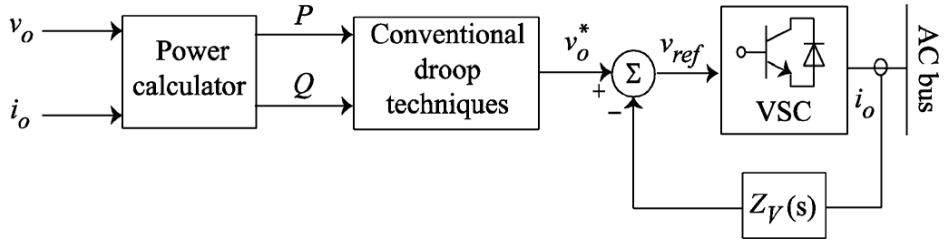

Figure 27. Virtual output impedance (Bidram et al. 2012: 1968).

The virtual impedance affect can be seen by the following equation, where the impedance is multiplied with grid current and then subtracted with reference voltage to generate voltage reference for the power converter.

$$V_{ref} = V_{Ref}^* - Z_v(s) * i \tag{42}$$

Here $Z_v(s)$ is virtual output impedance, which can be either inductive or resistive. In case if $Z_v(s) = sL_v$ then output reference voltage of voltage source converter is drooped proportional to its derivative of its output current. In case of non-linear loads, the harmonic currents can be properly shared by modifying the above equation (Bidram et al. 2012: 1968):

$$V_{ref} = V_{Ref}^* - s\sum L_{Vh} i_h \tag{43}$$

Here, i_h is h_{ih} current harmonic and L_{Vh} is inductance value corresponds to the current harmonic needed to set to effectively share current harmonics (Guerrero et al. 2009: 729). Since we know the non-linear loads can cause high total harmonic distortion in output voltages, thus to mitigate this issue a high pass filter is implemented instead in equation (43) as shown below (Bidram et al. 2012: 1968):

$$V_{ref} = V_{Ref}^{*} - L_V \frac{s}{s+\omega_c} i_o \quad (44)$$

Where ω_c is cutoff frequency of high pass filter as shown in (Guerrero et al. 2005: 1130-1131). If Z_V is properly adjusted, then occurrence of current spikes can be prevented when DER connects to the grid at first. So the easy initial connection can be shown in time-variant virtual output impedance as (Bidram et al. 2012: 1968):

$$Z_V(t) = Z_f - \left(Z_f - Z_i\right)e^{-\frac{t}{T}} \quad (45)$$

Here Z_i and Z_f are initial and final value of virtual output impedance and T is the time constant. The virtual output impedance method eases the dependencies of droop technique on system parameters. This method has such advantages as this can be used during non-linear loads, but it comes with a disadvantage of prone voltage and frequency fluctuations while adjusting closed loop time constants, as it might cause undesired deviations in DER voltage/frequency.

E. Adaptive voltage droop control

Bidram& Davoudi 2012:1968 explains that in this method, two terms are added to the conventional reactive power control as shown in droop equation (16) and (17). In here additional terms are considered to adjust voltage drop across the transmission line that delivers power DER to the loads. A typical two-way DER system is shown in Figure 28 below, where the voltage at first and second buses are (Bidram et al. 2012: 1968):

$$V_i\angle\alpha_i = E_i\angle\delta_i - (r_i + jx_i)(I_i\angle - \theta_i) \quad i = 1,2 \quad (46)$$

where $I_i\angle - \theta_i$ is the output current of i_{th} DER system.

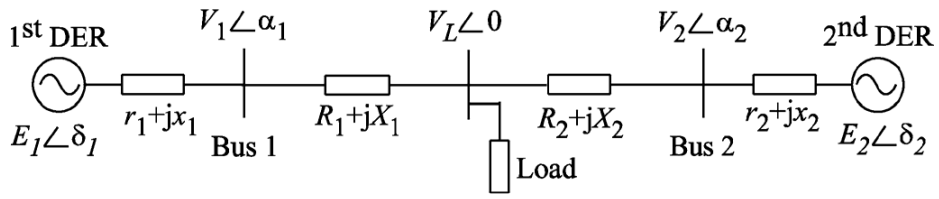

Figure 28. Two DER system (Bidram et al. 2012: 1969).

Now after comparing both droop equation and equation (46), the voltage from DER can be written as (Bidram et al. 2012: 1969):

$$V_i = E_i^* - D_{Qi}Q_i - r_i I_i cos\gamma_i - x_i I_i sin\gamma_i \quad (47)$$

where $\gamma_i = \alpha_i + \theta_i$. Similarly, the above equation can be also written in terms of active and reactive power as (Bidram et al. 2012: 1969):

$$V_i = E_i^* - D_{Qi}Q_i - \frac{r_i P_i}{E_i^*} - \frac{x_i Q_i}{E_i^*} \quad (48)$$

Here the terms $\frac{r_i P_i}{E_i^*}$ and $\frac{x_i Q_i}{E_i^*}$ represent voltage drop on internal impedance $r_i + jx_i$. These terms can be arranged in following manner to incorporate with internal impedance.

$$E_i = E_i^* + \left(\frac{r_i P_i}{E_i^*} + \frac{x_i Q_i}{E_i^*}\right) - D_{Qi}Q_i \quad (49)$$

From the above equations (Bidram et al. 2012: 1969), we can see that reactive power control improves the voltage regulation, but it still depends on active power. This issue can be resolved by adding voltage droop coefficients as a function of active and reactive powers as mentioned in Rokrok & Golshan 2010: 563.

$$\begin{cases} E_i = E_i^* + \left(\frac{r_i P_i}{E_i^*} + \frac{x_i Q_i}{E_i^*}\right) - D_i(P_i, Q_i)Q_i \\ D_i = D_{Qi} + m_{Qi}Q_i^2 + m_{Pi}P_i^2 \end{cases} \quad (50)$$

Here, D_{Qi}, m_{Qi} and m_{Pi} in equation (50) (Bidram et al. 2012: 1969) are voltage droop coefficients as discussed above and terms $m_{Qi}Q_i^2$ and $m_{Pi}P_i^2$ remove the impacts of active power control and MG parameters in reactive power control. From the equation, we can see that the higher order terms improve reactive power sharing under heavy load conditions. Adaptive voltage droop method still have some disadvantages, such as the method not being fully functional under non-linear loads. Similarly, just like adjustable load sharing method, varying time constants in this control method may lead to fluctuations in DER voltage and frequency.

F. Signal injection method

As the name suggests each DER injects a small amount of AC signal to the MG. Here frequency control signal ω_q can be controlled by reactive power Q of the corresponding

DER. ω_{q0} is nominal angular frequency of injected voltage signal and D_Q is the boost coefficient (Bidram et al. 2012: 1969).

$$\omega_q = \omega_{q0} + D_Q Q \tag{51}$$

Similarly, active power is sent through small injection method and calculated and output RMS value is calculated. The RMS output E can be written as (Bidram et al. 2012: 1969):

$$E = E^* - D_P P_q \tag{52}$$

where E^* is RMS value of DER under no-load conditions and D_P is droop coefficient, so this process is continued until all the power converters produce same frequency for the controlled signal (Bidram et al. 2012: 1969). If signal injection method is implied on two or multiple DER system as mentioned in Figure 29, then angular frequencies of both DER system can be shown as (Bidram et al. 2012: 1969):

$$\begin{cases} \omega_{q1} = \omega_{q0} + D_Q Q_1 \\ \omega_{q2} = \omega_{q0} + D_Q Q_2 \end{cases} \tag{53}$$

If $Q_1 > Q_2$ then,

$$\Delta\omega = \omega_{q1} - \omega_{q2} = D_Q(Q_1 - Q_2) = D_Q \Delta Q \tag{54}$$

And the phase difference between two voltage signals can be obtained as (Bidram et al. 2012: 1969):

$$\delta = \int \Delta\omega dt = D_Q \Delta Q t \tag{55}$$

As we see, there is some phase shift between power flowing from one DER to another. So, if we assume inductive impedance for a DER system, then actual power flow between one DER to another can be written as (Bidram et al. 2012: 1969):

$$p_{q1} = \frac{V_{q1} V_{q2}}{x_1 + x_2 + X_1 + X_2} sin\delta \tag{56}$$

Here p_{q1} is power flow from DER1 to DER2 and x_1, x_2, X_1 and X_2 are reactance of both DERs with phase shift δ. Hence the transmitted power from DER 2 to DER1 will be in reverse direction so the polarity of active power also reverses.

$$p_{q2} = -p_{q1} \tag{57}$$

And DER voltages can be written as (Bidram et al. 2012: 1969):

$$\begin{cases} E_1 = E^* - D_P p_{q1} \\ E_{12} = E^* - D_P p_{q2} \end{cases} \quad (58)$$

Herein, it is assumed that D_P is same for both DERs, so the difference between two DERs from equation (57) and (58) can be specified as (Bidram et al. 2012: 1969):

$$\Delta E = E_1 - E_2 = 2D_P p_{q1} \quad (59)$$

When the load is non-linear, parallel DERs can be controlled to supply current harmonics by proportionally adjusting the voltage loop bandwidth (Tuladhar et al. 2000: 324). This is because frequency of the injected voltage signals is droop based on distortion power (D),

$$\begin{cases} \omega_d = \omega_{d0} - mD \\ D = \sqrt{S^2 - P^2 - Q^2} \end{cases} \quad (60)$$

Where, ω_{d0} is nominal angular frequency of the injected voltage signal, m is droop coefficient and S is apparent power of DER system (Bidram et al. 2012: 1970). A similar procedure like (43)–(46) can be implemented to calculate power transmitted by injected signal, p_d, hence the bandwidth of the VSC can be written as (Bidram et al. 2012: 1970):

$$BW = BW_0 - D_{bw} p_d \quad (61)$$

where BW is bandwidth of VSC, BW_0 is the nominal bandwidth of the voltage loop and D_{bw} is droop coefficient. Block diagram of signal injection method is shown in Figure 29 as explained in Tuladhar et al. (2000: 323).

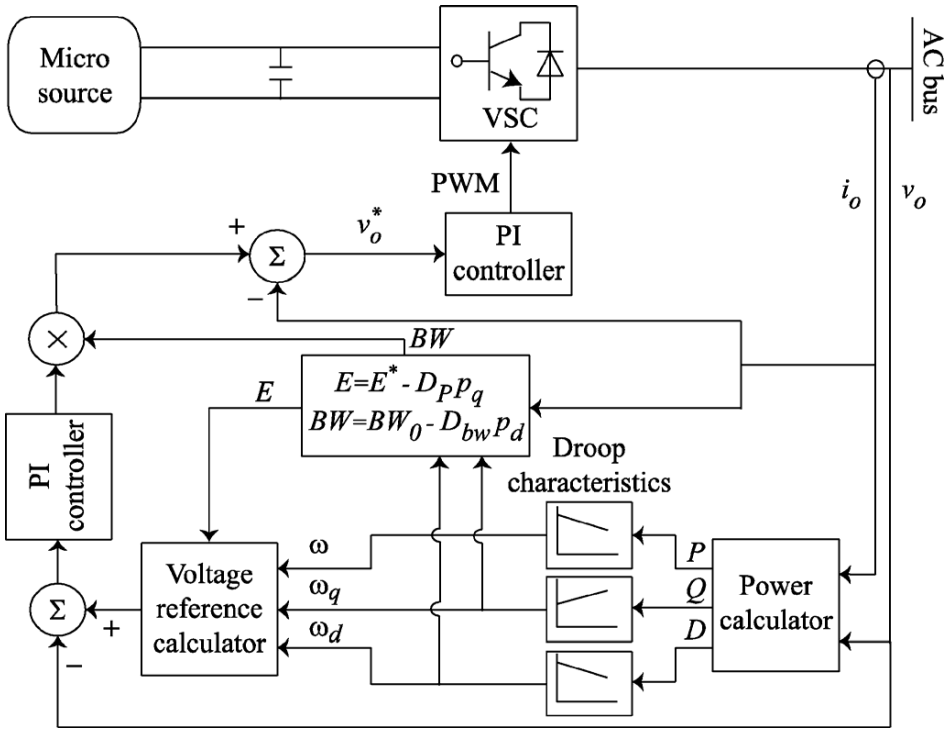

Figure 29. Signal injection method updated block diagram (Bidram et al. 2012: 1970).

As mentioned above, signal injection method is best suited for reactive power control and is not sensitive to line impedances hence it works well with linear and non-linear loads.

G. Nonlinear load sharing

Solution for the challenges, during the presence of non-linear load in droop control is being discussed in Bidram et al. (2012: 1970). In first solution the DERs equally share the linear and non-linear loads. Hence, for this, each load harmonic load current I_h is sensed to measure the corresponding voltage harmonic drop in the output terminals of DERs. Voltage harmonics are compensated by adding a phase shift of 90° for each current harmonics to the DER voltage reference. The real and imaginary parts of the harmonic voltage can be presented as (Bidram et al. 2012: 1970):

$$\begin{cases} Re(V_h) = -k_h Im(I_h) \\ Im(V_h) = k_h Re(I_h) \end{cases} \quad (62)$$

Here, k_h is droop coefficient for h^{th} harmonic, therefore the output voltage of total harmonic distortion is significantly improved. In another one the traditional droop method is altered to compensate the harmonics of DER output voltage. In Figure 30, the harmonic cancellation technique is explained.

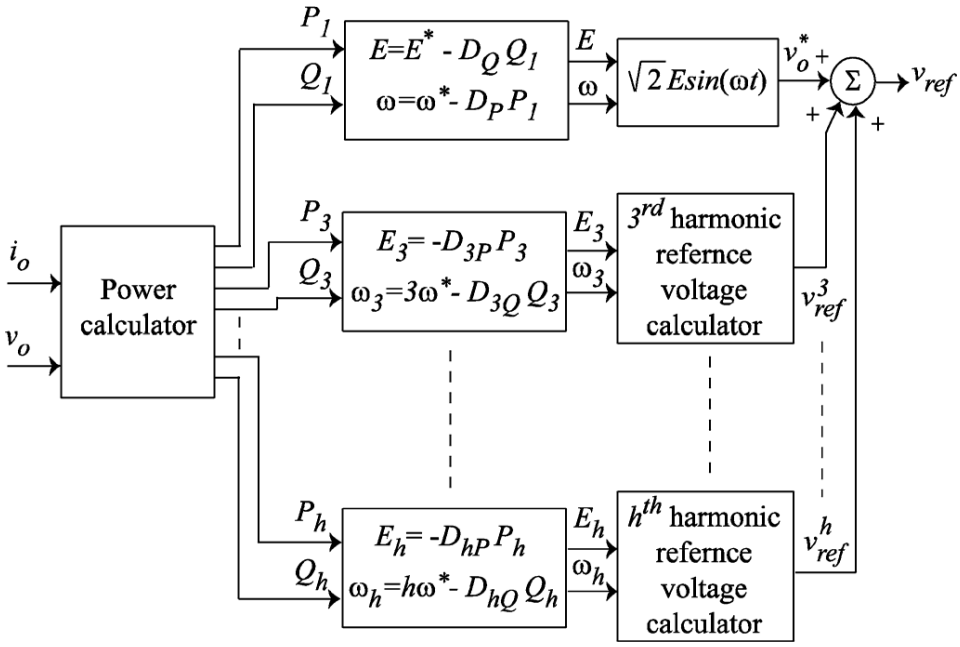

Figure 30. Control block diagram for harmonic cancellation technique (Bidram et al. 2012: 1971).

Here the DER's output voltage and current is used to calculate fundamental term and harmonic components of both active and reactive power, where P_h and Q_h are harmonic powers respectively. Here h is harmonic component and has odd values because distorted voltage and current normally have odd numbers and are never even. From the block diagram we can see that $P_1$and Q_1 are fed to droop control to generate reference voltage v_{ref} from fundamental voltage term v_0^*. To cancel the effect of voltage harmonics, set of droop characteristics are placed for individual harmonics. An additional term is characterized by each droop characteristic to VSC output reference voltage v_{ref}, to cancel the corresponding voltage harmonics. In Figure 31 $E_h\angle\theta_h$ is voltage representation in phasor format, and $E_h\angle\theta_h$ is the VSC output impedance associate with h^{th} current harmonic. The active and

reactive powers delivered to the harmonics current source are shown below (Bidram et al. 2012: 1970):

$$\begin{cases} P_h = E_h I_h cos\delta_h - Z_h I_h^2 cos\theta_h \\ Q_h = E_h I_h sin\delta_h - Z_h I_h^2 sin\theta_h \end{cases} \quad (63)$$

where δ_h is very small, which makes $sin\delta_h \approx \delta_h$. P_h and Q_h are harmonic components and are proportional to δ_h and E_h respectively. The droop characteristic equation, which is used to eliminate h^{th} harmonic output voltage of a DER system, is shown below (Bidram et al. 2012: 1970).

$$\begin{cases} \omega_h = h\omega^* - D_{hQ} Q_h \\ E_h = -D_{hP} P_h \end{cases} \qquad h \neq 1 \quad (64)$$

here, ω^* is fundamental frequency of MG, D_{hQ} and D_{hP} are droop coefficient.

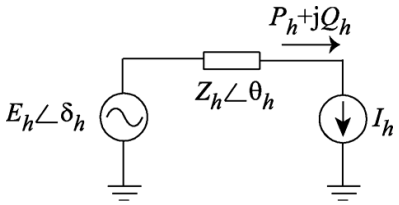

Figure 31. h^{th} harmonic equivalent circuit of a DER (Bidram et al. 2012: 1971).

Hence, from Figure 31 we can conclude that the harmonic reference voltage v_{ref}^h is used for eliminating h^{th} voltage harmonics, which can be formed by individual voltage harmonic E_h and the phase angle generated from the integration of ω_h.

4.2.3. Secondary control

The primary control mechanism as discussed earlier still has issues regarding voltage and frequency deviations. Even though use of battery or flywheel will overcome this fluctuation, but there is an advanced level control called secondary control, which can mitigate this issue. Secondary control is conceived to compensate voltage and frequency deviations produced by virtual impedances at primary control of MG. This control works such a way that it maintains frequency and voltage deviations towards zero or within prescribed limits. But this control has much slower dynamic response than primary control (Palizban et al. 2015: 808).

Secondary control can be divided into two categories, centralized and decentralized control. Detailed approach on both centralized and decentralized control is discussed by Shafiee et al. (2014: 1020-1025). The structure of secondary control can be seen in Figure 32.

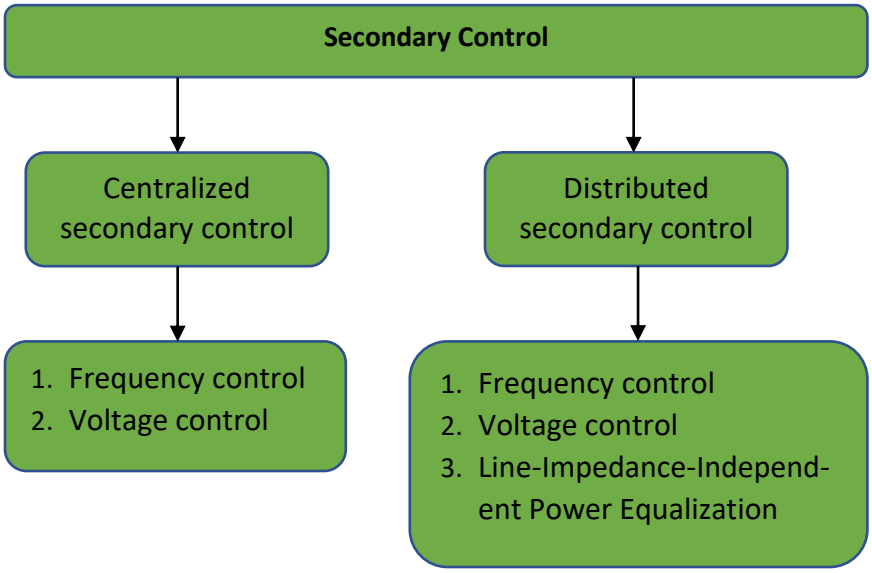

Figure 32. Secondary control structure in a microgrid

4.2.3.1 Centralized secondary control of a microgrid

As primary control mostly do not have intercommunication with different distributed systems so secondary control is used for controlling MG globally. A traditional centralized secondary control for a microgrid is shown in Figure 33.

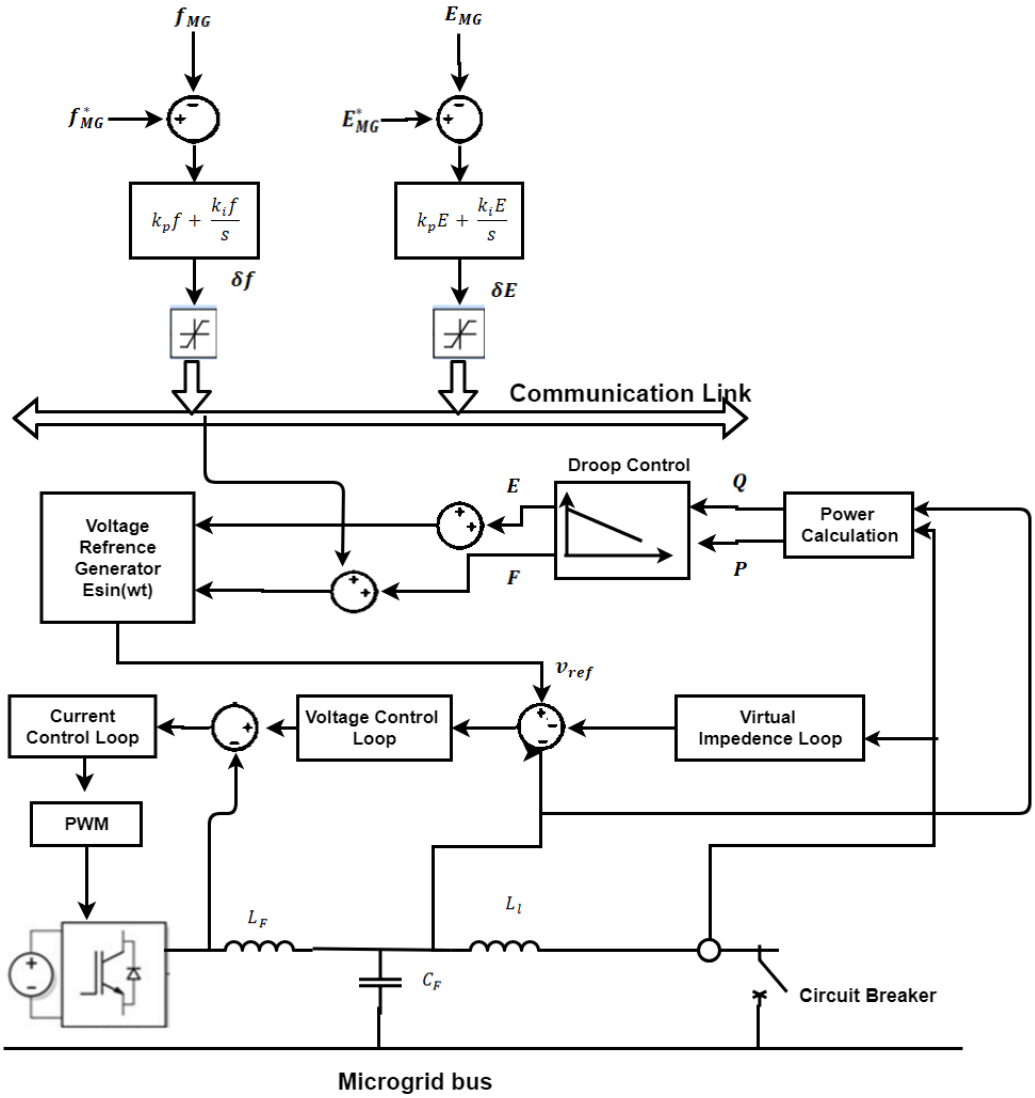

Figure 33. The centralized way of Secondary control in a MG Shafiee et al. (2014: 1022).

In this figure the DGs are different electrical sources and each DG has its own primary control using mostly droop-based mechanism. The remote sensing will send the utility parameters to the secondary control and the primary control will communicate with secondary control using a low bandwidth communication channel. Hence, the variables, which sent to these control, will be optimized after controlling process, then these are sent to primary control of DG units using same communication channel. Even though the secondary control is bit slower in operation due to its dynamic response, but passing values to the primary control compensates

it as mode of communication is completely unidirectional. But this comes with a drawback, as it's centralized control, so in case if there is failure of secondary control, then all units will get affected. The centralized control can be divided in to two:

A. Frequency control

Secondary control system for large power systems depends on frequency restoration as these generator-dominated grids highly rely on active power. Hence this factor can be used as an advantage as frequency is a control variable, which can give information about consumption/generation balance of a grid. Nowadays this frequency control for centralized system has PI control, which has slow response that restores the frequency of the grid, when the error is higher than a certain value for example (greater than +/- 50 MHz in Northern Europe). The frequency restore compensator can be written as follows (Shafiee et al. 2014: 1020):

$$\delta f = K_{pf}(f_{MG}^{*} - f_{MG}) + k_{if}\int(f_{MG}^{*} - f_{MG})\,dt \quad (65)$$

Here K_{pf} and k_{if} are secondary control parameters of a PI compensator. The frequency levels in MG (f_{MG}) are measured and compared with its reference frequency f_{MG}^{*} and then the resultant error after processing sent through PI controller, will be passed through DG units in order to restore the frequency of MG.

B. Voltage control

Similar to frequency control, voltage can be controlled using same procedure (Guerrero et al. 2011: 164). When an output of MG voltage is passed through a PI compensator along with the reference voltage, then the error signal will pass through dead band and send voltage information through a low-bandwidth communication channel. So this voltage control can be implemented similar to frequency control in a microgrid central controller. Similar to frequency, the voltage restoration can be written as (Shafiee et al. 2014: 1020):

$$\delta E = k_{PE}(E_{MG}^{*} - E_{MG}) + k_{iE}\int(E_{MG}^{*} - E_{MG})dt \quad (66)$$

Here k_{PE} and k_{iE} are PI controller parameters for voltage secondary control. The error signal δE is then sent to primary control of all DG units in order to remove the steady state errors caused by droop control. Shafiee et al. (2014: 1023) says, this approach can be implemented to resistive microgrids by using $P - V$ droops in the primary control and restoring voltage of

MG by sending voltage information to adjust voltage references as discussed before. Hence voltage and frequency controllers can be used in any R/X conditions under Park transformation in primary control. In below figure a detailed secondary control using centralized system is explained. As we see the frequency and voltage levels are measured at the grid and then compared with their references, then the resultant error signal after processing from these compensators is sent to primary control of all DG systems simultaneously.

4.2.3.2 Distributed secondary control of a microgrid

The main problem for implementing centralized MG controller is that, if there is a failure occurring during processing in secondary level then all DGs will get affected. Therefore, in order to avoid the issue due to centralized control, a decentralized way of secondary control is proposed by Shafiee et al. (2014: 1019). Here the initial ideology behind secondary control is to have a primary and secondary control in the same block as shown in Figure 34.

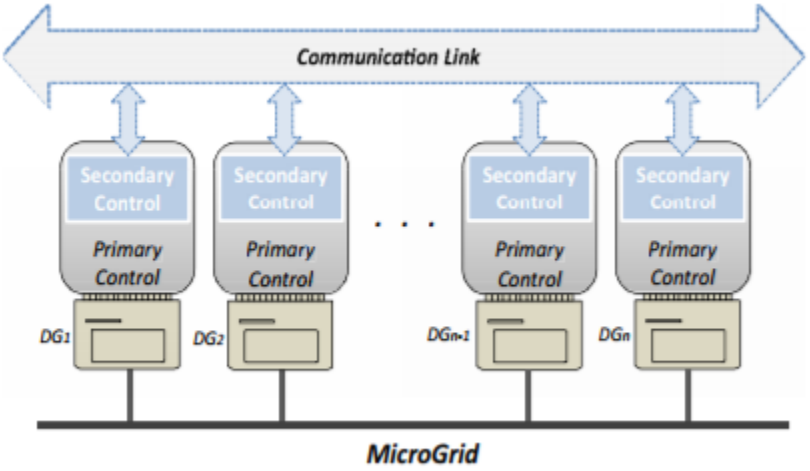

Figure 34. Networked control system in a microgrid Shafiee et al. (2014: 1022).

In above figure, the primary and secondary control are placed onto each other next to DG system. Primary control is closer to DG, which act as first level of control and then secondary control, which act as next level is placed near to communication link. This control can be used to share active power under high reactance conditions (R/X). In this control, parameters

like voltage, frequency, power values from DG units are communicated using communication link after averaging them and producing appropriate control signal to subsequent primary control level. The detailed block diagram of decentralized secondary control is shown in Figure 35.

A. Frequency control

Frequency deviations for large power systems are controlled by droop control as discussed in primary control. The frequency control of secondary control as proposed by Shafiee et al. (2014: 1021) states that frequency measurement values from first DG are sent through communication link to others, similarly the measured frequencies from other DGs are averaged and taken as reference for the first DG and the frequency of first DG is restored. The restored frequency of DG as mentioned above can be written as (Shafiee et al. 2014: 1021):

$$\delta f_{DG_k} = k_{Pf}\left(f^*_{MG} - f^-_{DG_k}\right) + k_{if}\int\left(f^*_{MG} - f^-_{DG_k}\right)dt \tag{67}$$

$$f^-_{DG_k} = \sum_{i=1}^{N}\frac{f_{DG_i}}{N} \tag{68}$$

Here, k_{Pf} and k_{if} are PI controller coefficients, f^*_{MG} is microgrid frequency reference, $f^-_{DG_k}$ is the average frequency for all DG units and δf_{DG_k} is the control signal produced by distributed secondary control of k^{th} DG systems in every sample time.

In Figure 36, we can see how secondary control resolves the frequency and voltage deviation as compared to primary control. Here we can see that secondary control helps to shift the response up, so that both the voltage and frequency can attain its nominal value even though the power rating of various DGs are different. To understand the system and also to tune the frequency and voltage variation, a small signal model was developed for low R/X microgrids as discussed in Guerrero et al. (2011: 162). According to droop control (Shafiee et al. 2014: 1022):

$$\omega_{DG_k} = \omega^*_{DG_k} + G_P(s)\left(P^*_{DG_k} - P_{DG_k}\right) \tag{69}$$

The active power of DG in low R/X microgrid system as mentioned in Guan et al. (2011: 21) can be written as (Shafiee et al. 2014: 1022):

$$P_{DG_k} = \frac{E_{DG_k}E_{com}\cos(\emptyset_{DG_k} - \emptyset_{com})}{X_k} \tag{70}$$

where E_{DG_k} is voltage at PCC, $\emptyset_{com}$ is phase difference between DG_k and PCC and X_k is reactance between PCC and DG_k. After linearizing equations (4) and (5) at an operating point P_{k0} and $\emptyset_{k0}$, the droop equations can be represented as (Shafiee et al. 2014: 1022):

$$\Delta\omega_{DG_k} = \Delta\omega^*_{DG_k} + G_P(s)\left(\Delta P^*_{DG_k} - \Delta P_{DG_k}\right) \quad (71)$$

$$\Delta P_{DG_k}(s) = \frac{\Delta E_{DG_k}\,\Delta E_{com}\cos(\emptyset_{DG_k} - \emptyset_{com})}{X_k} \quad (72)$$

or equation (72) can be written as (Shafiee et al. 2014: 1022)

$$\Delta P_{DG_k}(s) = G.\Delta_{\emptyset DG_k}(s) \quad (73)$$

Where $G = \frac{E_{DG_k}\,E_{com}\cos(\emptyset_{DG_k} - \emptyset_{com})}{X_k}$

Figure 36 depicts how a secondary control detaches frequency and voltage deviation caused by primary control. In both figures, primary and secondary control for two DGs with different droop coefficients has been showed. Here, when droop curve gets misplaced after primary control, then secondary control will shift up the frequency and voltage cure back to nominal value. The small signal model for frequency control of distributed secondary control can be seen in Figure 37, which includes a droop control model. In droop control block, we can see a low pass filter $G_{LPF}(s)$ that has a cut-off frequency of 0.2Hz as mentioned in Shafiee et al. (2014: 1022). And the secondary control has a simple PLL with a first order transfer function as mentioned as $G_{PLL}(s)$, which takes the DG frequencies, proportional gain constant k_a, average angular frequencies from other DGs and a PI controller. The characteristic equation of below small signal model is (Shafiee et al. 2014: 1023):

$$\Delta f = 1 + G_{LPF}(s) * G_P(s) * \frac{1}{s} * G + G_{PLL}(s) * k_a * G_{f\,sec}(s) \quad (74)$$

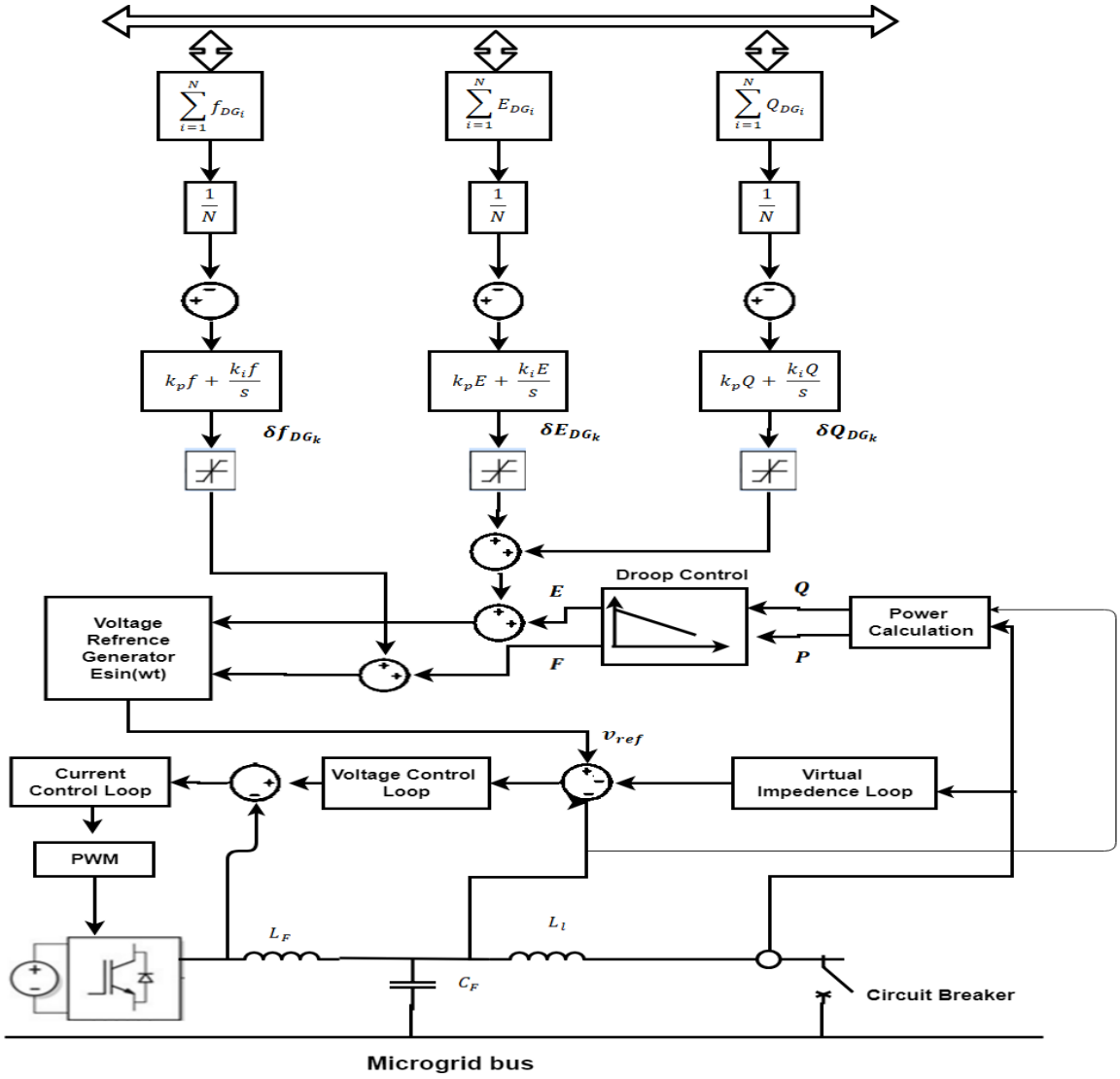

Figure 35. Distributed secondary control Shafiee et al. (2014: 1022).

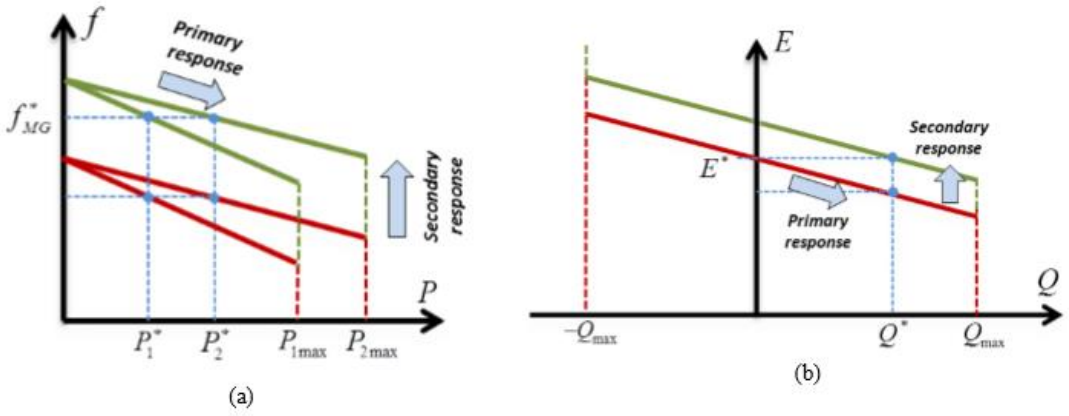

Figure 36. Secondary control response vs primary control response (a) Frequency restoration (b) Voltage amplitude restoration (Shafiee et al. 2014: 1023).

Where $k_a = \frac{1}{N}$ is a parameter to get average of frequency. Transfer function of blocks in the model are shown as (Shafiee et al. 2014: 1023):

$$G_{LPF}(s) = \frac{1}{1+\tau_p s} \quad (75)$$

$$G_{PLL}(s) = \frac{1}{1+\tau s} \quad (76)$$

$$G_P(s) = \frac{k_{pP}s + k_{iP}}{s} \quad (77)$$

$$G_{f\,sec}(s) = \frac{k_{pf}s + k_{if}}{s} \quad (78)$$

Here k_{iP} is droop coefficient, where as k_{pP} can be considered as virtual inertia of the system. The eigen values calculated from the small signal model equation (74) can be used to produce control parameters.

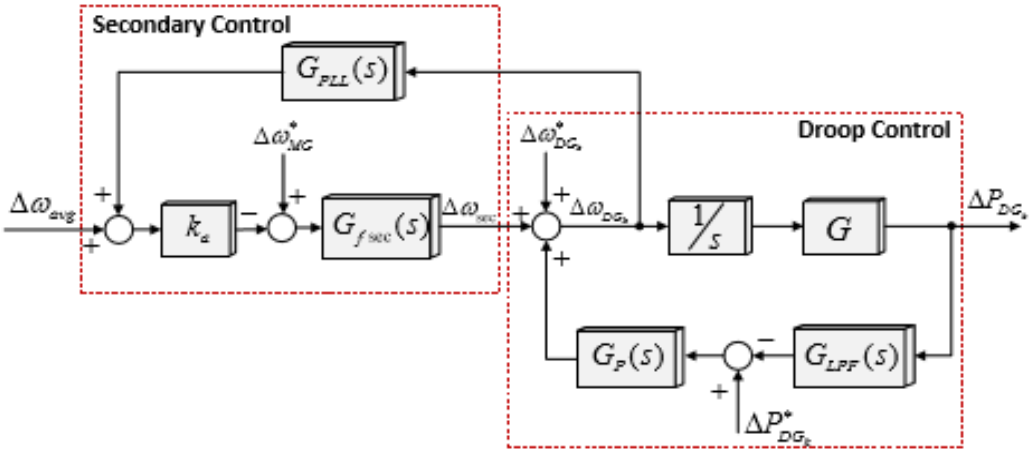

Figure 37. Small signal model for distributive frequency control for a DG unit (Shafiee et al. 2014: 1023)

B. Voltage Control

Voltage control uses similar strategy like frequency control as discussed above. So here each inverter will measure voltage error and then it tries to mitigate the voltage deviation caused by droop control ($Q - E$). The voltage restoration is obtained as follows (Shafiee et al. 2014: 1023):

$$\delta E_{DG_k} = k_{PE}\left(E^*_{MG} - E^-_{DG_k}\right) + k_{iE}\int\left(E^*_{MG} - E^-_{DG_k}\right)dt \quad (79)$$

where δE_{DG_k} is voltage restoration coefficient of DG that is generated from PI controller. Here, the error is calculated between voltage reference of MG (E^*_{MG}) and average voltage of all DG units, which can be specified as $E^-_{DG_k} = \sum_{i=1}^{N}\frac{\sum E_{DG_i}}{N}$.

The main benefit of using this method over traditional droop is that the remote sensing used by secondary control is not needed, hence, each DG terminal voltage can be different from one and another if required Shafiee et al. (2014: 1023). From this method, we can see that secondary control can reduce the voltage deviation issue caused by primary control as discussed in Figure 36 (b).

C. Line-impedance-independent power equalization

From previous theories it is notable that, in low impedance or low (R/X) microgrids, reactive power control sharing is not accurate and similarly, for high (R/X) microgrids, active power sharing is also not proper. Hence, using voltage as a variable is not sufficient to control reactive power. As we saw before, the voltage and phase between two distributive generators can be different so, the reactive control sharing between two DGs will be a problem. In preceding explanations, we have discussed different methods to overcome reactive power sharing by using primary control. However, in all those methods we cannot achieve equitable reactive power because voltage was used as a controlled variable in those methods.

An achievable solution as discussed by Shafiee et al. (2014: 1024) is to implement a reactive power sharing locally, so that each unit can send the active and reactive power to other DG units in order to be averaged. By this way as the information is common, all the DGs will have same reference values. The reactive power sharing of distributed control can be expressed as (Shafiee et al. 2014: 1024):

$$\delta Q_{DG_k} = k_{PQ}\left(Q^{-}_{DG_k} - Q_{DG_k}\right) + k_{iQ}\int Q^{-}_{DG_k} - Q_{DG_k})dt \qquad (80)$$

where $\mathrm{Q}^{-}_{\mathrm{DG_k}} = \frac{\sum_{i=1}^{N} \mathrm{Q_{DG_i}}}{\mathrm{N}}$

Here k_{iQ} is integral coefficient and k_{PQ} is proportional coefficient, Q_{DG_k} is reactive power of kth DG systems, $Q^{-}_{DG_k}$ is the average reactive power of all DGs. The resultant error signal δQ_{DG_k} is secondary control signal in every sample time to share the reactive power between different DGs. A small signal model of reactive control sharing model can be seen in Figure 38.

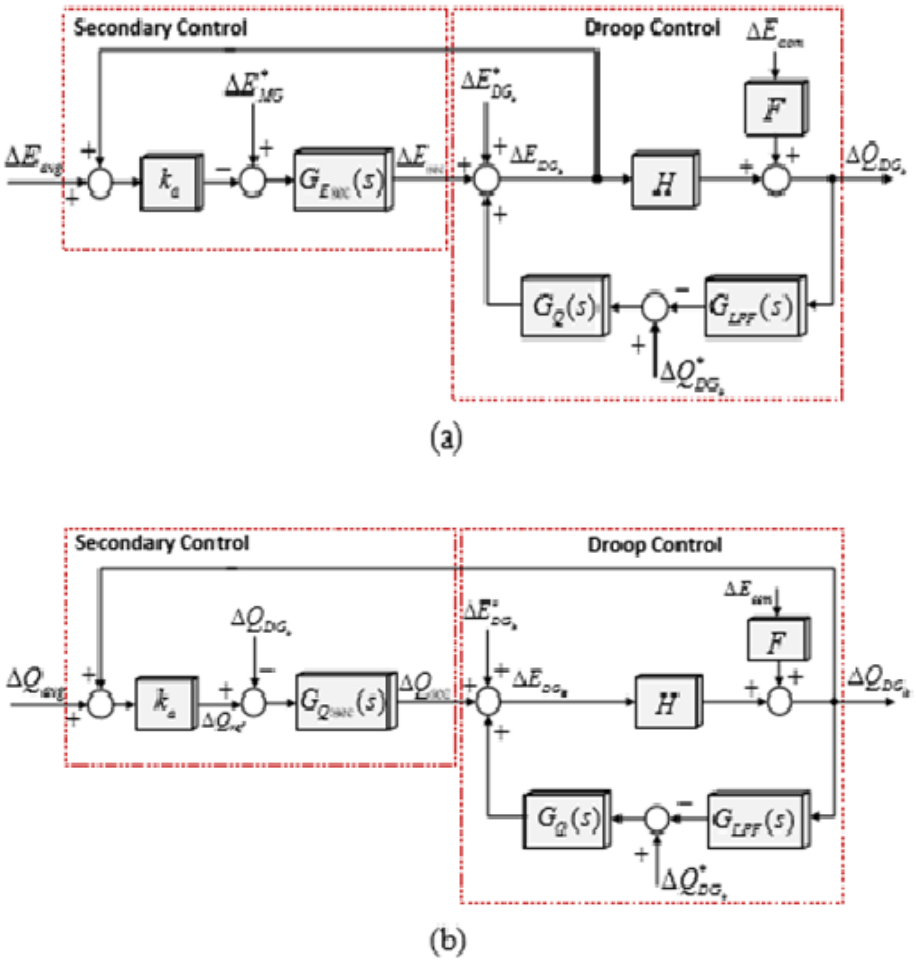

Figure 38. Small signal model of distributed control of a DG unit in a low R/X islanded microgrids (a) Voltage Control (b) Reactive power sharing Shafiee et al. (2014: 1024).

Small-scale model as explained for frequency control can be seen here in voltage control and reactive power sharing control from equations 79 and 80 (Shafiee et al. 2014: 1024).

$$E_{DG_k} = E^*_{DG_k} + G_Q(s)\left(Q^*_{DG_k} - Q_{DG_k}\right) \tag{81}$$

Similarly, the reactive power of DG_k in a low impedance islanded microgrid can be shown as (Shafiee et al. 2014: 1024):

$$Q_{DG_k} = \frac{E^2_{DG_k} - E_{DG_k}E_{comm}\cos(\emptyset_{DG_k} - \emptyset_{comm})}{X_k} \tag{82}$$

After linearizing both (81) and (82) at operating points $Q_{k0}, \emptyset_{k0}$ andE_{k0}, we get

$$\Delta E_{DG_k} = \Delta E^*_{DG_k} + G_Q(s)\left(\Delta Q^*_{DG_k} - \Delta Q_{DG_k}\right) \quad (83)$$

$$\Delta Q_{DG_k}(s) = H.\Delta E_{DG_k}(s) + F.\Delta E_{com}(s) \quad (84)$$

where $F = -\frac{E_{DG_k}\cos(\emptyset_{k0}-\emptyset_{com})}{X_k}$ and $H = -\frac{2E_{k0}-E_{com}\cos(\emptyset_{k0}-\emptyset_{com})}{X_k}$

Figure 38(a) and 38(b) depicts the small signal model of secondary control for voltage restoration and reactive power sharing, which has been derived from equation 79 and 80 respectively. The characteristic equation of small signal model in Figure 32 can be written as (Shafiee et al. 2014: 1024):

$$\Delta_E = 1 + \left(G_{LPF}(s) * G_Q(s) * H\right) + (k_a * G_{E\,sec}(s)) \quad (85)$$

$$\Delta_Q = 1 + \left(G_{LPF}(s) * G_Q(s) * H\right) + \left(k_a * H * G_{E\,sec}(s)\right) \quad (86)$$

where transfer functions can be expressed as (Shafiee et al. 2014: 1025):

$$G_Q(s) = k_P \quad (87)$$

$$G_{E\,sec}(s) = \frac{k_{PE}s + k_{iE}}{s} \quad (88)$$

$$G_{Q\,sec} = \frac{k_{PQ}s + k_{iQ}}{s} \quad (89)$$

where k_{PQ} is droop coefficient and $G_{E\,sec}(s)$ and $G_{Q\,sec}(s)$ are transfer functions of PI controller respectively.

4.2.4 Tertiary control

Tertiary control is the last type of control strategy in hierarchical control network. Here the long term and optimum set points are provided depending on the requirement of the DER. When multiple DERs are connected in parallel, then in order for them to connect to the grid a third level of synchronization is required called tertiary control. Tertiary control is responsible for synchronizing the operation of multiple microgrids within the system. The overall reactive power management of a grid that contains several microgrids could be acquired by properly synchronizing through tertiary control approach, reactive power injection of generators and MG at PCC, based on centralized loss minimization approach for the entire grid (Cañizares et al. 2014: 1913). This control level provides information to

secondary control and other subsystems to form a full grid. Tertiary control handles the economic concerns of a MG and handles the power flow between main grid and microgrid. In grid-connected mode, the control of power flow between MG and main grid is done by adjusting the amplitude and frequency of individual DER system. Block diagram of tertiary control can be shown in Figure 39.

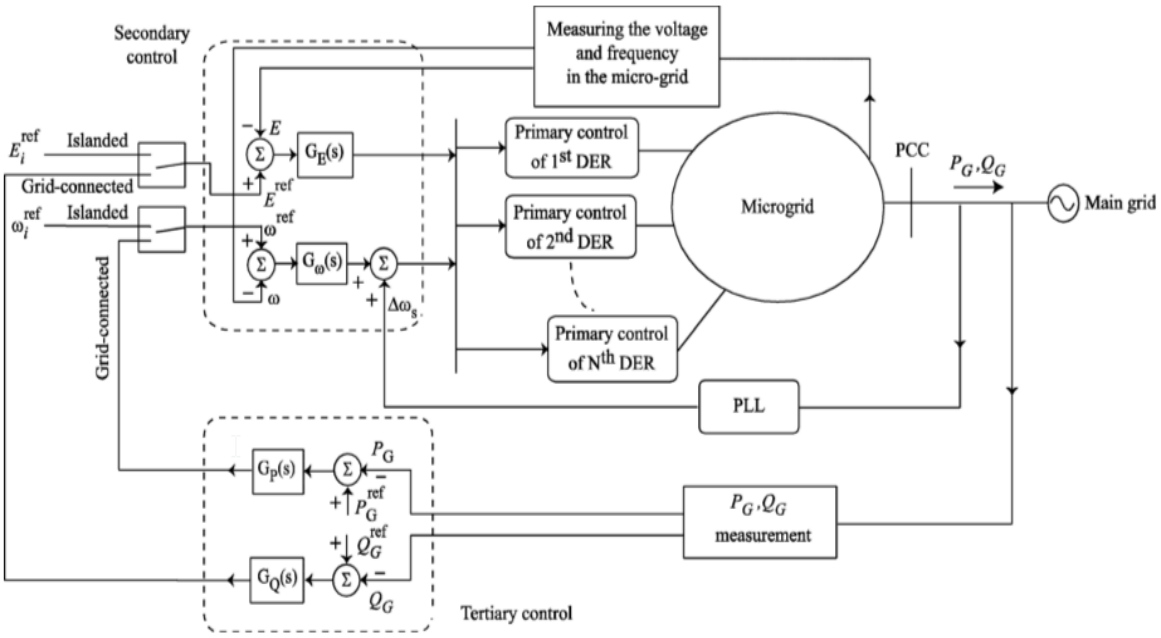

Figure 39. Block diagram of tertiary control (Bidram et al. 2012: 1973)

Here, the active and reactive power of the individual MGs are calculated and then these values are compared with the reference values P_G^{ref} and Q_G^{ref} to produce reference frequency and voltage (ω^{ref} and E^{ref}). Based on above description, the reference values can be written as (Bidram et al. 2012: 1972):

$$\begin{cases} \omega^{ref} = K_{PP}\left(P_G^{ref} - P_G\right) + K_{IP}\int\left(P_G^{ref} - P_G\right)dt \\ E^{ref} = K_{PQ}\left(Q_G^{ref} - Q_G\right) + K_{IQ}\int\left(Q_G^{ref} - Q_G\right)dt \end{cases} \quad (90)$$

Here, K_{PP}, K_{PQ}, K_{IP} and K_{IQ} are proportional constants of PI controller and ω^{ref}, E^{ref} are reference values to secondary control respectively. The tertiary control also provides an economically optimal operation for example using gossiping algorithm. In general, the economically optimal operation is fulfilled if all DERs operate at minimal cost. Gossiping

algorithm as aforementioned works such a way that, initially random power set points P_i^0 and P_j^0 are considered for $i^{th}$and j^{th}DER system. Then by looking at the antecedent information about the marginal cost curves of DER, the most favorable output power of two DERs $P_i^{opt}$and P_j^{opt} are determined. The similar procedure is performed for other DERs in grid systems until overall stability and stable performance is achieved. (Bidram et al. 2012: 1972).

5. SIMULATIONS AND RESULTS

In this chapter the simulations of the grid controls are implemented and discussed. Models are implemented in Simulink and scopes are taken from MATLAB, which is a programming language build by Mathworks. MATLAB/Simulink is a tool used to design and test system models. A special power systems library named Simscape Power Systems is used to execute the models (Mathworks).

5.1 Single inverter model islanding mode:

For single inverter model a PV array model is used, which will simulate a solar panel with a given irradiation. A PV array is a module consisting of several solar panels, which can be connected both serial and parallel. The circuit of the model can be seen in Figure 40.
In Figure 40, a single inverter MG control with a PV module and control system is modeled. This microgrid is using a resistive load. The first component of this model is PV module, which is driven by an illumination source and this is enabled by a signal generator. In PV array module there are five main elements: illuminated light source, diode, series resistance, shunt resistance and temperature of the module. In this model MPPT algorithm is not implemented.

$$I_d = I_0 \left[\exp\left(\frac{V_d}{V_t}\right) - 1\right] \quad (91)$$

$$V_T = \frac{kT}{q} nIN_{cell} \quad (92)$$

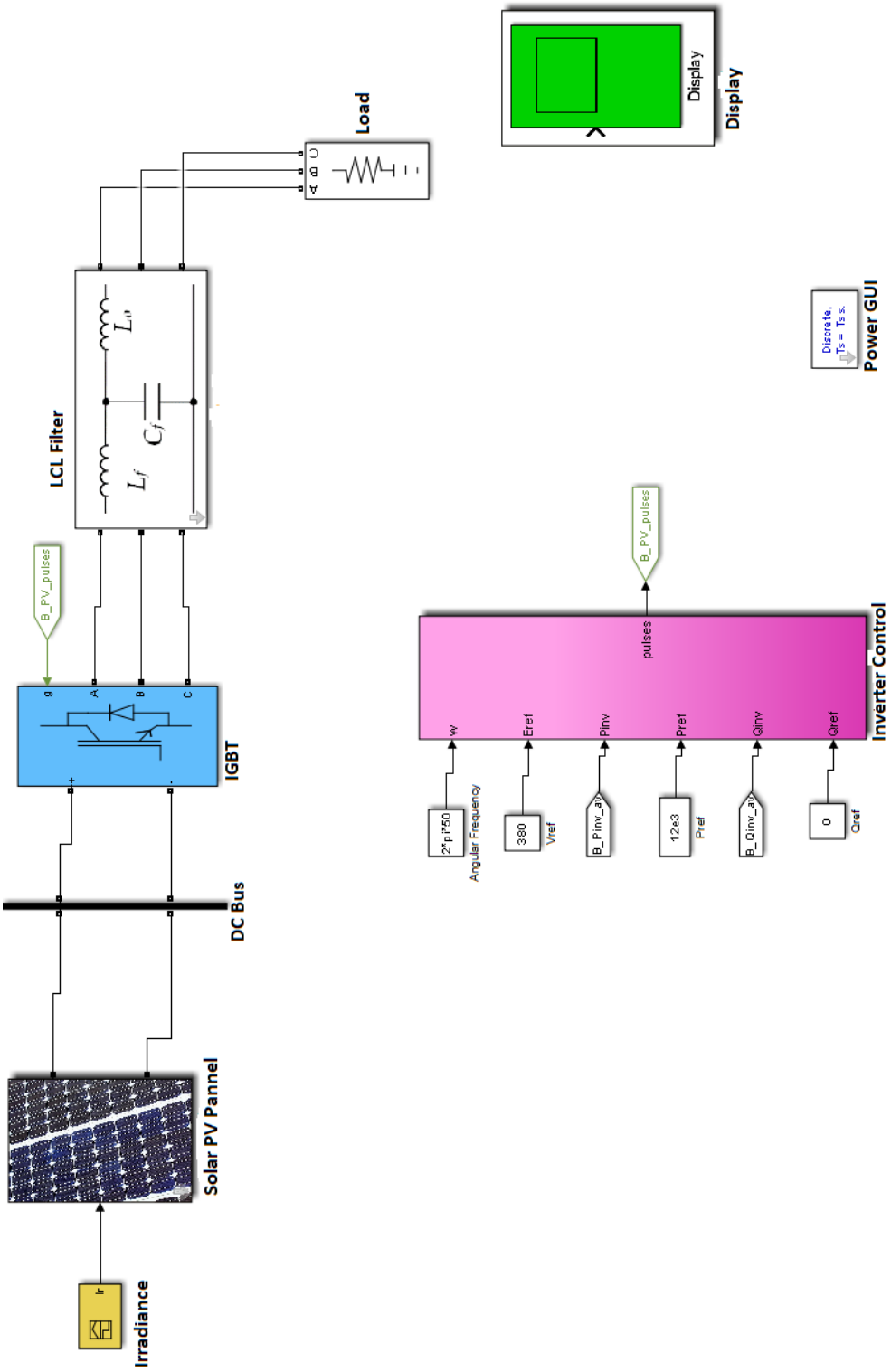

Figure 40. Single inverter control model

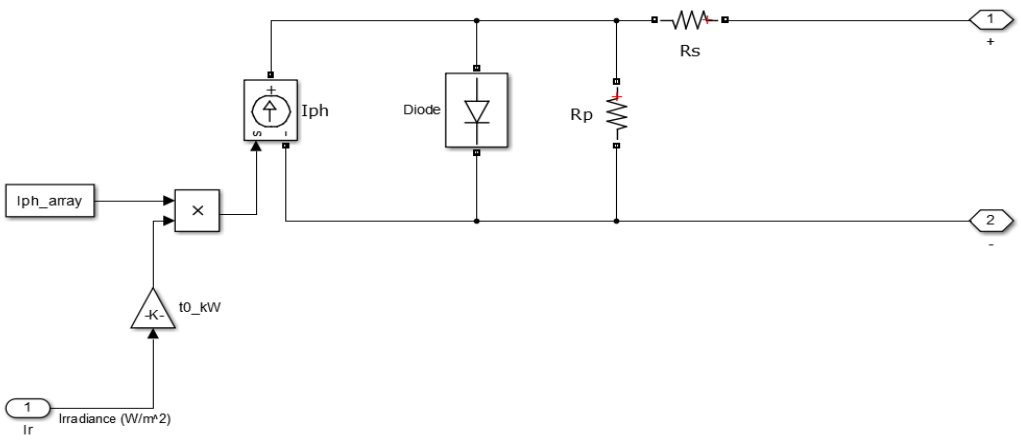

Figure 41. PV array circuit

The above figure is a circuit used to generate DC voltage from the illumination source. A 12 kW single inverter MG is simulated here, which consists of a P and Q calculation, then droop control and then voltage and current control technique. Active and reactive power can be calculated as:

$$P = \frac{v_d i_d + v_q i_q}{2} \text{ and } Q = \frac{v_q i_d - v_d i_q}{2} \quad (93)$$

A resistive and inductive virtual impedance combination is used then in model with ratings 24mH and 0.5 ohms. A $abc - dq$ frame transformation block is used to convert a three phase AC from abc to dq and back to abc.

Here the phase angle for the block is provided by the phase lock loop block (PLL), which will generate frequency and phase for a signal by taking mean and passing through a 2nd order low pass filter with a cut off frequency of 25Khz. This block is taken from an open source model by Pierre Giroux (Hydro-Quebec Research Institute IREQ). Droop control is implemented using a PI control, whose control parameters Kpf, Kif,Kpe and Kie are given in start script Start.m. The sine wave generator is formed by adding phase shift with phase angles 0,180 and 360 respectively. In this block a discrete time integrator is used to generate a phase angle from angular frequency.

$$wt = \int_0^{2pi} w \, dt \quad (94)$$

The generated direct and quadrature components can be passed through a mean value generator block of sampling time Ts to generate an average signal. This mean block is taken and modified from Control & Measurements library of Mathworks called Simscape, which is used to model and simulate multi-domain physical systems. The signal from voltage control and dq current from inverter is passed to current control block, which generates a V_{dq}, that will be transformed back to V_{abc} and then given to a PWM generator block to produce 6-pulse for voltage source inverter. VSI has 6 IGBT's, here serially connected IGBT pairs will be connected parallel to produce three phase signal. A unit delay of sampling time Ts is used to switch the transistors so that the impact of all the blocks can be reduced while generating the pulses for IGBT's. Internal structure of control model can be seen in Figure 42.

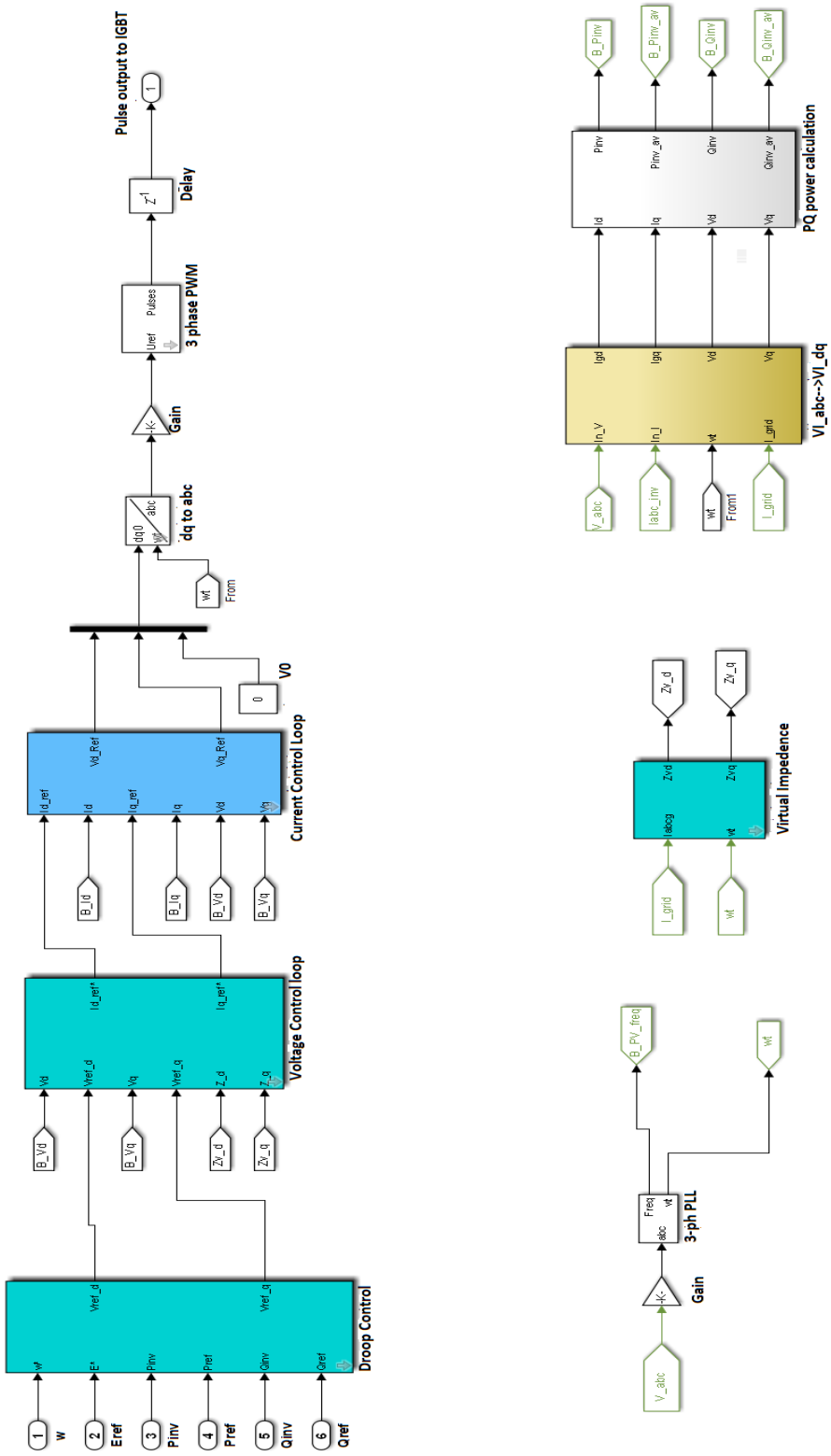

Figure 42. Internal control structure

The simulation result of single inverter MG model shows active power, reactive power, voltage at PCC and frequency. As we see active power will raise, when inverter is turned on due to irradiation and after a short raise time, P value gets to saturation near to active reference value.

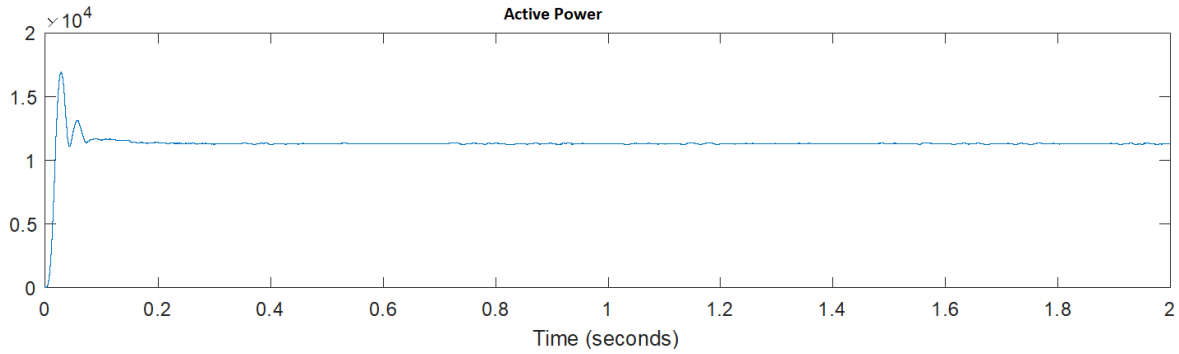

Figure 43. Active power from inverter

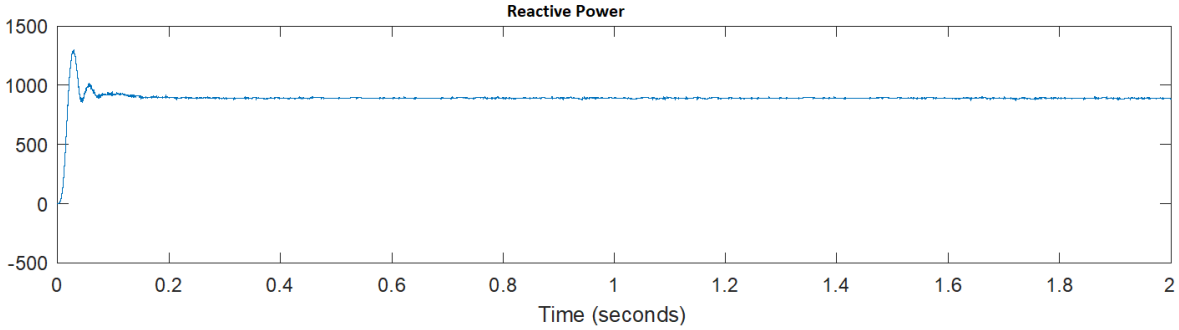

Figure 44. Reactive power from the inverter

The active power generated to load is more or less equal to the reference power. There is some reactive power generated in the inverter side due to line impedance, which is as shown. The voltage and current across the inverter output are as shown:

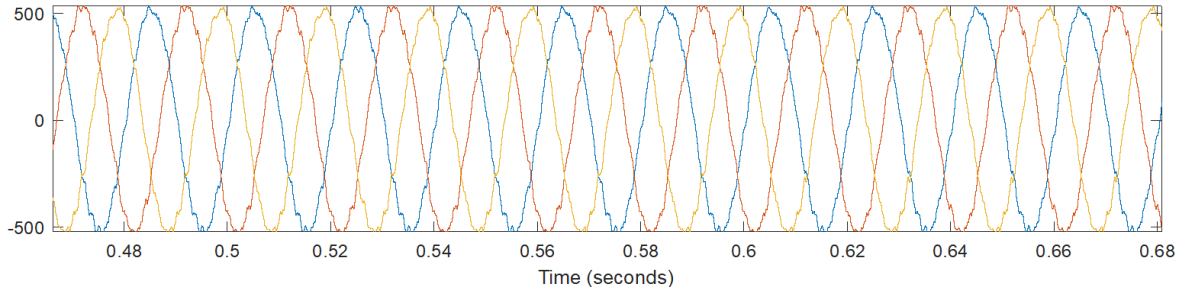

Figure 45. Three phase voltage from the output of inverter

Inverter current is taken across line inductance L and voltage is taken across line capacitance, which is acting as a LC filter to eliminate the ripples.

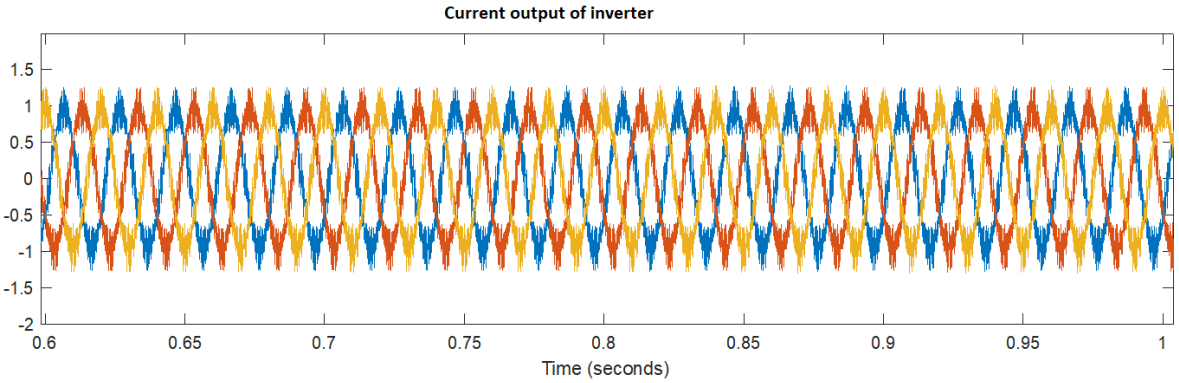

Figure 46. Current across output of inverter

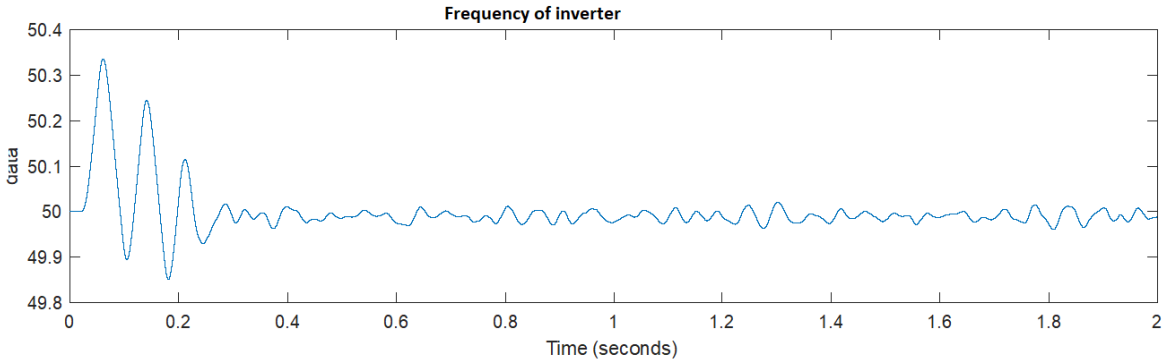

Figure 47. Frequency of inverter output voltage (Vabc)

5.2 Grid connected single inverter model

When a DG is connected to the grid, a synchronization is needed so that transition from islanding to grid-connected mode can happen smoothly.

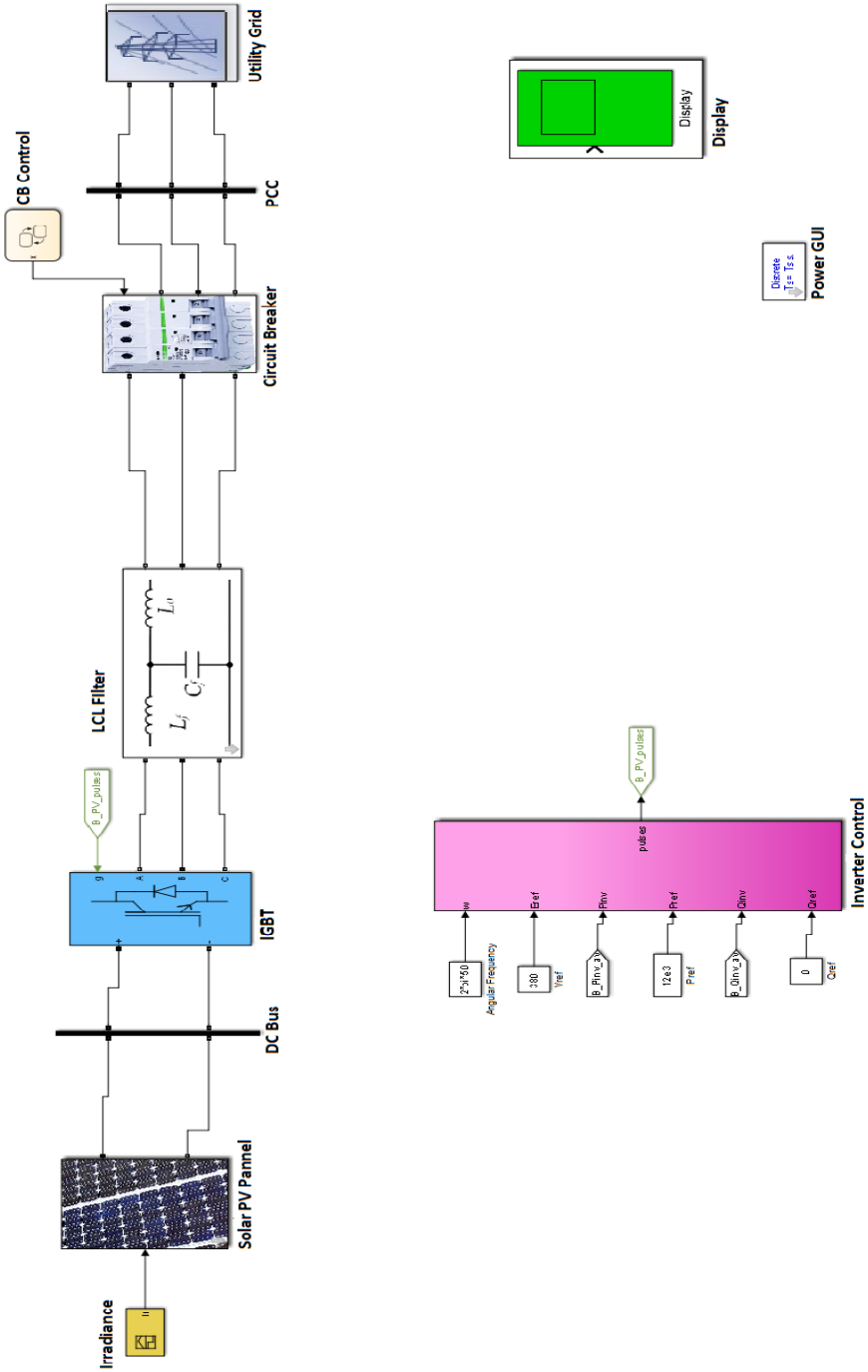

Figure 48. Single inverter MG in grid-connected mode

In this model as shown above, there is a contactor circuit, which is programmed to turn on every second by means of a state flow diagram.

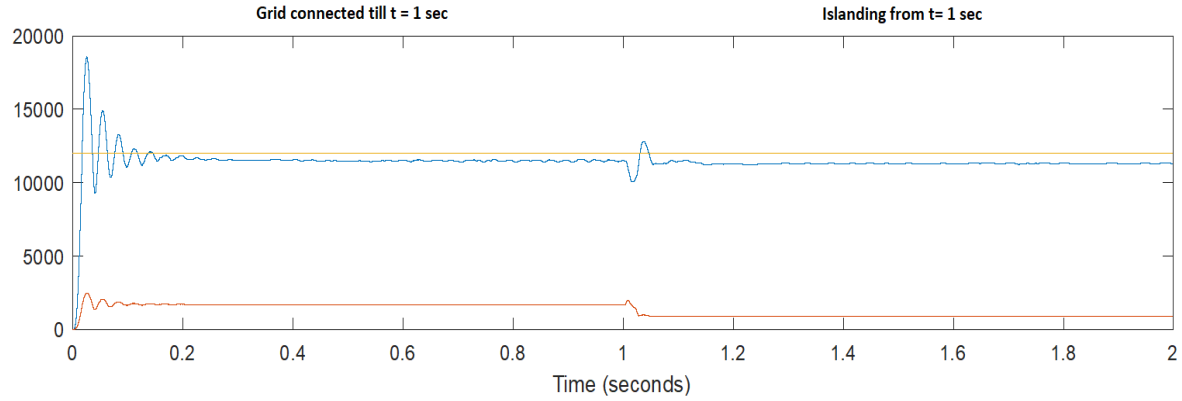

Figure 49. Active and Reactive power during transition from islanding to grid-connected mode.

As we can see from the plot that active power glitches, when switching happens at t=1 seconds and P gets back to same level, but Q reduces as grid doesn't have any reactance components. Same effect can be seen in inverter voltage output and grid voltage outputs. Frequency in both grid-connected and islanding mode remains stable with some transition glitch during t=1 seconds, when breaker switch closes. Similarly, voltage at the output of inverter can be seen below, here during switching of circuit breaker, the voltage at the output of inverter experiences a distortion, which is then overcome after synchronization with grid.

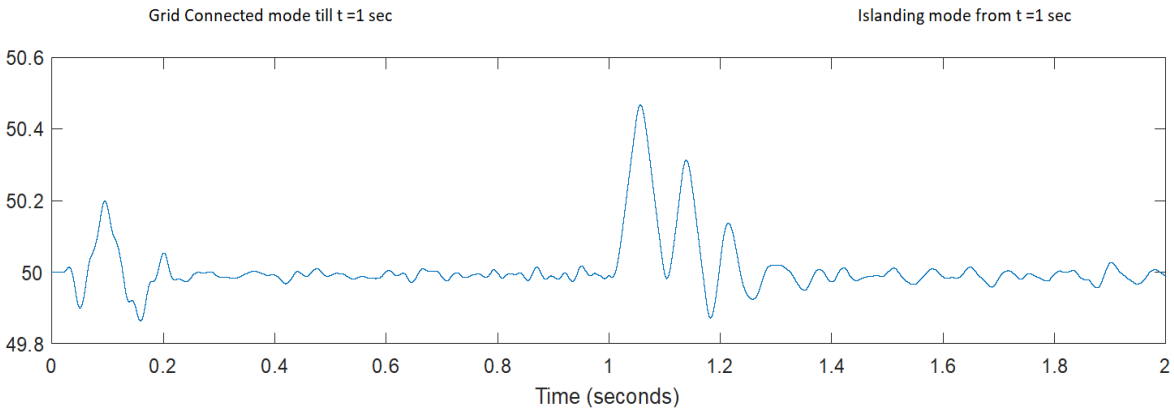

Figure 50. Frequency transition between islanding and grid-connected mode

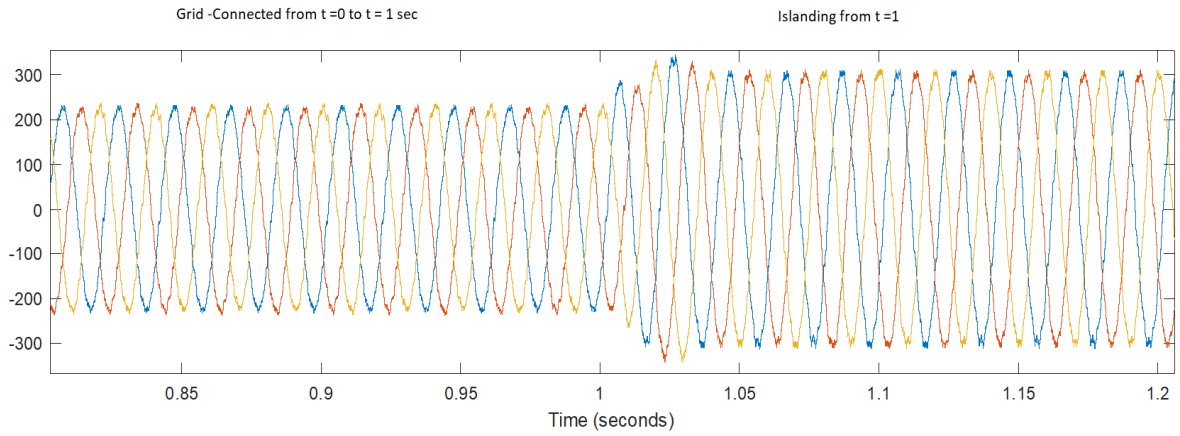

Figure 51. Voltage at inverter output

5.3 Parallel inverter in a microgrid

When two inverters are connected in parallel then as discussed, it can be done in two ways: centralized and de-centralized manner. Two parallel connected MGs are shown in Figure 52.

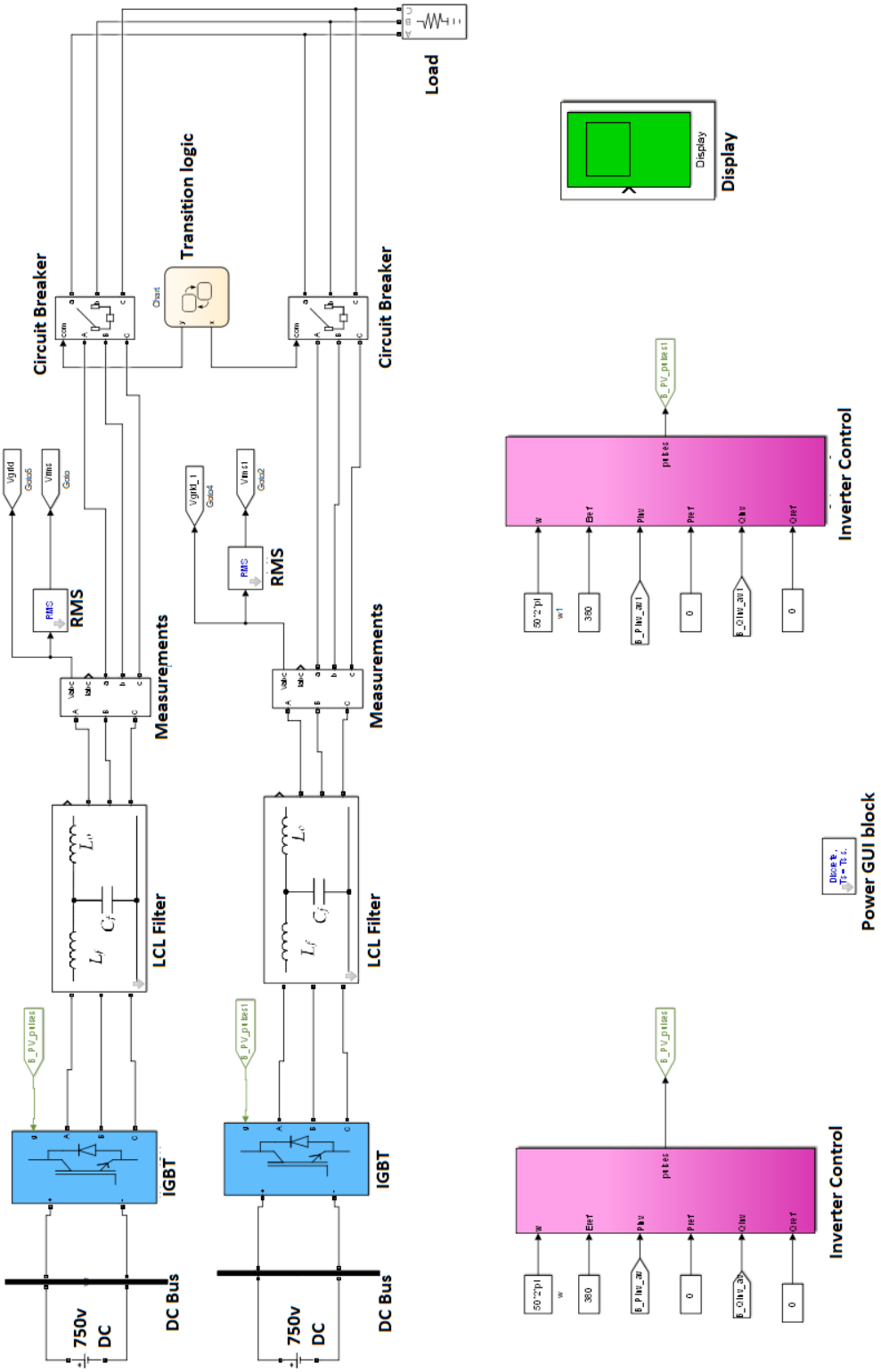

Figure 52. Two inverters connected in parallel

5.3.1 De-centralized microgrid control

Parallel inverter in de-centralized mode of operation has following active and reactive power output. Here the active power of the utility grid synchronizes with the inverter and constant 12 kW flows through the load.

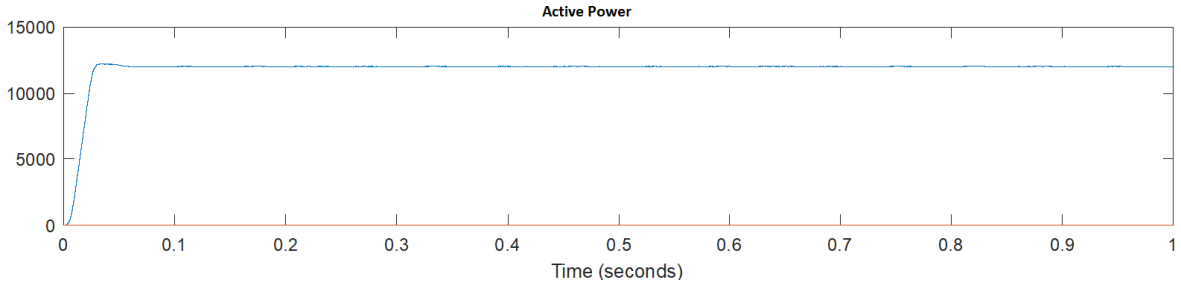

Figure 53. Active power of parallel inverters

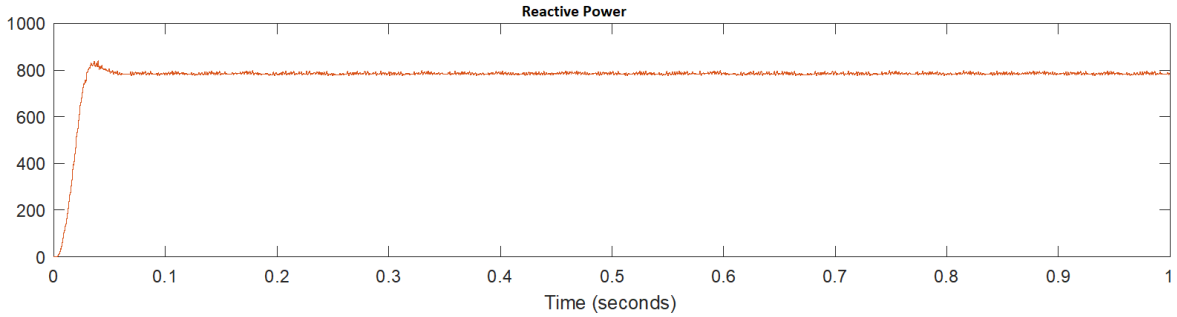

Figure 54. Reactive Power of parallel inverters

Frequency and voltage synchronization is needed to achieve, especially when multiple inverters are connected in parallel. The frequency as we can see is maintained with 50 Hz due to the implementation of secondary control in droop, which will try to maintain P-F characteristic curve. In the curve we can notice a small raise in active power in order to restore the frequency deviations.

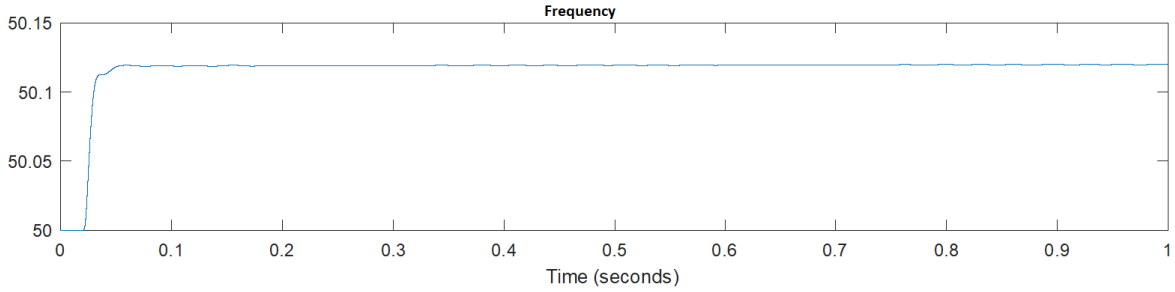

Figure 55. Frequency restoration from P-F

Now when different inverters are switched at different instants of time, the impact of load is supposed to be checked. At time t = 0 seconds the inverter 1 is switched on by closing breaker switch and at t = 0.3 seconds the breaker is closed for inverter 2 and opening for inverter 1, and at t = 0.6 seconds switch is closed for both inverters and after 0.3 seconds again circuit breaker of inverter 1 is closed and that of inverter 2 is opened. As we notice in Figure 56 the frequency drops during transition and the active power delivered to load increases almost double.

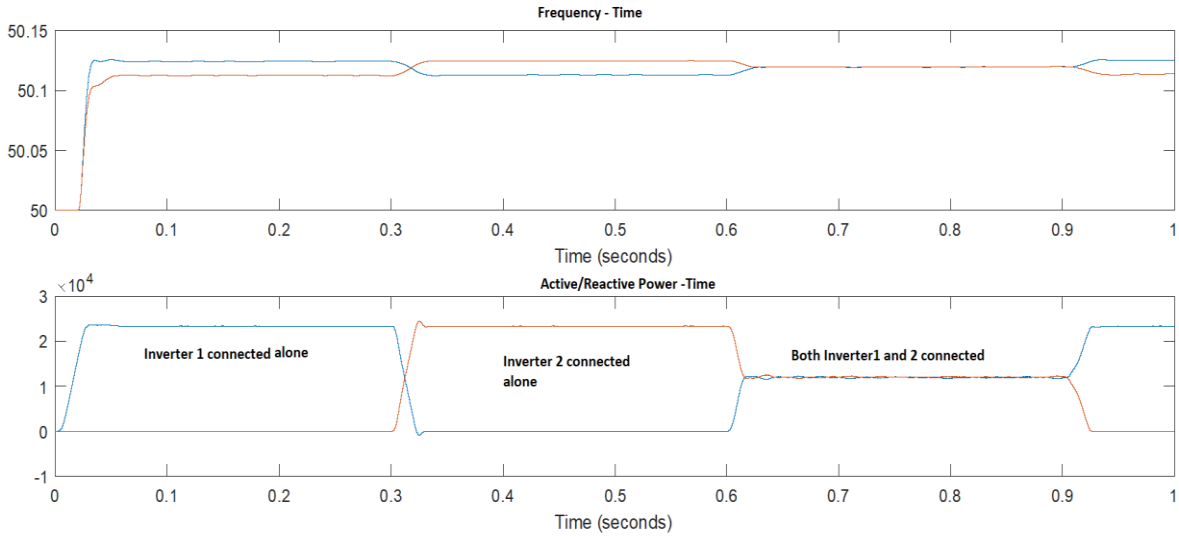

Figure 56. Active load sharing and frequency between two inverters with switching time at t =0.3, 0.6 and 0.9 seconds

After both inverters are turned on during t=0.6 sec, the power is shared equally between two inverters to the load. Similarly voltage across the inverters, while switching from one inverter to another, can be seen below. As we see, when both inverters are switched together then there are some harmonics, which can be resolved by controlling PI of voltage controller.

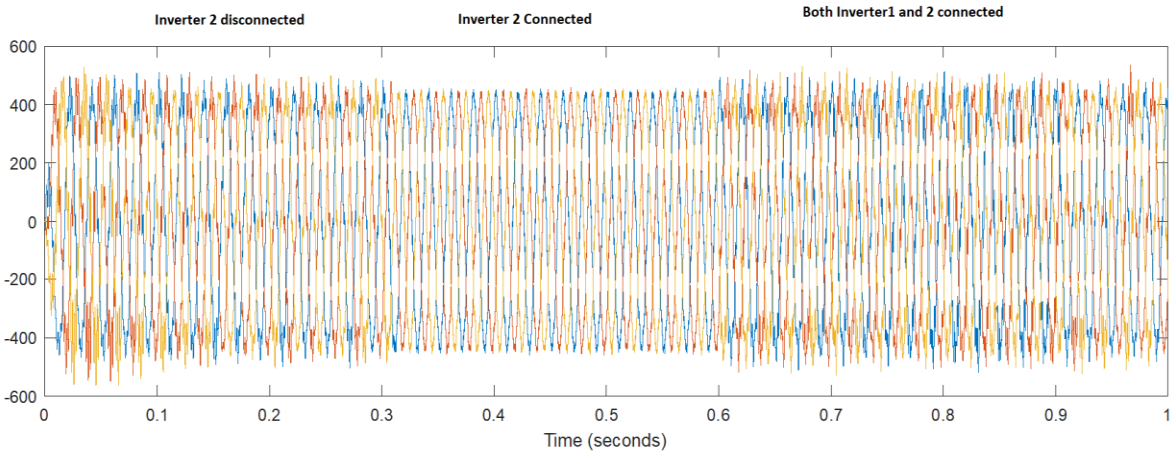

Figure 57. Voltage transition between two inverters

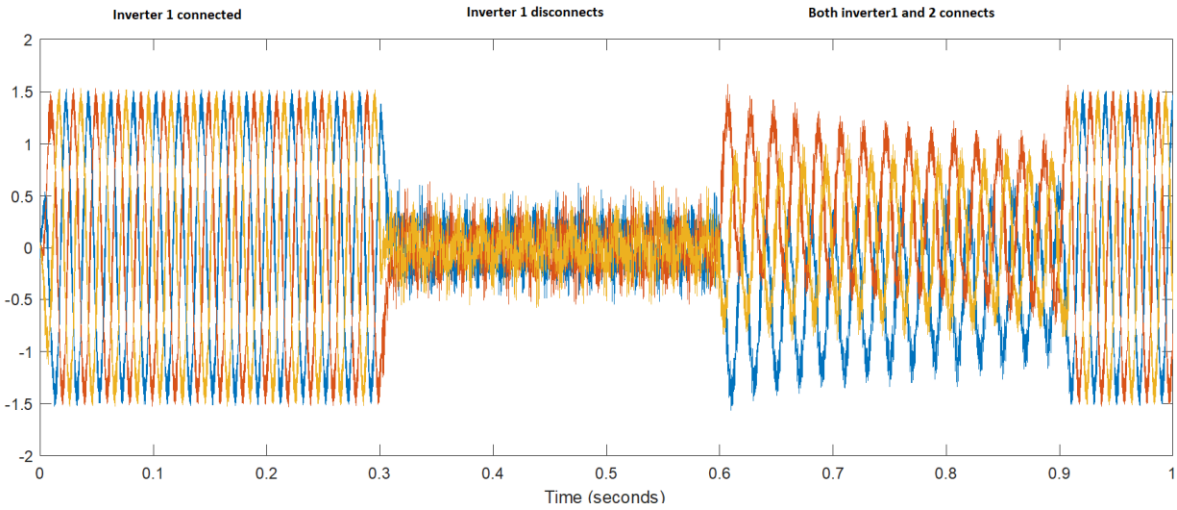

Figure 58. Current transition between two inverters

The inner control of de-centralized control can be seen from Figure 59.

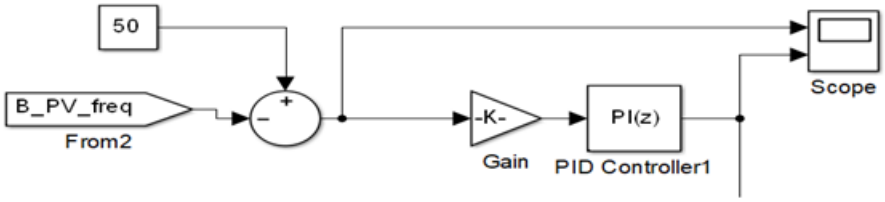

(a)

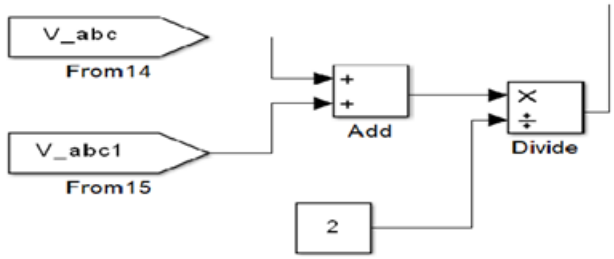

(b)

Figure 59. Inner control of de-centralized parallel inverter. (a) P-F control (b) Q-E control

5.3.2 Centralized microgrid control

Similarly, when parallel-connected inverters are following centralized control strategy, then the frequency restoration and voltage at the output of inverter can be seen below:

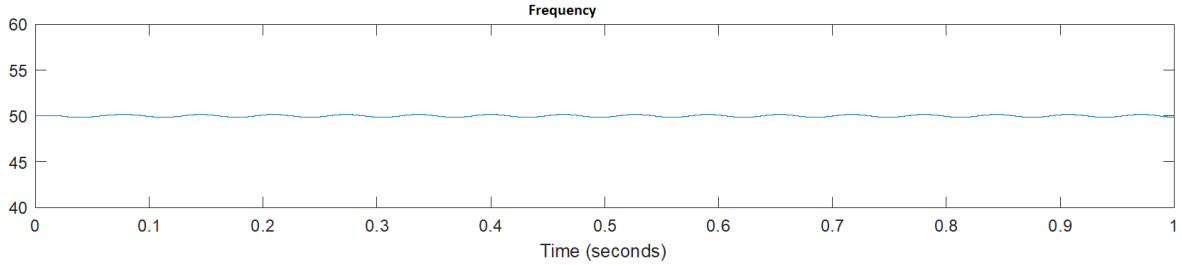

Figure 60. Frequency restoration of centralized MG

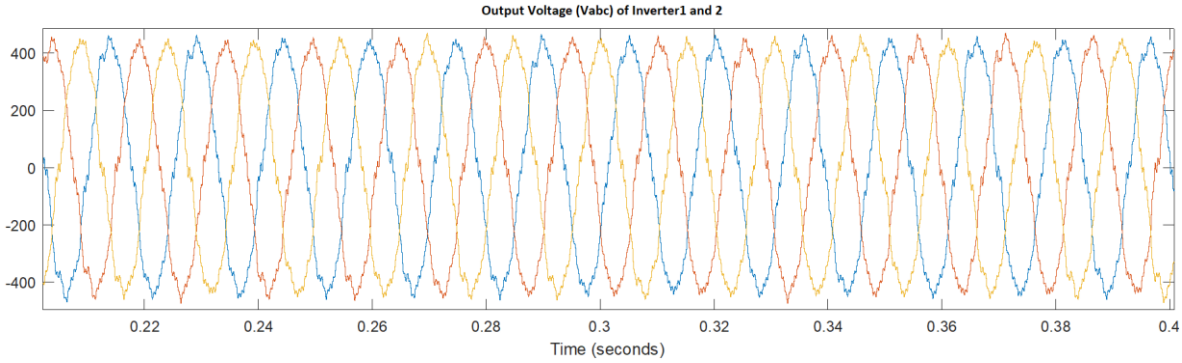

Figure 61. Voltage restoration of centralized MG

As we see the frequency is restored within the range of 49.95 to 50.05, but the fluctuation is

the case of communication latency of centralized load, i.e. here the load is same as like in de-centralized type, but the control values for droop are centralized unlike in de-centralized, where control is distributed. The centralized part of the Simulink can be seen below.

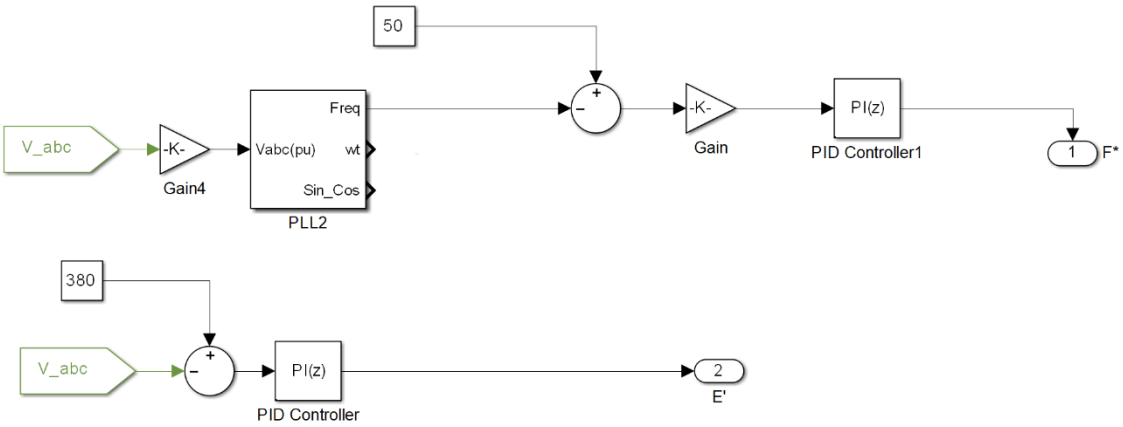

Figure 62. Model snapshot of centralized control inside droop strategy

Active power and reactive power output of centralized type secondary control can be seen in figure.

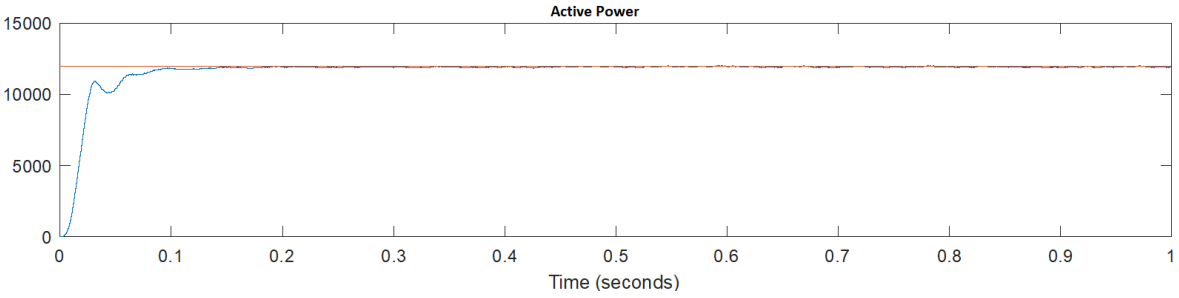

Figure 63. Active power in load during centralized MG control

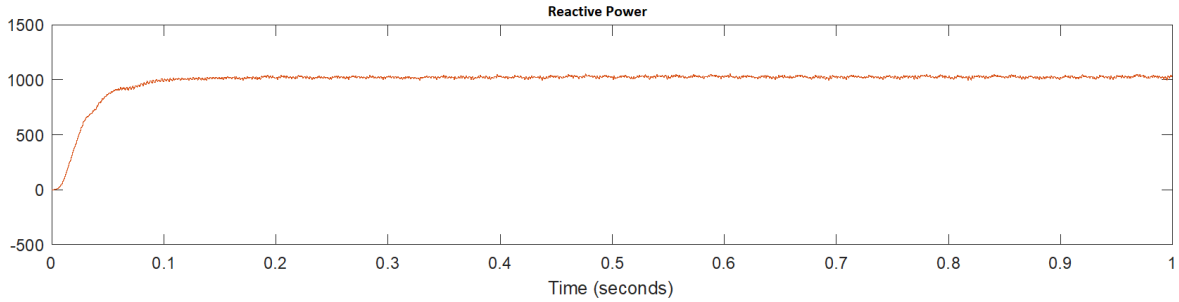

Figure 64. Reactive power in load during centralized MG control

Now when load is distributive, then frequency is restored properly and output current and

voltage fluctuation is shown to be reduced as we can see from figure below. We can see that both frequency and power avoids steady state error, which is produced in primary control.

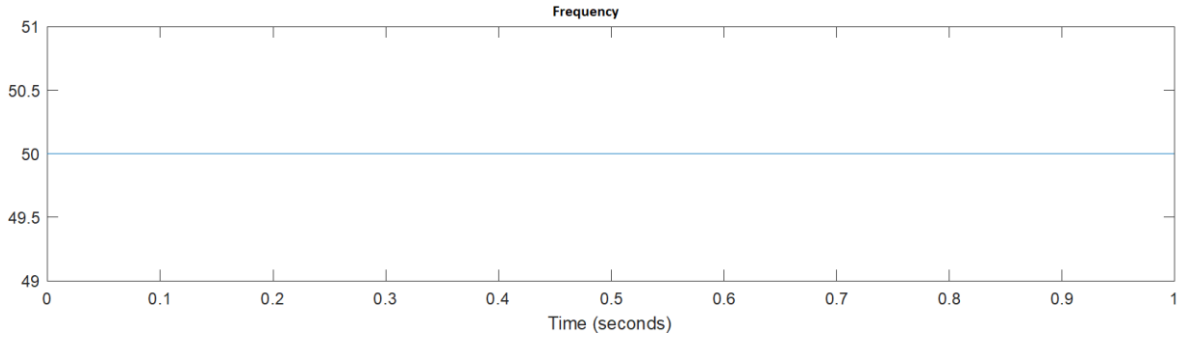

Figure 65. Frequency of centralized MG control with distributive load

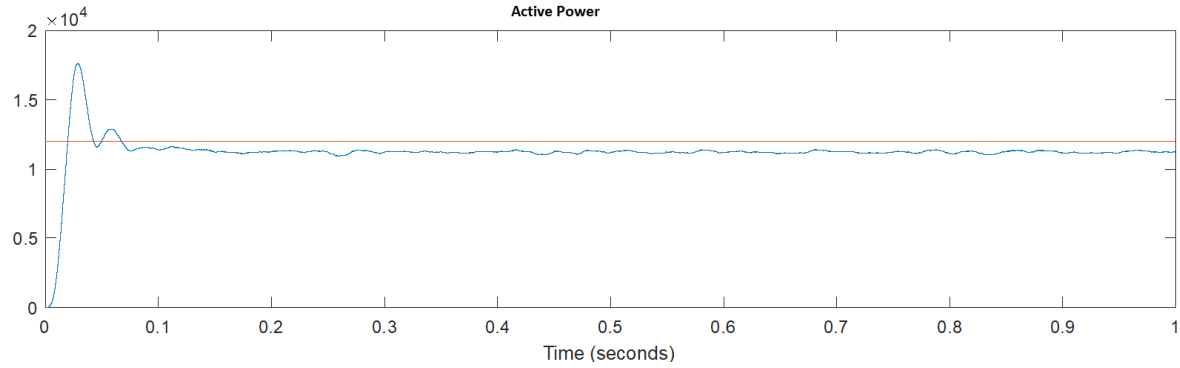

Figure 66. Active power of centralized MG control with distributive load

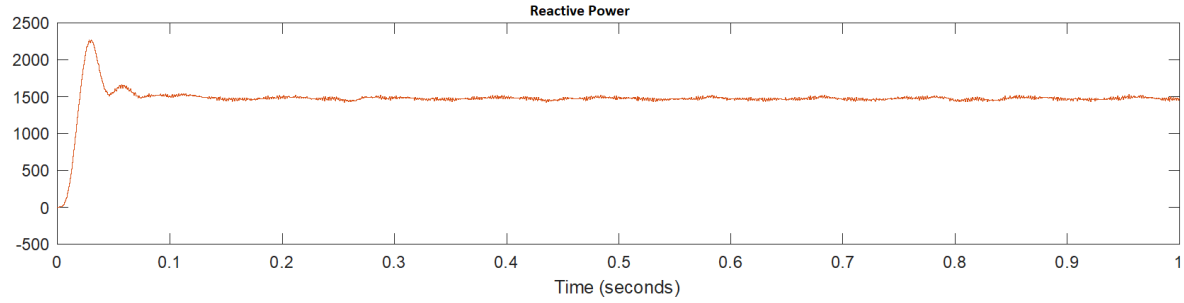

Figure 67. Reactive power of centralized MG control with distributive load

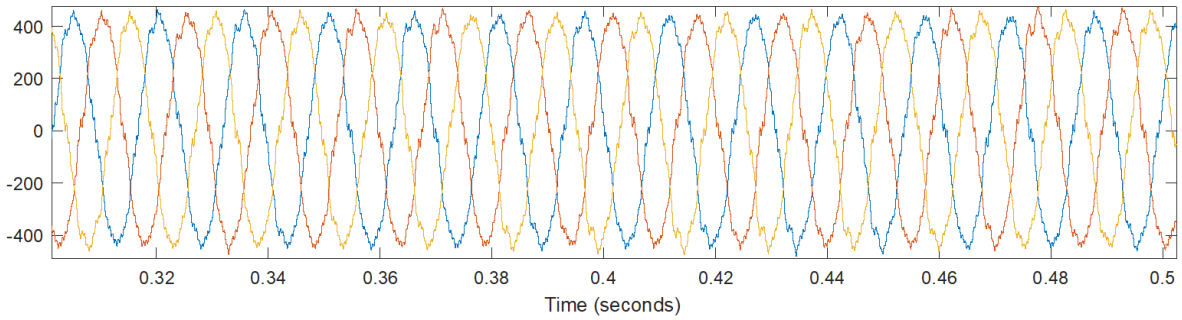

Figure 68. Inverter output voltage of centralized MG control with distributive load

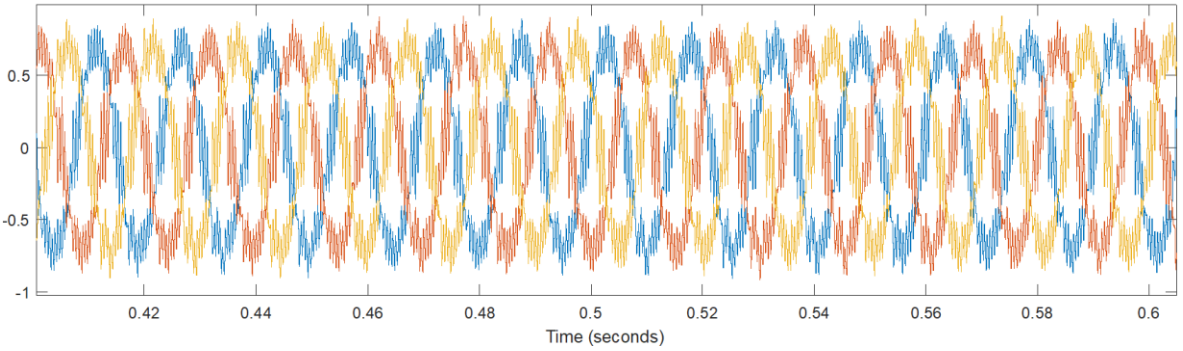

Figure 69. Inverter output current of centralized MG control with distributive load

5.4 Parallel inverter grid-connected mode

Parallel inverters in grid-connecting mode in Simulink model can be seen in Figure 61. When both the inverter in islanding mode are connected to the grid, then synchronization issue needs to be resolved again. Here we can see the frequency is restored for both centralized and de-centralized mode. For de-centralized control, the restoration happens quickly as the control does not need communication, whereas for centralized control it happens after few seconds.

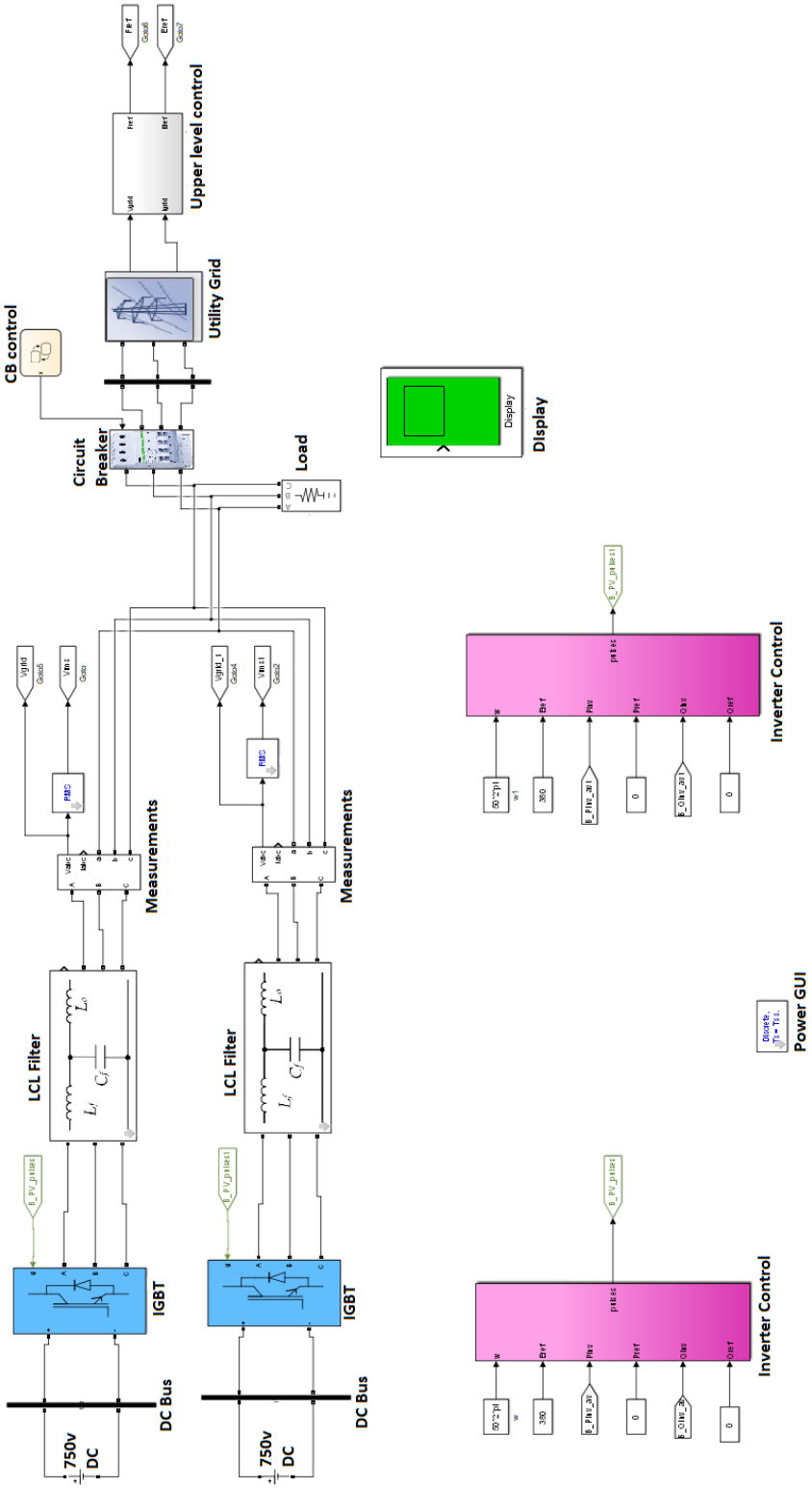

Figure 70. Grid connected in parallel inverter operation

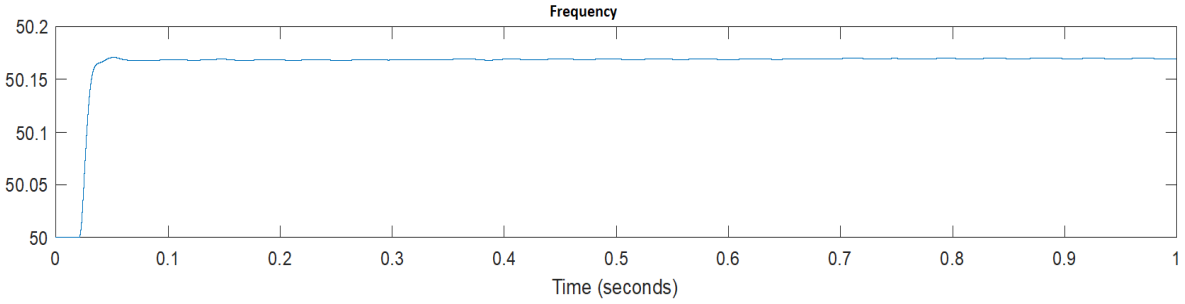

(a)

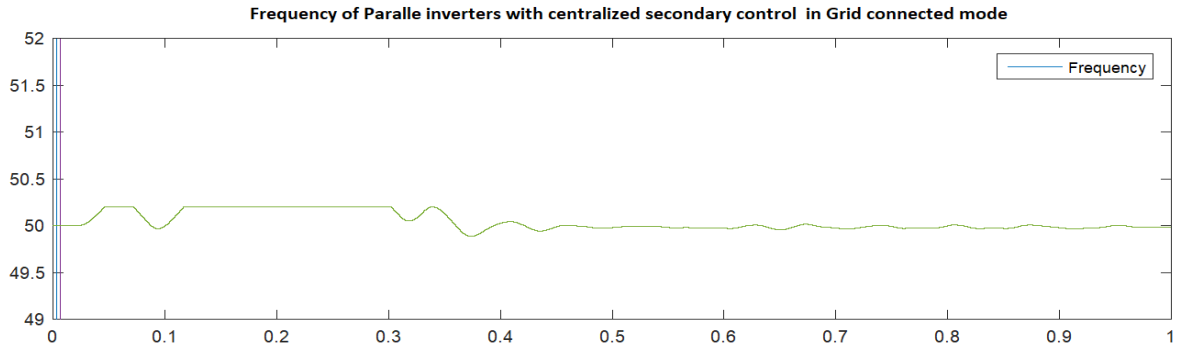

(b)

Figure 71. Frequency restoration in grid- connected mode. (a) centralized control, (b) decentralized control. Similarly, the output voltage and current of inverter during grid-connected mode can be seen below.

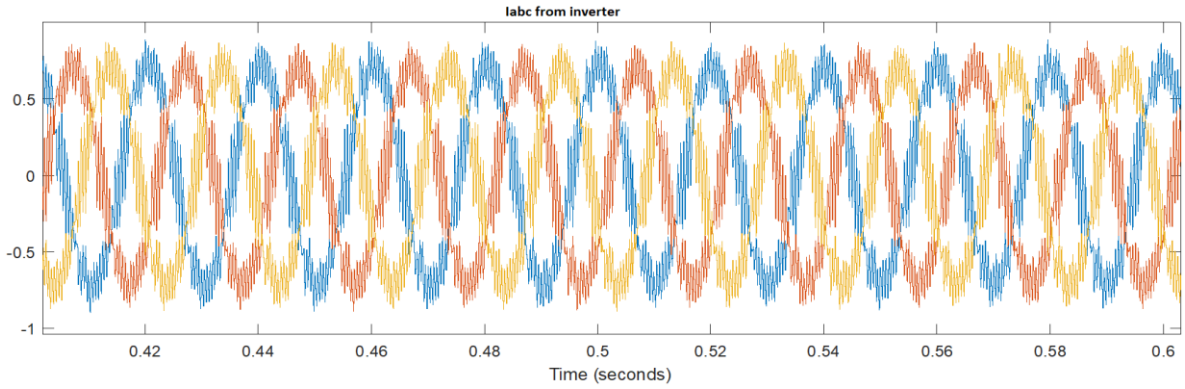

Figure 72. Current at output of inverter during grid-connected mode.

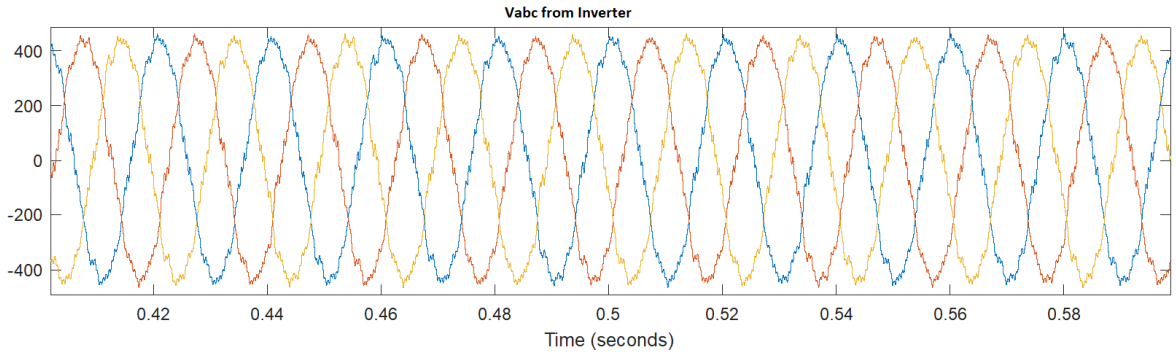

Figure 73. Voltage at the output of inverter during grid-connected mode

Now when the grid is connected to islanding inverters the transition needs to be tested, hence circuit breaker is added with a timing logic implemented in state flow and a 400 v 14 kW grid is simulated, which is connected to islanding load. As shown below the frequency curve, during transition from islanding to grid-connected mode the frequency drops and power flowing to the load increases to 16 kW.

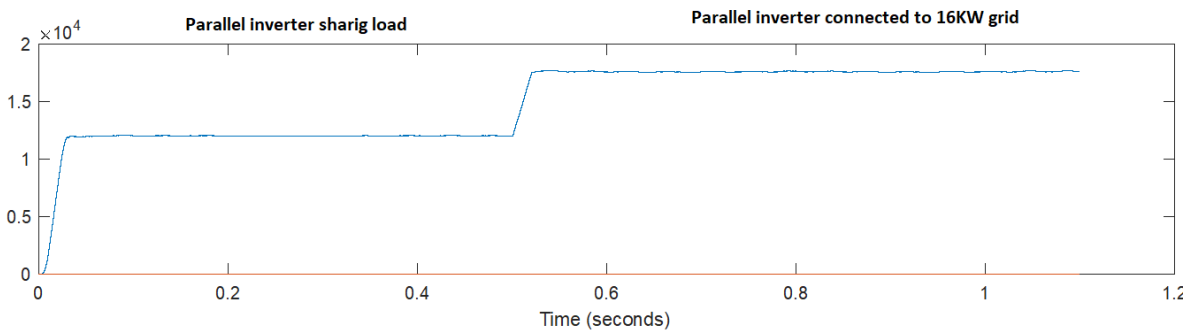

(a) (b)

Figure 74. (a) Active power during transition (b) Frequency during transition

The voltage at PCC seems to have a small glitch while transition from islanding to grid-connected mode at t=0.5 seconds as shown in below figure.

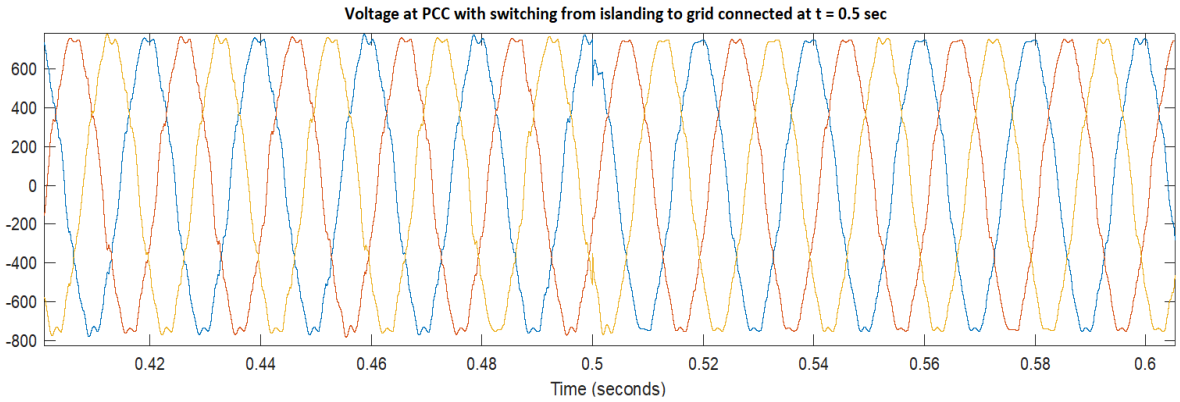

Figure 75. Voltage at PCC in grid-connected mode

Current output during and after transition can be seen below.

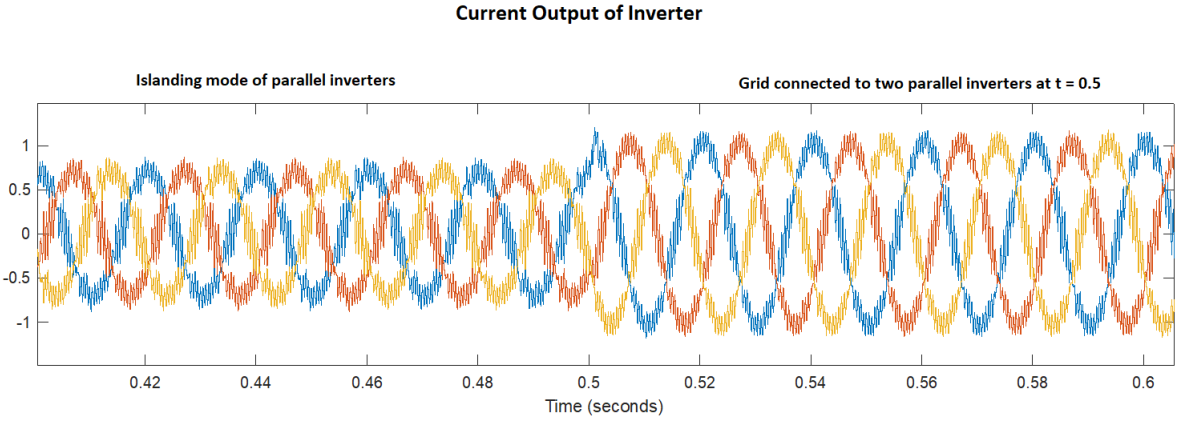

Figure 76. Current output of inverter during and after switching to grid

Table 2. Parameter values used in simulation

Parameter	Symbol	Value	Units
Power stage			
Grid Voltage	V_g	400	Volts(V)
Grid Frequency	f	50	Hz
Grid Inductance	L_g	0	H
Grid Resistance	R_g	1000	Ohm
Loss Resistance of Inverter	R_{loss}	0	Ohm
Inverter filter Inductance	L_f	5e-3	H
Line Inductance	L_l	3e-3	H
Inverter filter capacitance	C_f	25e-6	F
Load	R_L	12e3	Ohm
Directive frequency droop	m_d	1e-4	W/rd
Proportional frequency droop	m_p	1e-3	Ws/rd
Proportional Amplitude droop	n_p	1e-5	V Ar/V
Proportional gain Voltage control	K_{vp}	1	W/rd
Integral gain Voltage control	K_{vi}	15	Ws/rd
Proportional gain Current control	K_{ip}	1.5	W/rd
Integral gain Current control	K_{ii}	40	Ws/rd
Secondary Control			
Proportional Frequency droop	K_{pf}	1e-2	Ws/rd
Integral Frequency droop	K_{if}	1e-4	W/rd
Proportional Amplitude droop	K_{pe}	.1	W/rd.s
Integral Amplitude droop	K_{ie}	1e-4	V Ar.s/V

6. CONCLUSION

This chapter will summarize the information and work done. In this thesis the main area of focus was how to achieve synchronization in microgrids when it is connected in islanding mode and grid-connected mode and also when multiple voltage source inverters are connected in parallel. Various controls of power converters are discussed in the beginning chapter, which mainly focuses on islanding and grid-connected modes.

A hierarchical model is introduced to overcome the issue of synchronization and improving power quality. Two types of inner controls, with and without communication type, are explained in detail. The control with communication (master-slave, ALS, 3C, etc.) is explained and compared with non-communication type (droop control). Inside primary control implications of virtual impedance with resistance and impedance with reactance are explained.

For secondary control apart from traditional centralized approach, a new decentralized method is explained. In this method, the control structure is not common to all DER, but rather segregated to each unit. Finally, theory of tertiary control is given with explanation of working procedure.

Simulations for single and multiple inverter systems are verified, where we saw the effect of synchronization plays a crucial role. In addition, we saw how the secondary control technique helps to overcome the synchronization issues while connecting two voltage source inverters in parallel. The parallel inverter system as discussed, follows same control strategy except the usage of voltage and frequency control inside droop control mechanism, which will make the P-F and Q-E curve stable like single inverter control.

For future work, a detailed analysis of transition between parallel inverters and grid-connected inverters can be done for better understanding of synchronization between the inverter during switching. Different types of communication type models that have been discussed, need to be simulated for better analysis. Even though droop control seems very apt for present day inverter control designs, there are some drawbacks as mentioned in the theory that are needed to be studied deeper and tests should be conducted to analyze the

results. Similarly, for secondary control, we saw that decentralized control has advantages over centralized, but there are issues with latency, which needs more investigation. In this thesis only control of AC microgrid is explained, for future works control of DC microgrid can also be undertaken. Tertiary control is only explained in theory and simulations or tests were not conducted in this thesis, hence testing tertiary control in multiple inverters can give a good insight on how the active and reactive power is exported to or imported from the grid.

REFERENCES

Ambrosio, R. & S.E. Widergren (2007). A framework for addressing interoperability issues. *Power Engineering Society General Meeting*, 2007, IEEE 1–5. ISSN**:** 1932-5517.

Blaabjerg, F., R. Teodorescu, M. Liserre & A. V. Timbus (2006). Overview of control and grid synchronization for distributed power generation systems. *IEEE Transactions on Industrial Electronics,* 53:5, 1398-1409. ISSN**:** 1557-9948.

Bouzid, Allal, Josep M. Guerrero, Ahmed Cheriti, Mohamed Bouhamida, Pierre Sicard & Mustapha Benghanem (2015). A survey on control of electric power distributed generation systems for microgrid applications. *Renewable & Sustainable Energy Reviews,* 44, 751-766. ISSN: 1364-0321.

Chen, Dong & Lie Xu (2017). AC and DC microgrid with distributed energy resources. *Technologies and Applications for Smart Charging of Electric and Plug-in Hybrid Vehicles*, 39-64. ISBN: 978-3-319-43651-7.

Clarke, E. (1943). *Circuit Analysis of AC Power Systems.* vol. 1. New York: Wiley.

Driesen, J. & K. Visscher (2008). Virtual synchronous generators. *Power and Energy Society General Meeting – Conversion and Delivery of Electrical Energy in the 21st Century*, 2008 IEEE, [online] 1–3. ISSN**:** 1932-5517

Guerrero, Josep M., J. Matas, L. G. de Vicuna, M. Castilla & J. Miret (2006). Wireless-control strategy for parallel operation of distributed-generation inverters. *IEEE Transactions on Industrial Electronics,* 53:5, 1461–1470. ISSN**:** 1557-9948.

Guerrero, Josep M., Lijun Hang & Javier Uceda (2008). Control of distributed uninterruptible power supply systems. *IEEE Transactions on Industrial Electronics,* 55:8, 2845-2859. ISSN**:** 1557-9948

Guerrero, Josep M, Juan C. Vásquez, José Matas, Miguel Castilla & Luis García de Vicuña (2009). Control strategy for flexible microgrid based on parallel line-interactive UPS systems. *IEEE Transactions on Industrial Electronics,* 56, 726-736. ISSN**:** 1557-9948.

Guerrero, Josep M., J. C. Vásquez, J. Matas, L. G. D. Vicuña & M. Castilla (2011). Hierarchical control of droop-controlled AC and DC microgrids – A general approach towards standardization. *IEEE Transactions on Industrial Electronics,* 58:1, 158-172. ISSN: 1557-9948.

Hamilton, S. L, E. W. Gunther, R. V. Drummond & S. E. Widergren (2006). Interoperability – A key element for the grid and DER of the future. *Transmission and Distribution Conference and Exhibition,* 2005/2006, IEEE PES [online], [02 Feb 2018], 927–931. ISBN**:** 0-7803-9194-2.

Hsieh, H. M., T. F. Wu, H. S. Nien, Y. E. Wu & Y. K. Chen (2005). A compensation strategy for parallel inverters to achieve precise weighting current distribution. *Conf. Rec. IEEE IAS Annual Meeting,* 954-960. ISBN: 0-7803-9208-6.

Iwade, T, S. Komiyama & Y. Tanimura (2003). A novel small-scale UPS using a parallel redundant operation system. *Telecommunications Energy Conference*, 2003, INTELEC '03, The 25th International 480–483. ISBN**:** 4-88552-196-3.

Kroposki, Benjamin, Thomas Baso & Richard DeBlasio (2009). Microgrid standards and technologies. *Power and Energy Society General Meeting - Conversion and Delivery of Electrical Energy in the 21st Century,* 2008 IEEE, 1-4. ISBN: 978-1-4244-1905-0.

Kundur, P. (1993). *Power System Stability and Control*. Emeryville, CA: McGraw-Hill. ISBN: 978-0070359581.

Li, Yan & Yun Wei Li (2009). Decoupled power control for an inverter based low voltage microgrid in autonomous operation. *Power Electronics and Motion Control Conference*, 2009, IEEE 6th International, 2490-2496. ISBN: 978-1-4244-3556-2.

Liserre, M., R. Teodorescu & F. Blaabjerg (2006). Multiple harmonics control for three-phase grid converter systems with the use of PI-RES current controller in a rotating frame. *IEEE Transactions on Power Electronics*, 21:3, 836–841. ISSN**:** 1941-0107.

Lopes, J. A. P., C. L. Moreira & A.G. Madureira (2006). Defining Control Strategies for Microgrids Islanded Operation. *IEEE Transactions on Power Systems*, 21, 916-924. ISSN: 0885-8950.

Manandhar, Ujjal, Abhisek Ukil & Tan Keng Kiat Jonathan (2016). Efficiency comparison of DC and AC microgrid. *Innovative Smart Grid Technologies - Asia (ISGT ASIA)*, 2015 IEEE. ISSN**:** 2378-8542.

Martins, P., A. S. Carvalho & A. S. Araújo (1995). Design and implementation of a current controller for the parallel operation of standard UPSs. *Industrial Electronics, Control, and Instrumentation*, 1995, Proceedings of the 1995 IEEE IECON 21st International Conference on Industrial Electronics, Control, and Instrumentation, 584–589. ISBN**:** 0-7803-3026-9.

Mastromauro, Rosa A., (2014). Voltage control of a grid-forming converter for an AC microgrid: a real case study. *Renewable Power Generation Conference 2014, 3rd*, 1-6. ISBN**:** 978-1-84919-917-9.

Olivares, Daniel E., A. Mehrizi-Sani, A. H. Etemadi, C. A. Canizares, R. Iravani, M. Kazerani, A. H. Hajimiragha, O. Gomis-Bellmunt, M. Saeedifard, R. Palma-Behnke, G. A. Jimenez-Estevez & N. D. Hatziargyriou (2014). Trends in microgrid control. *IEEE Transactions on Smart Grid*, 5, 1905 – 1919. ISSN: 1949-3061.

Palizban, Omid & Kimmo Kauhaniemi (2015). Hierarchical control structure in microgrids with distributed generation: islanded and grid-connected mode. *Renewable and Sustainable Energy Reviews*, 44, 798-811. ISSN: 1364-0321

Peng, F. Z., Y. W. Li & L. M. Tolbert (2009). Control and protection of power electronics interfaced distributed generation systems in a customer-driven microgrid. *Power & Energy Society General Meeting*, 2009, IEEE 1–8. ISBN**:** 978-1-4244-4241-6.

Rocabert, Joan, Luna Alvaro, Frede Blaabjerg & Pedro Rodriguez (2012). Control of power converters in AC microgrids. *IEEE Transactions on Power Electronics*, 27:11, 4734-4749. ISSN: 1941-0107.

Rodriguez, P., A. Timbus, R. Teodorescu, M. Liserre & F. Blaabjerg (2009). Reactive power control for improving wind turbine system behavior under grid faults. *IEEE Transactions on Power Electronics*, 24:7, 1798-1801. ISSN**:** 1941-0107.

Rokrok, E. & M. E. H. Golshan (2010). Adaptive voltage droop scheme for voltage source converters in an islanded multibus microgrid. *IET Generation, Transmission & Distribution* 4, 562-578. ISSN**:** 1751-8695.

Sao, C. K. & P. W. Lehn (2005). Autonomous load sharing of voltage source converters. *IEEE Transactions on Power Delivery*, 20, 1009-1016. ISSN: 1937-4208.

Shafiee, Qobad, Josep M. Guerrero & Juan C. Vasqez (2014). Distributed secondary control for islanded microgrids – A novel approach. *IEEE Transactions on Power Electronics*, 29:2 1018-1030. ISBN: 1941-0107.

Timbus, A., M. Liserre, R. Teodorescu, P. Rodriguez & F. Blaabjerg (2009). Evaluation of current controllers for distributed power generation systems. *IEEE Transactions on Power Electronics*, 24:3, 654–664. ISSN**:** 1941-0107.

Tuladhar, A, H Jin, T Unger & K. Mauch (2000). Control of parallel inverters in distributed AC power systems with consideration of the line impedance effect. *Applied Power Electronics Conference and Exposition*, 1998. APEC '98. Conference Proceedings 1998, *Thirteenth* Annual, 321-328, ISBN**:** 0-7803-4340-9.

Vandoorn, T. L., J. D.M. De Kooning, B. Meersman & L. Vandevelde (2013). Review of primary control strategies for islanded microgrids with power electronics interfaces. *Renewable and Sustainable Energy Reviews*, 19, 613-628. ISSN: 1364-0321.

Vasquez, J. C., J. M. Guerrero, Alvaro Luna, Pedro Rodriguez & Remus Teodorescu (2009). Adaptive droop control applied to voltage-source inverters operating in grid-connected and islanded modes. *IEEE Transactions on Industrial Electronics*, 56, 4088-4096. ISSN: 1557-9948.

Vilathgamuwa, D. M., L. Poh Chiang & Y. Li (2006). Protection of microgrids during utility voltage sags. *IEEE Transactions on Industrial Electronics*, 53:5, 1427–1436. ISSN**:** 1557-9948.

Wu, T. F., Y. K., Chen & Y. H. Huang (2000). 3C strategy for inverters in parallel operation achieving an equal current distribution. *IEEE Transactions on Industrial Electronics*, 47:2, 273-281. ISSN: 1557-9948.

Zhong, Qing-Chang & George Weiss (2009). Static synchronous generators for distributed generation and renewable energy. *Power Systems Conference and Exposition*, 2009, PSCE '09, IEEE/PES 1-6. ISBN: 978-1-4244-3810-5.

MathWorks, Simscape Power Systems – Model and simulate electrical power systems, Available from Web: https://se.mathworks.com/products/simpower.html

APPENDIX I

MATLAB Startup script for test

```
clc;
disp(sprintf('Hierarcheal Control Of Micro Grid Simulink Models:\n 1. Single Inverter Islanding Mode\n 2. Single Inverter Grid Connected Mode\n 3. Two Parallel Inverters Islanding Moden (de-centralized secondary)\n 4. Two Parallel Inverters In Islanding mode (Centralized secondary )\n 5. Two Parallel Inverters In Islanding mode (Centralized secondary with Distributive load) \n 6. Two Parallel Inverter in Grid COnnected mode(Centralized Secondary)\n 7. Two Parallel Inverter in Grid Connected Mode (De-centralized Secondary)\n 8. Two parallel inverter in Tertiary Mode'));
prompt = 'Which Modle to select? ';
x = input(prompt);
Ts = 2e-5;%sampling time
PVinit;
if isempty(x)
   disp('Select between 1 to 6');
   x = input(prompt);
end
switch x
   case 1
      disp('Single Inverter Islanding Mode is selected');
    case 2
      disp('Single Inverter ¨Grid Connecting Mode is selected');
   case 3
      disp('Parallel Inverter Islanding Mode decentralized is selected');
   case 4
      disp('Parallel Inverter Islanding Mode centralized  is selected');
   case 5
      disp('Parallel Inverter Islanding Mode centralized with distributed load is selected');
   case 6
      disp('Parallel Inverter Grid Mode centralized is selected');
   case 7
      disp('Parallel Inverter Grid Mode decentralized is selected');
   case 8
      disp('Parallel Inverter Tertiary control is selected');
end

if(x == 1 || x==2)
    disp('Simulating....');
    if(x==1)
       mdl = 'singleinvertermodel';
       mdl1='singleinvertermodel/Display/Scope2'
    else
       mdl = 'singleinvertermodel_gridconnected';
       mdl1='singleinvertermodel_gridconnected/Display/Scope2'
    end
   open(mdl);
   open_system(mdl1);
   set_param(mdl,'StopTime','2')
   load_system(mdl);
```

```
    sim(mdl);
    figure('Name','Active and Reactive power measurements');
    title('Active and Reactive power measurements');
    grid;
    P1= plot(Pinv);
    hold on
    P2 =plot(Qinv);
    legend([P1,P2],'Active power','Reactive Power');
    figure('Name','Frequency measurements');
    title('Frequency measurements');
    plot(Freq)
    legend('Frequency');
    axis([0 2 40 60])
    figure('Name','Voltage measurements');
    title('Voltage measurements');
    plot(Vpcc)
    figure ('Name','PV VOltage ');
    axis([0 2 0 1000])
    plot(PV);
end
if(x==3)
     disp('Simulating....');
    mdl = 'parallelldecentrilized';
    open(mdl);
    Kpf=.2;    Kpf1=.2;
    Kif=0;   Kif1=0;
    Kpe=.2;     Kpe1=.2 ;
    Kie=0.00001;   Kie1=0.00001;
    set_param('parallelldecentrilized','StopTime','1');
    open_system('parallelldecentrilized/Display/Scope2');
    load_system('parallelldecentrilized');
    sim('parallelldecentrilized');
    figure('Name','Active and Reactive power measurements');
    title('Active and Reactive power measurements');
    grid;
    P1= plot(Pinverter);
    hold on
    P2 =plot(Qinverter);
    plot(Freq)
%     legend('Frequency');
%     axis([0 1 49 52])

end

if( x==4)
     disp('Simulating....');
    mdl = 'parallelcentralized';
    open(mdl);
    Kpf=.2;    Kpf1=.2;
    Kif=1.1;   Kif1=1.1;
    Kpe=0.2000;     Kpe1=.20000 ;
    Kie=0.000;   Kie1=0.000;
```

```
    set_param('parallelcentralized','StopTime','1');
    open_system('parallelcentralized/Display/Scope2');
    load_system('parallelcentralized');
    sim('parallelcentralized');
    figure('Name','Active and Reactive power measurements');
    title('Active and Reactive power measurements');
    grid;
    P1= plot(Pinverter);
    hold on
    P2 =plot(Qinverter);
    figure('Name','Frequency');
    plot(Freq);
    legend('Frequency');
     axis([0 1 49 52])

end
if( x==5)
     disp('Simulating....');
    mdl = 'parallelcentralized_distributive_load';
    open(mdl);
    Kpf=0.11;    Kpf1=0.11;  Kpft=1.2001;
    Kif=1e-4;   Kif1=1e-4; Kift=0;
    Kpe=.11;     Kpe1=.15 ;  Kpet=1.2001;
    Kie=1e-4;   Kie1=1e-4; Kiet=0;

    set_param('parallelcentralized_distributive_load','StopTime','1');
    open_system('parallelcentralized_distributive_load/Display/Scope2');
    load_system('parallelcentralized_distributive_load');
    sim('parallelcentralized_distributive_load');
    figure('Name','Active and Reactive power measurements');
    title('Active and Reactive power measurements');
    grid;
    P1= plot(Pinverter);
    hold on
    P2 =plot(Qinverter);
    plot(Freq);
    legend('Frequency');
    axis([0 1 49 52])

end
if( x==6)
     disp('Simulating....');
    mdl = 'parallelcentralized_gridconnected';
    open(mdl);
    Kpf=.11;    Kpf1=.11;       Kpft=1.2001;
    Kif=0;   Kif1=0            ;Kift=0;
    Kpe=0.0000;     Kpe1=0.0000 ; Kpet=1.2001;
    Kie=0.0000;   Kie1=0.0000;    Kiet=0;
      set_param('parallelcentralized_gridconnected','StopTime','1');
      open_system('parallelcentralized_gridconnected/Display/Scope2');
    load_system('parallelcentralized_gridconnected');
    sim('parallelcentralized_gridconnected');
```

```
    figure('Name','Active and Reactive power measurements');
    title('Active and Reactive power measurements');
    grid;
    P1= plot(Pinverter);
    hold on
    P2 =plot(Qinverter);
     plot(Freq);
    legend('Frequency');
    axis([0 1 49 52])

end

if( x==7)
     disp('Simulating....');
    mdl = 'parallelldecentrilized_grid_connected_test123';
    open(mdl);
    Kpf=.2;    Kpf1=.2;  Kpft=1.2001;
    Kif=0.1;   Kif1=0.1;  Kift=0;
    Kpe=0.2000;     Kpe1=.20000 ;  Kpet=1.2001;
    Kie=0.000;   Kie1=0.000;  Kiet=0;
    set_param('parallelldecentrilized_grid_connected_test123','StopTime','1');
    open_system('parallelldecentrilized_grid_connected_test123/Display/Scope2');
    load_system('parallelldecentrilized_grid_connected_test123');
    sim('parallelldecentrilized_grid_connected_test123');
    figure('Name','Active and Reactive power measurements');
    title('Active and Reactive power measurements');
    grid;
    P1= plot(Pinverter);
    hold on
    P2 =plot(Qinverter);
    plot(Freq);
    legend('Frequency');
    axis([0 1 49 52])

end
if( x==8)
     disp('Simulating....');
    mdl = 'Tertiarymodelslx';
    open(mdl);
    Kpf=0.20;    Kpf1=0.2;Kpft= .2001;
    Kif=0.001;   Kif1=0.001;Kift = 1e-4;
    Kpe=0.2000;     Kpe1=2.0000 ;Kpet=.2001;
    Kie=0.0001;   Kie1=0.001; Kiet=0;
    set_param('Tertiarymodelslx','StopTime','1');
    open_system('Tertiarymodelslx/Display/Scope2');
    load_system('Tertiarymodelslx');
    sim('Tertiarymodelslx');
    figure('Name','Active and Reactive power measurements');
    title('Active and Reactive power measurements');
    grid;
    P1= plot(Pinverter);
    hold on
```

```
   P2 =plot(Qinverter);
   plot(Freq);
   legend('Frequency');
   axis([0 1 49 52])

end
%%%%%%%%%%%%%%%     Plotting   %%%%%%%%%%%%%%%%%%


%%%%%%%%%%%%%%%%%%%%%%%%%%%%%%%%%%%%%%%%%%%%%%%%%%%%%
 PV initialization
nCells= 36;             % Number of cells in series
Pmp= 12000;             % Maximum power (W)
Vmp= 750;               % Maximum power voltage (V)
Imp= 16;            % Maximum power current (A)
Voc= 800;           % Open circuit voltage (V)
Isc= 20;           % Short circuit current (A)
TempC_Pmp= -6.445e-001;  % Maximum power temp. coefficient (W/deg.C)
TempC_Vmp= -8.200e-002;  % Maximum power voltage temp. coefficient (V/deg.C)
TempC_Imp= -1.068e-003;  % Maximum power current temp. coefficient (A/deg.C
TempC_Voc= -8.000e-002;  % Open circuit voltage temp. coefficient (V/deg.C)
TempC_Isc= 5.022e-003;   % Short circuit current temp. coefficient (A/deg.C)
Rs= 0.10593;             % Series resistance of PV model (ohms)
Rp= 142.84;              % Parallel resistance of PV model (ohms)
Isat= 9.845e-07;         % Diode saturation current of PV model (A)
Iph=  8.3758;            % Light-generated photo-current  of PV model (A)
Qd= 1.5;                 % Diode quality factor of PV model
Npar =66;%Paralle number of pannels
Nser = 36; %series number of pannels
k= 1.3806e-23; % Boltzman constant (J.K^-1)
q=1.6022e-19;  % electron charge  (C)
T=273+25;
 %set_param(BlockName,'Ncell',num2str(nCells));
 %set_param(BlockName,'ModuleParameters',str);
VT=k*T/q*nCells*Qd;
%set_param(BlockName,'ModelParameters',str)
Iph_array=Iph*Npar;
Isat_array=Isat*Npar;
VT_array=VT*Nser;
Rs_array=Rs*Nser/Npar;
Rp_array=Rp*Nser/Npar;
```

APPENDIX II

Simulink model of virtual impedance

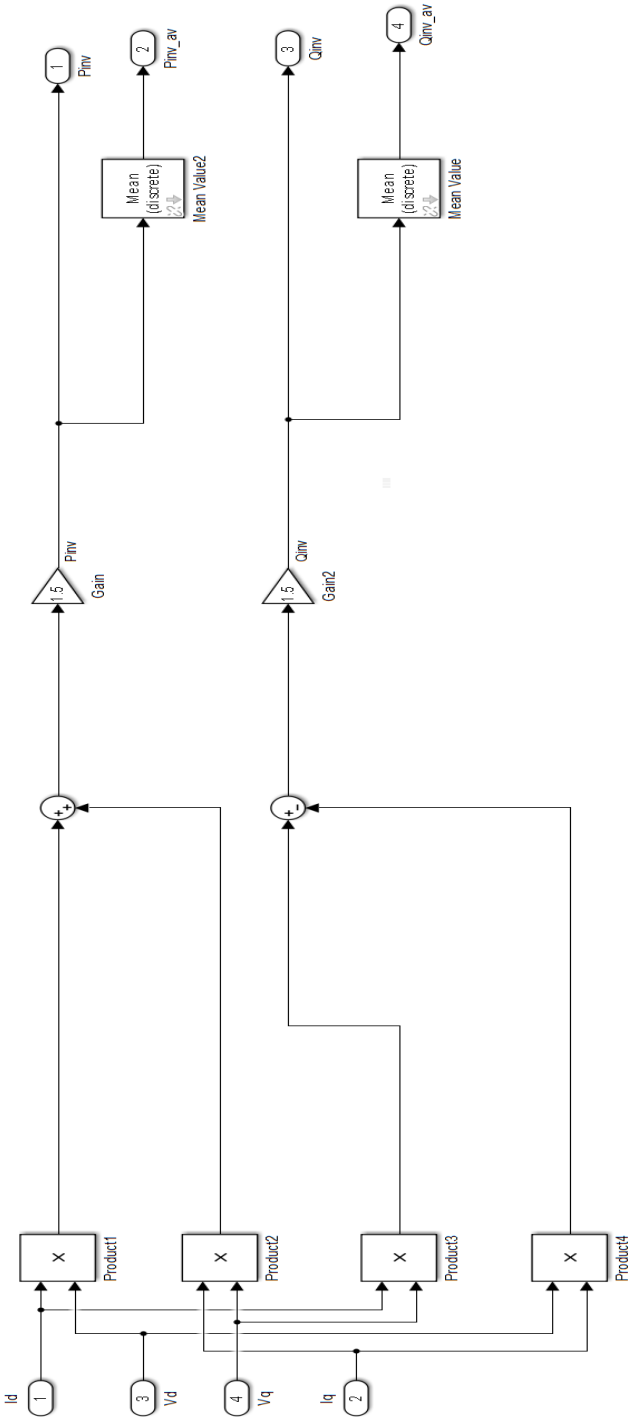

APPENDIX III

Simulink model of voltage controller

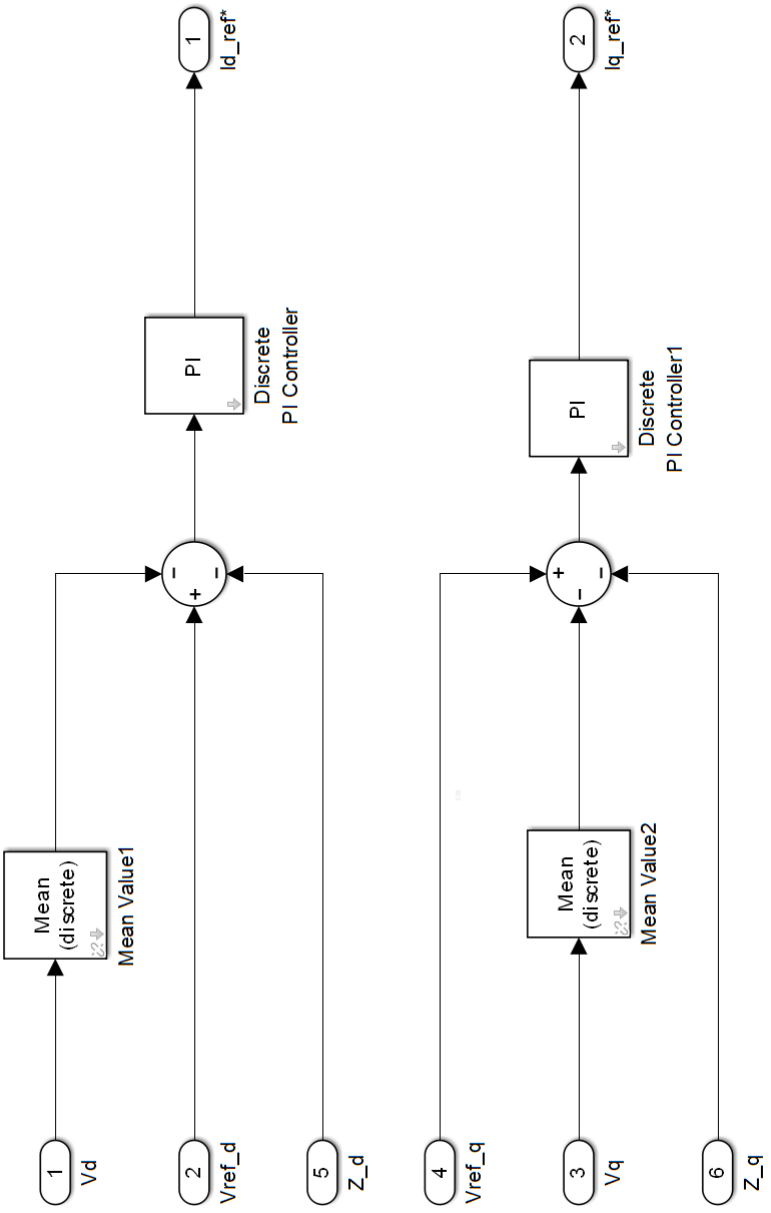

APPENDIX IV

Simulink model of current controller

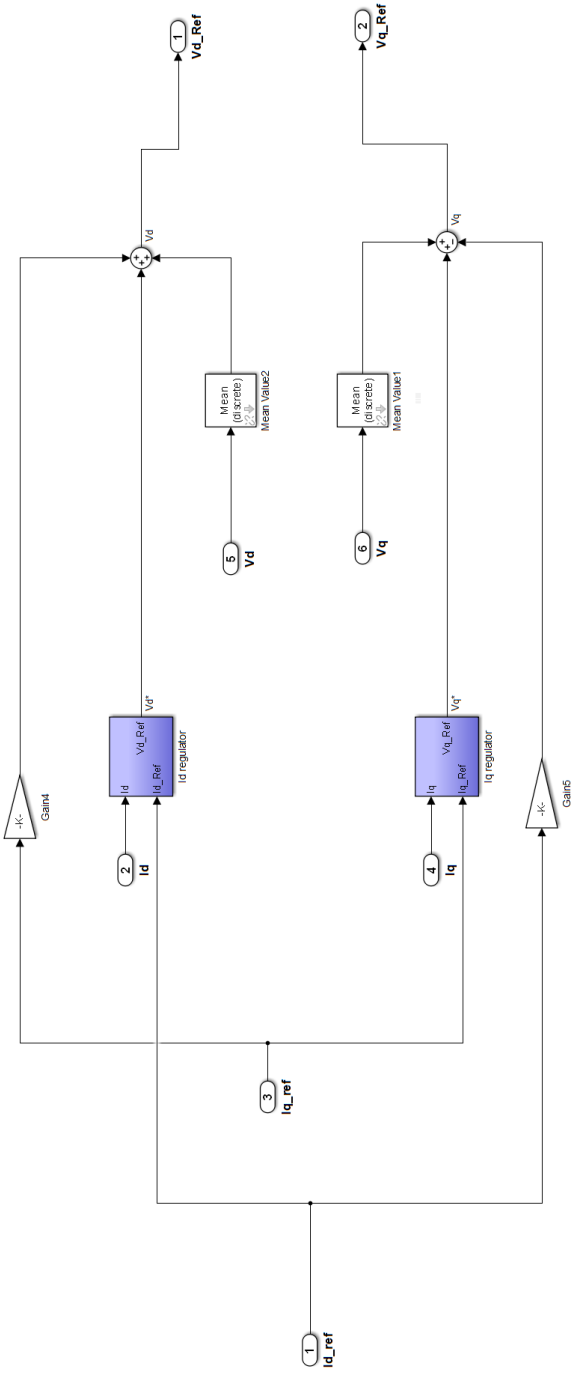

APPENDIX V

Simulink model of virtual impedance

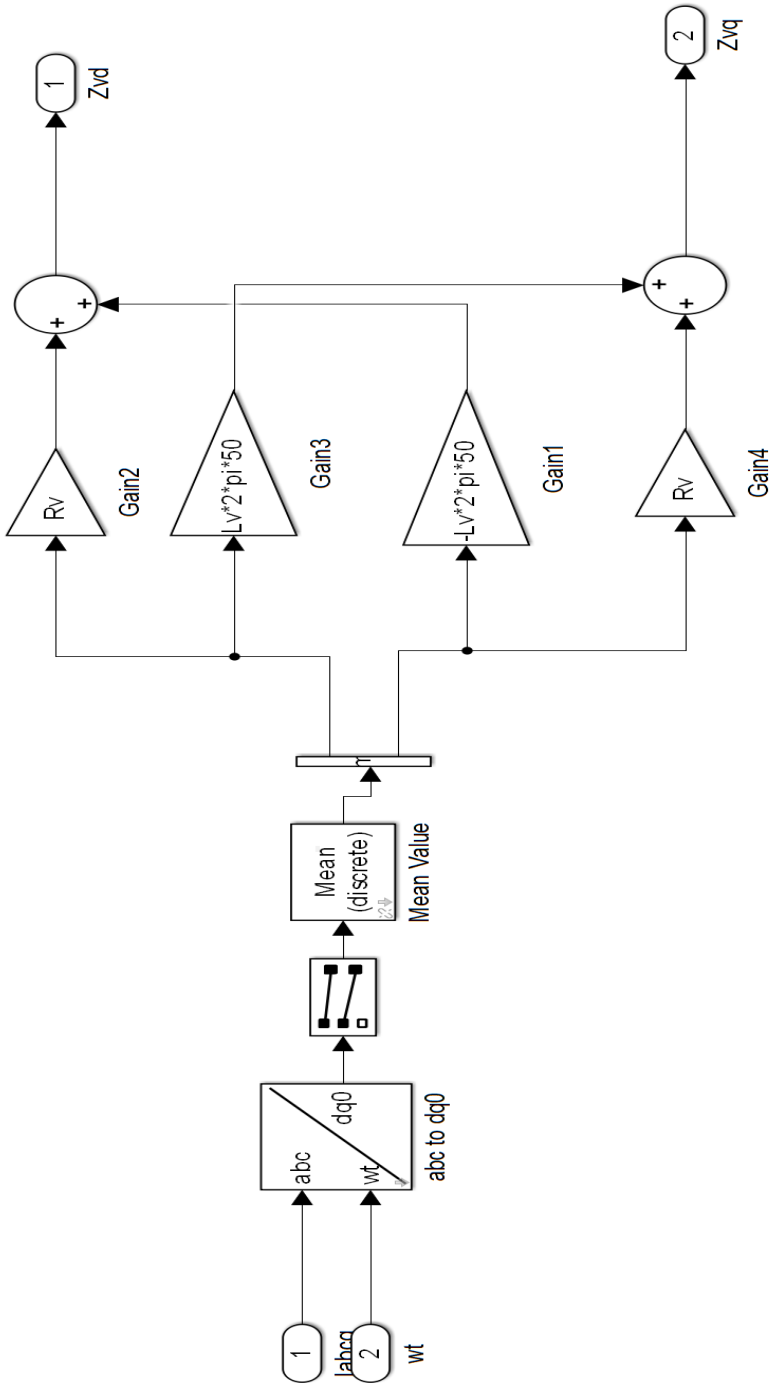

APPENDIX VI

Simulink model of power calculation